CORRELATION BETWEEN MICROSTRUCTURE AND TEXTURE OF TWO STEELS

By

ANUPRIYA PRASAD

DEPARTMENT OF MATERIALS AND METALLURGICAL ENGINEERING

INDIAN INSTITUTE OF TECHNOLOGY KANPUR

JANUARY, 1994

DEDICATED

TO

MY PARENTS

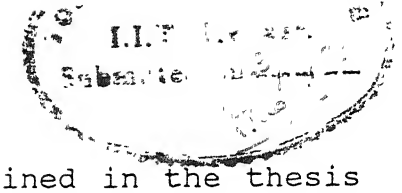

CERTIFICATE

It is certified that the work contained in the thesis entitled "Correlation between microstructure and texture of two steels" by "Anupriya Prasad" has been carried out under my supervision and that this work has not been submitted elsewhere for a degree.

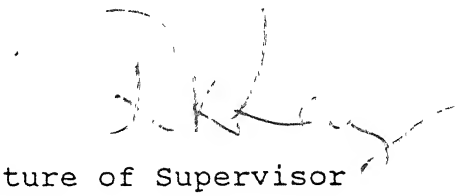

Signature of Supervisor

Professor R.K.Ray

Materials and Metallurgical Engineering.

Indian Institute of Technology. Kanpur.

January, 1994.

ACKNOWLEDGEMENT

I wish to record my deep sense of gratitude and indebtedness to my guide and teacher, Dr. R. K. Ray, Professor, Department of Materials and Metallurgical Engineering, I.I.T. Kanpur, for his constant guidance, thought provoking discussions and suggestions that he has very kindly made during different phases of the investigation and preparation of this thesis.

I am also thankful to Mr. K. P. Mukherjee, Mr. H. C. Srivastava, Mr. P. K. Paul and Mr. B. K. Jain for their help at different stages of the experimental work.

My sincere thanks are due to Ms. K. Vidya, Mr. Yash Pal and Mr. Pavitra Sandilya for their intelligent and flawless typing, and also to Mr. Amitava Sinha for his timely and untiring help in preparing this thesis.

Finally, I wish to express my special thanks to Ms. M. P. Butron-Guillen, of the Department of Metallurgical Engineering, McGill University, Montreal, Canada, for making available her texture results on the two steels.

Anupriya Prasad

CONTENTS

LIST OF FIGURES

LIST OF TABLES

ABSTRACT

An attempt has been made to correlate the microstructures and textures of a plain C steel and a Nb-microalloyed steel. For this purpose, the two steels (each soaked at 1250°C as well as at 1150°C) were controlled rolled, upto 90% and 75% reductions, at five different finishing temperatures viz. 1020°C(in the $\gamma_{recryst}$ range), 870°C(in the $\gamma_{nonrecryst}$ range), 770°C (in the upper $\gamma+\alpha$ range), 730°C(in the lower $\gamma+\alpha$ range) and 630°C (in the lower α range). Measurements of crystallographic textures of these controlled rolled steels have been carried out at the mid-thickness sections. The major texture component in both the steels, rolled upto 90% is {100}<011> and that in the steels rolled upto 75% is {111}<112>. In general, the texture intensities are more severe in the Nb-microalloyed than in the plain C steel. A detailed quantitative study of the changes in microstructure of the controlled rolled steels with (a)finishing temperature, (b)composition, (c)amount of deformation and (d)austenitizing temperature, was undertaken, by measuring certain metallographic parameters such as (a)the grain shape parameter, (b)degree of orientation, (c)grain thickness along ND and (d)the rose-of-the-number-of-intersections.

It has been found that the degree of orientation and the rose-of-the-number-of-intersections correlate well with the texture severity in both the steels. However, the correlation with the other two parameters i.e. the grain shape parameter and the grain thickness along ND is not meaningful.

CHAPTER I
INTRODUCTION

Controlled rolling is well known as a process to refine the structure of steel and, thereby, to enhance its mechanical properties. This refinement of structure is achieved mainly through γ-grain refinement which in turn is achieved by controlling the austenitizing temperature, steel composition, amount of deformation, etc. The finishing temperature is another factor which controls the final steel structure. For example, controlled rolling in the $\gamma_{nonrecryst}$ range yields a finer structure than that in the $\gamma_{recryst.}$ range. This is because the austenite grains are divided into several blocks by the introduction of deformation bands when the steel is finished in the former temperature range. Deformation in the intercritical region yields a mixed structure consisting of equiaxed grains and subgrains, which increases the strength and toughness of the steel to a large extent.

The composition of steel, especially when microalloyed with Nb, has an important influence on the final microstructure. This is because Nb(C,N) tends to suppress the recrystallization of γ and further, they precipitate at certain preferential sites, due to which the grains boundary movement, of the nucleated grains, is inhibited. This results in finer structures in case of Nb-microalloyed steel as compared to those in case of plain C steel. Furthermore, grain refinement is also sensitive to the austenitic grain size, which depends on the austenitizing temperature. Lower austenitizing temperatures yield finer γ-grains which in turn are expected to produce finer α-grains.

In addition to the microstructural changes observed during controlled rolling, textural changes have also been reported in literature. During controlled rolling, the parent γ acquires a crystallographic texture, the sharpness of which depends on the finishing temperature as well as the composition of the steel. This texture is then inherited in a definite way by α after transformation, because of the particular orientation relationship existing between the two phases. If γ is allowed to recrystallize before transformation, {100}<001> cube texture develops in γ which later on transforms to rotated cube {100}<011> in α. However, if γ-recrystallization does not take place, sharp γ rolling textures are developed which give rise to {332}<113> and {113}<110> type of orientations in the product α. The sharpness of the rolling textures generally increases with (a) increase in the amount of deformation, (b) decrease in finishing temperature and (c) alloying with Nb.

Although much study has been done, separately, on the microstructural as well as the textural changes during controlled rolling, no attempt has so far been made to correlate the two. Reports in the literature, however, indicate that there should be some kind of correlation between the two features, since both are produced as a result of mechanical processing. In view of this a detailed investigation involving quantitative microscopic characterization, of the plain C steel and a Nb-microalloyed steel, has been undertaken in the present work. Attempts were then made to correlate the microstructure with the crystallographic texture of these steels, by considering various microstructural parameters.

In the following pages, a detailed review ;of the literature has been presented in Chapter II. Here the fundamentals of controlled rolling and, microstructural and textural changes associated with it have been reviewed. Further, the applicability of quantitative microscopy to the controlled rolled steel structures has been examined and the studies involving various microstructural parameters have been stated.

Chapters III and IV have been devoted to the experimental procedure and the results obtained, respectively.

In Chapter V, the results of the investigation have been critically evaluated and discussed. The possibility to correlate the microstructurees and textures of the two steels, has been examined and a detailed analysis leading to this correlation has been presented.

Finally in Chapter VI, the conclusions derived from the present work have been mentioned in the usual manner.

CHAPTER II
LITERATURE REVIEW

2.1 CONTROLLED ROLLING OF STEELS

2.1.1 Controlled rolling

It has been known that mechanical properties such as strength, toughness, weldability, etc., of structural steels can be improved by grain refinement, which can in turn be achieved by lowering the finish rolling temperature in the γ-range. Earlier the refinement of microstructure was carried out by Al-killing, Normalizing, increasing the Mn to C-content ratio, etc., whereby high strength as well as high notch toughness was obtained in rolled steel. Later on, marked increase in strength was observed by small additions of Nb. But this caused reduction in the notch toughness. In order to prevent this reduction, controlled rolling of Nb-bearing steels was studied. Further research on controlled rolling was carried out by BISRA group [1] which has evolved into the modern controlled rolling process. A detailed study of the evolution of controlled rolling process has been made by Tanaka[1].

The basic idea behind controlled rolling is to refine the γ-grain size so as to obtain fine ferrite after transformation. This is done by controlling the rolling process so that it takes place within a particular temperature range. Earlier, steels were hot rolled i.e. rolled in the $\gamma_{recryst.}$ region only, but later on, the effect of recrystallization of γ on texture development was realised which gave way for controlled rolling of steels in $\gamma_{nonrecryst.}$ range also(This will be discussed in detail in a subsequent section on textural changes during controlled rolling). Controlled rolling has now been

further extended to the γ-α range and α range also, due to textural requirements.

2.1.2 Purpose of controlled rolling

It has already been stated that controlled rolling is superior to conventional hot rolling with respect to texture. This is important mainly in case of low cost deep drawing quality steels. These steels require a sharp {332}<113> texture which is sensitive to austenite grain size, and very fine austenite grains can be obtained by cold rolling and annealing. But a sharp {100}<001> component forms in austenite due to this and gives rise to {100}<011> texture in transformed ferrite, which caused delamination in the rolled steel[1]. So this route cannot be followed.

It has also been observed [1] that controlled rolling produces finer ferrite grains as compared to those produced by hot rolling and subsequent recrystallization, since in the latter case, α-nucleation takes place only at the austenite grain boundaries as well as grain interiors, due to the presence of deformation bands.

2.1.3 Controlled rolling practice

Tanaka has proposed three stages of controlled rolling process, as illustrated in Fig 2.1 [2]. The three stages correspond respectively to (a) rolling in $\gamma_{recryst.}$ range, (b) rolling in $\gamma_{nonrecryst.}$ range and (c) rolling in the γ-α intercritical range[1]. As stated earlier, controlled rolling is also sometimes done in the upper ferritic region before

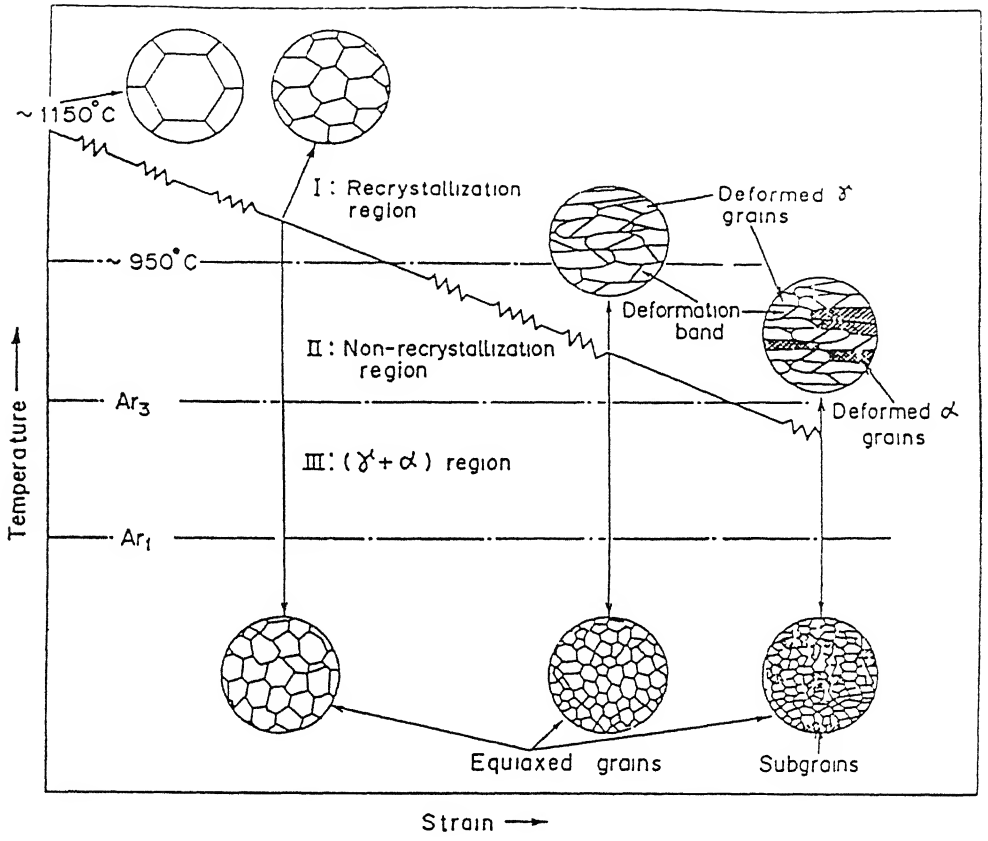

Figure 2.1: Schematic diagram illustrating the three stages of the controlled rolling process and changes in microstructure with deformation in each stage [2].

controlled cooling to room temperature.

The two very important factors that affect the controlled rolling process in the production mill are (a) lowering of slab reheating temperature, so as to obtain a fine and uniform γ-structure and (b) selection of a suitable roll pass schedule. If the roll pass schedule is not proper, one may obtain a mixed grain structure, which causes reduction in the toughness value.

In the production mill, controlled rolling is often carried out in three steps (a) roughing, (b) soaking for sufficient time to ensure uniform structure and (c) finishing[1]. However, the soaking stage may lead to recrystallization which should be avoided by taking care while selecting the soaking temperature and time.

2.1.4 Microstructural changes during controlled rolling

2.1.4.1 Deformation in the $\gamma_{recryst.}$ range

As already stated, the main idea behind controlled rolling is to obtain a fine and uniform ferrite grain size, which obviously requires uniform parent austenite grains. It has been established[1] that it is almost impossible to refine γ through dynamic recrystallization, instead grain refinement can be achieved by static recrystallization. The nucleation sites in the latter case are predominantly the triple junctions of grains and the grain boundaries.

As evident from Fig.2.2, the recrystallized grain size decreases rapidly with increasing amount of deformation and becomes constant after a critical value[3]. Although the effect

of deformation temperature on the recrystallized γ grain size is not very significant, the trend is that recrystallized grain size is slightly smaller in case of lower deformation temperatures (Fig.2.2).

The initial grain size plays an important role in determining the recrystallized grain size, because the nucleation occurs predominantly at the grain boundaries, as stated earlier. Ouchi et al[4] showed that recrystallized grain size decreases linearly with the product of strain and total grain boundary area. They also showed that the limiting value of recrystallized grain size (defined earlier with Fig.2.2) decreases with initial grain size. Towle and Gladman[5] showed that in case of stainless steels, the recrystallized grain size, $d_{rex.}$, can be related to the strain and initial grain size by,

$$d_{rex.} = k\varepsilon^{-0.5} d_0 Z^{-0\ 06} \qquad \ldots(2.1)$$

where k is a constant, ε is the strain, d_0 is the initial grain size and z is the Zener-Hollomon parameter.

Tanaka et al [3] have studied the effect of composition on the recrystallization behaviour of steels. The effects of deformation temperature and initial grain size on the critical amount of deformation (for recrystallization) have been shown in Fig.2.3 [1]. It is evident from the figure that critical reduction needed in case of Nb steel is much higher than that in case of C-Mn steel and recrystallization is virtually suppressed below 950°C in case of Nb steel. Ouchi et al [6] and Tanaka et al [7] later on found out that the reason for higher critical reduction in case of Nb steel is the strain-induced precipitation of fine Nb(C,N).

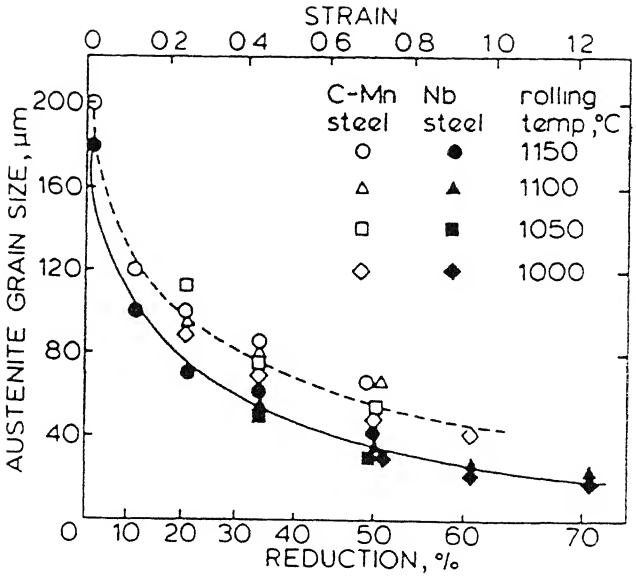

Figure 2.2: Influence of amount of single pass deformation and deformation temperature on recrystallized austenite grain size in plain C and Nb steels [1].

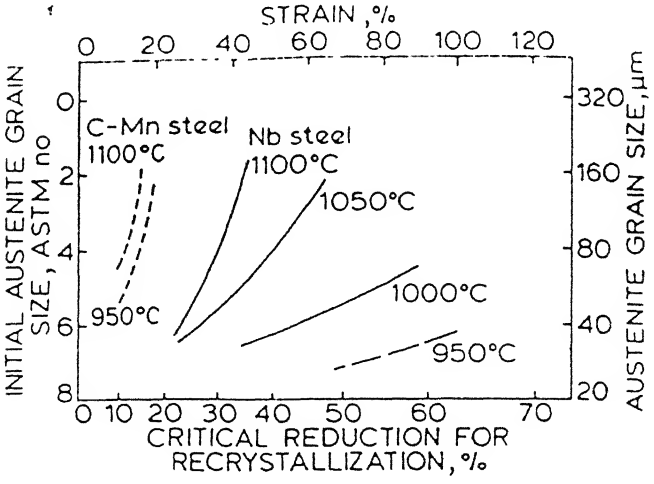

Figure 2.3: Effects of deformation temperature and initial grain size on critical amount of deformation required for completion of recrystallization in plain C and Nb steels [1].

Fig.2.4[1] shows the persistent recrystallization behaviours of steel at various rolling temperatures and amount of deformation. This figure has been used by Ouchi et al and Tanaka et al for determining the proper conditions i.e. the rolling temperature and amount of reduction[1]. They have established that if a reduction per pass, slightly greater than that for partial recrystallization, is given successively, a uniform and refined grain structure is obtained.

Sometimes, a mixed grain structure consisting of fine and coarse α grains and/or upper bainite, is obtained due to improper controlled rolling conditions. This is often observed when partial recrystallization of γ occurs[8], whereby fine recrystallized grains form at the γ grain boundaries, leaving an unrecrystallized region in the grain interior. The steel should thus be soaked for a sufficient time [1] to prevent the formation of mixed grain structure. Alternatively, a continuous rolling schedule can be carried out in the whole temperature range as proposed by Jones and Rothwell [8].

2.1.4.2 Deformation in the $\gamma_{nonrecryst.}$ range

The ferrite grains obtained after deformation in this range have been found to be finer than those obtained after transformation of recrystallized γ. This is due to the fact that in this temperature range, γ gets warm worked and thus deformation bands are produced within the grains. This tends to increase the number of potential nucleation sites in the structure since α nucleation takes place at the grain boundaries as well as in the grain interiors[1]. According to Ouchi et al

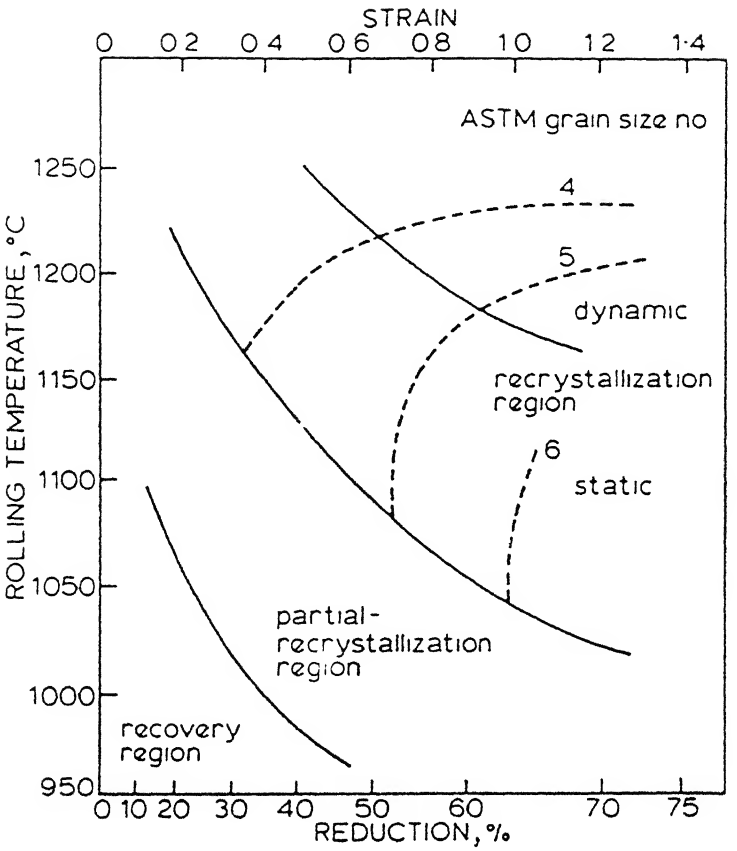

Figure 2.4: Austenite recrystallization and resulting grain size as function of rolling temperature and reduction for 0.03% Nb steel; steel was reheated to 1250°C for 20 minute, rolled with one pass, and quenched; initial grain size number was 1.0 [1].

[6], the unrecrystallized γ contains high dislocation density and substructure besides elongated grain boundaries and deformation bands.

The deformation band density has been found, by some investigators, to increase rapidly after 30% deformation[1]. It remains however unaffected by the deformation temperature. Sekine and Maruyama[9] have reported that the γ grain boundary area appears to increase with an increasing amount of reduction, reaching a steady level above about 30% reduction[1]. This means that beyond 30% reduction the refinement of grains due to deformation in the $\gamma_{nonrecryst.}$ range occurs mainly due to increase in the deformation band density [1].

In plain C steel the $\gamma_{nonrecryst.}$ range starts at about 900°C[1]. But alloying elements, especially Nb has been found, by Irvine et al [10] and Kozasu[11], to raise this limit, i.e. in presence of Nb, recrystallization starts becoming sluggish at much higher temperatures than 900°C. This is evident from Fig.2.5[1]. It has been suggested by many investigators[1] that the retardation of recrystallization, due to Nb is possible only when Nb is in solution in γ before deformation. Tanaka has attributed the recrystallization retardation, due to Nb alloying, to

(i) a solute drag effect,

(ii) strain induced precipitation of fine Nb(C,N) and

(iii) combined effects of both (i) and (ii).

Furthermore, it has been reported by Coladas et al [12] that the effect of Nb is only on the incubation time and not on the recrystallization kinetics.

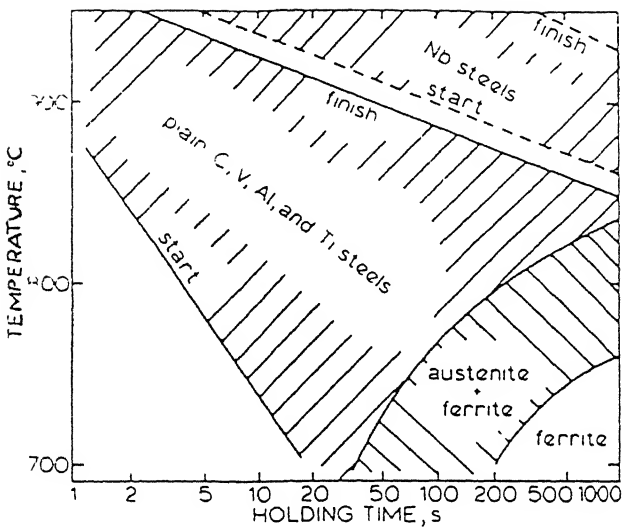

Figure 2.5: Recrystallization of austenite following single deformation of 50% in various steels [1].

Since the effect of Nb alloying is to suppress $\gamma_{recryst.}$ at even at relatively higher temperatures the α grains obtained after transformation will obviously be finer than those obtained in the absence of Nb.

2.1.4.3 Deformation in $\gamma+\alpha$ region

Deformation in this region produces some equiaxed α grains and cold worked α grains. The deformed γ transforms to polygonal α and deformed proeutectoid α remains as cold worked α. When considered in terms of an electron microscopic scale, the cold worked α is found to consist of subgrains which are formed because of the stabilization of the α sub-boundary network due to strain induced precipitation of of Nb(C,N)[1].

Priestner and de los Rios [13] have postulated that during transformation of deformed γ to α ,α nucleates on the unrecovered dislocation substructure in γ. These grains soon impinge on existing γ subgrains and thus are unable to grow further. This has been considered to be the cause of grain refinement during rolling in this region.

The deformed α in the parent structure does not recrystallize but only recovers because of strain induced precipitation of Nb(C,N) in the α-substructure. This too leads to fine α grain structure[1]. However Priestner and de los Rios have reported that grain refinement is obtained due to the substructure and not due to Nb(C,N) precipitates. This can be considered to be the operating mechanism in the grain refinement of Nb-free steels. Melloy and Dennison and others[1] have attributed grain refinement to dynamic recovery and/or dynamic

recrystallization of α.

2.1.4.4 Deformation in the α region

Controlled rolling in the α-range produces a structure consisting of elongated α grains. Here the equiaxed α grains, obtained by transformation of γ also, get deformed due to which the whole structure appears elongated. No further information is available in literature about the microstructural changes during controlled rolling in the α range. The textural changes, however, have been extensively studied (section 2.1.5.3) since very sharp α rolling textures are observed when the steels are finish rolled in this temperature range.

2.1.5. Textural changes during controlled rolling

It has been well established that there are three processes which give rise to textural changes in steels namely deformation, recrystallization and transformation[2]. During controlled rolling, reductions are applied in the γ range, γ+α range as well as in the ferritic range. In the first two cases γ to α transformation plays an important role in texture formation. The parent γ develops a texture which is acquired by the material after transformation. This inheritance depends on the orientation relationships of the parent and product phases. In the third case however, texture can be controlled by controlling only deformation and recrystallization since, here γ to α transformation plays a minor role by providing the starting texture.

2.1.5.1. Finish rolling in the γ range

When steel is finish rolled in the $\gamma_{recryst.}$ region, a weak {100}<011> texture is found in the product ferrite. This is because the cube {100}<001> texture is formed in the parent austenite due to recrystallization[2]. However, if the finishing temperature is lowered down to the $\gamma_{nonrecryst.}$ range, sharp rolling textures {110}<112> and {112}<111> are formed in the parent austenite. These give rise to strong {332}<113> and {113}<110> textures respectively in the product ferrite . The strengths of these texture components have been found to increase with increase in the amount of deformation and decrease in the temperature of deformation within this range.

It has also been demonstrated by many investigators that the composition of steel affects the nature and sharpness of the final texture components. Inagaki[14] has compared the textures of Nb-V steel and Nb-free steel. The difference between the textures of the two steels is due to the difference in the parent austenite texture. In case of Nb-V steel, precipitation of NbC and VC suppresses the recrystallization of austenite, due to which strong austenite rolling texture is obtained. This results in sharper texture in this case. However, in case of Nb-free steel, austenite recrystallizes readily and hence weak recrystallization texture is obtained, resulting in weaker texture in the product ferrite. Similar observations were made by Ray et al [15] who worked on a plain C steel and a Nb-microalloyed steel. However, an additional and important orientation {110}<110> was found in

these steels when finish rolled in the $\gamma_{recryst.}$ range. The intensity of this component was found to decrease as the finishing temperature was lowered in this range.

2.1.5.2 Finish rolling in $\gamma+\alpha$ range

It has been observed by Inagaki that finish rolling in this range produces the following in the steel;(i) crystal rotation of the parent γ phase,(ii) γ to α transformation and (iii) crystal rotation and recrystallization of the product α phase [2]. Thus the resultant texture is invariably, decided by the relative contribution of the above processes. These in turn depend on various variables such as composition of the steel, amount of reduction, finishing temperature, etc., of which the finishing temperature has the most important effect.

At higher finishing temperatures in the $\gamma+\alpha$ range, the amount of proeutectoid α is very less as compared to the austenite and hence the product α inherits the transformed {332}<113> and {113}~{112}<110> components, since crystal rotation of α does not have any significant influence. However as the finishing temperature is lowered in the same range, the amount of α formed, before the final pass, increases which results in the increase in the effect of α crystal rotation on the final texture. This increases the sharpness of the final α texture. The remaining γ gets deformed more and more as the temperature is lowered and hence sharper γ texture is formed which is later on inherited by the product α, as sharp {332}<113> as well as {554}<225>.

The effect of composition on the textures,

obtained by controlled rolling in the range, has been studied by Inagaki[14] by considering the textures of Nb-V steel and Nb-free steel. It has been shown that in the upper $\gamma+\alpha$ range, the {332}<113> component is rather weak in the Nb-free steel, whereas it is stronger in case of Nb-V steel. Development of {100}<011> texture was also observed in the two steels. However, it was stronger in case of Nb-free steel since this component has been ascribed[14] to the recrystallization of α, which is observed to be suppressed by the presence of NbC and VC. Ray et al [15] have found that when the finishing temperature is in the lower $\gamma+\alpha$ range, in addition to the {100}<011>, two major components of the plain C steel texture are the {223}<110> and {554}<225> whereas, the corresponding texture of Nb-microalloyed steel are near {4411}<110> and {332}<113>/{554}<225>.

2.1.5.3 Finish rolling in the α range

It has been reported by Ray et al [15] that the texture components formed after finishing plain C and Nb-microalloyed steels, in the lower α range are {100}<001>, {223}<110>and {554}<225>. Here the deformation of α plays a much important role in the final texture formation than the transformation of γ, due to which the {113}<110> and {332}<113> are converted to {223}<110> and {554}<225> since the latter are much more stable during α-rolling. These give rise to a high $\bar{r}$ value in steels. Not much difference was found between the textures of the two steels.

However earlier, Inagaki had concluded that, since the textures formed after finishing in the $\gamma+\alpha$ range were near

the stable end, not very significant change will be observed after rolling in the α range[2] in Nb-V and Nb-free steels. It has been observed by Hashimoto et al that in interstitial free steels, finish rolling in the lower α range produces the {112}<110> texture which can change to {554}<225> giving a high $\bar{r}$ value[2].

Although finish rolling in the α range seems to be beneficial for the steel in achieving a high $\bar{r}$ value, a major problem associated with this process has been reported by Inagaki[14]. He has reported that a surface texture is observed in his steels which gives rise to inhomogeneity of texture through the thickness of the specimen. The surface texture consisted of partial fibre texture with <110> axes parallel to ND, and a weak {332}<113> component. The surface texture is related to the texture at the centre of the specimen by some rotation about the TD (Transverse Direction) depending upon the lubrication and rolling temperature.

2.1.5.4 Effect of austenitizing temperature and cooling rate on texture development

The austenitizing temperature (or γ grain size), has been reported by Inagaki and co-workers, to have significant influence on the final texture intensity. The effect is obvious from Fig.2.6[2], wherein the texture of the specimen soaked at 1100°C is observed to be sharper than that of the specimen soaked at 1250°C. Similar difference in the sharpness of textures of specimens soaked at 1250°C and 1050°C, and then quenched to get martensitic structure, was observed by Inagaki and Kodama. It

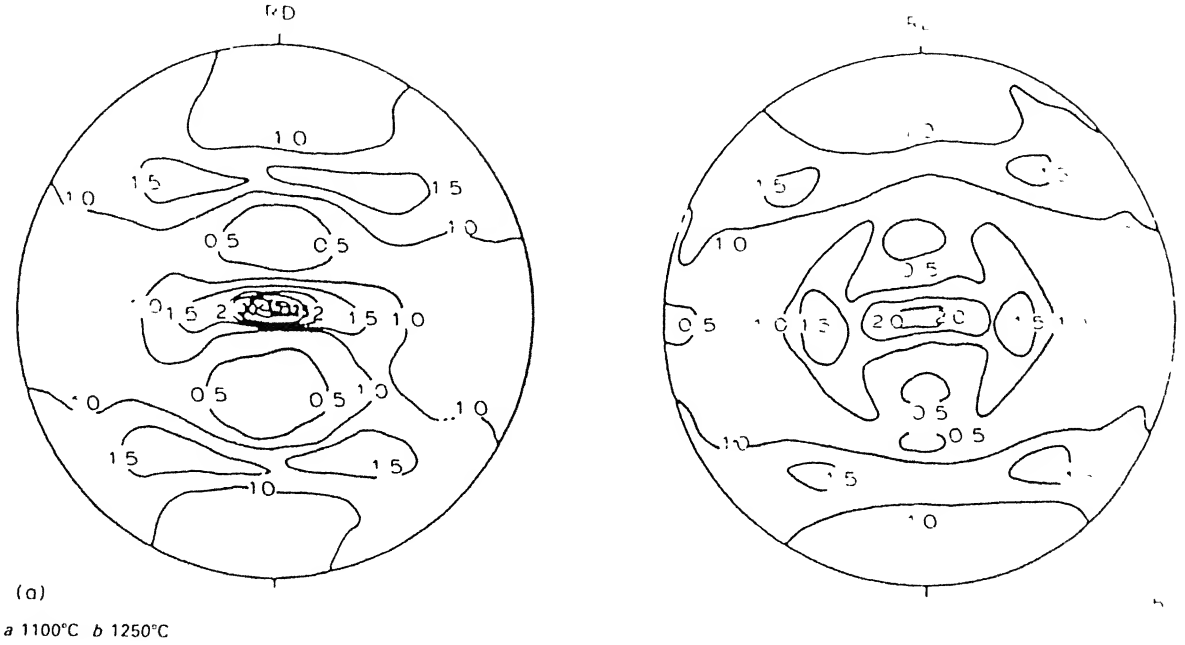

Figure 2.6: (200) pole figures showing effect of soaking temperature on texture of 0.1C-0.3Si-1.6Mn-0.04Nb Steel [2].

was found that the major component which is influenced by austenitizing temperature is {332}<113> while the {113}<110> component remains unaffected.

The work of many investigators has been reviewed by Ray and Jonas [2] which shows that the rate of cooling after controlled rolling in the γ and $\gamma+\alpha$ ranges has significant effect on the sharpness of the texture. Although the major components of the texture have been identified as {113}<110> and {332}<113>, irrespective of the final microstructure, their sharpness has been found to increase as the cooling rate increases. This means that the texture intensity of martensite is higher than that of bainite and that of bainite is higher than the texture intensity of ferrite. Furthermore, the {332}<113> component has been found to be influenced by the cooling rate whereas the other component remains unaffected[2].

The effects of various factors such as composition of steel, finishing temperature, austenitizing temperature, cooling rate, etc., on the texture of steel have been shown in Fig.2.7.

2.2 MICROSTRUCTURAL CHARACTERIZATION OF CONTROLLED ROLLED STEELS USING QUANTITATIVE METALLOGRAPHIC TECHNIQUES

As suggested by DeHoff [16] rolling operation yields a structure, deformed in a plane perpendicular to the direction of the applied force. Because of such kind of deformation the structure gets partially oriented along the rolling direction, as well as along the rolling plane. In literature, following metallographic parameters have been shown to adequately characterize this type of structure:

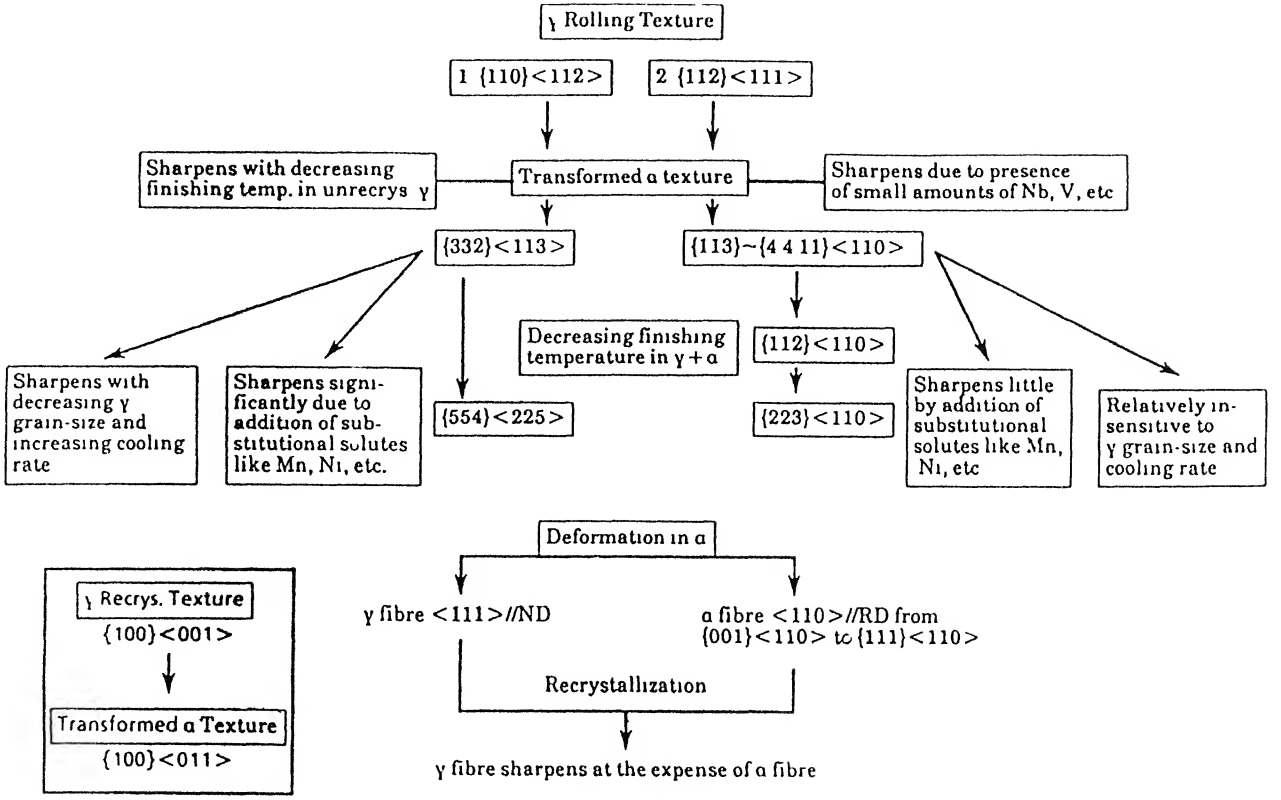

Figure 2.7: Schematic diagram showing effect of compositional and processing variables on the two major components of transformation texture in steels [2].

(i) grain shape parameter,

(ii) degree of orientation, and

(iii) rose-of-the-number-of-intersections.

2.2.1. Grain shape parameter

In the above mentioned state of microstructure, the shape of the grains has been approximated, by DeHoff [16], by triaxial ellipsoids (Fig.2.8), with their three axes aligned in the three orthogonal directions, RD, TD and ND. Assuming constant shape throughout the structure, he suggested that the shape of the grains can be uniquely determined by specifying any two of the three axial ratios,

$$g_{12} = \frac{d_1}{d_2} \qquad \ldots(2.2)$$

$$g_{13} = \frac{d_1}{d_3} \qquad \ldots(2.3)$$

$$g_{23} = \frac{d_2}{d_3} \qquad \ldots(2.4)$$

where d_1, d_2 and d_3 are the dimensions in the three orthogonal directions shown in Fig.2.9. These ratios have been shown, by DeHoff, to be equivalent to the ratios of the number of grains per unit area, N_{A1}; e.g if N_{A1} is the number of grains per unit area observed on the plane perpendicular to axis 1 and, N_{A2} and N_{A3} are similarly defined, then the ratios are defined as,

$$g_{12} = \frac{N_{A1}}{N_{A2}} \qquad \ldots(2.5)$$

$$g_{13} = \frac{N_{A1}}{N_{A3}} \qquad \ldots(2.6)$$

$$g_{23} = \frac{N_{A2}}{N_{A3}} \qquad \ldots(2.7)$$

2.2.2 Degree of orientation

Gleyn had studied the deformation of mild steel quantitatively, by measuring the length and width of the ferrite grains. Later on many more methods were devised to determine the extent of orientation of the structure. Underwood[17] has defined the degree of orientation, w', of a partially oriented system of lines as the ratio of the length of the oriented portions to the total length , i.e.,

$$w' = \frac{100(L_A)_{or}}{(L_A)_{or}+(L_A)_{is}} \text{ percent} \qquad \ldots(2.8)$$

where $(L_A)_{or}$= specific length of oriented portion of lines mm/mm^2 and $(L_A)_{is}$= specific length of isometric portion of lines mm/mm^2.

The method most popularly used for determining w' has been proposed by Saltykov. Various systems of surfaces have been classified by him into four types namely, isometric, linear, planar and linear-planar (Fig.2.8). The corresponding formulae for degrees of orientation, for each case, have been given in Table 2.1. In all the cases, the basic equation used is,

$$w'_{or} = \frac{100(S_V)_{or}}{S_V} \text{ percent} \qquad \ldots(2.9)$$

where "or" subscript refers to the particular oriented surface of interest i.e. linear, planar or linear-planar [17].

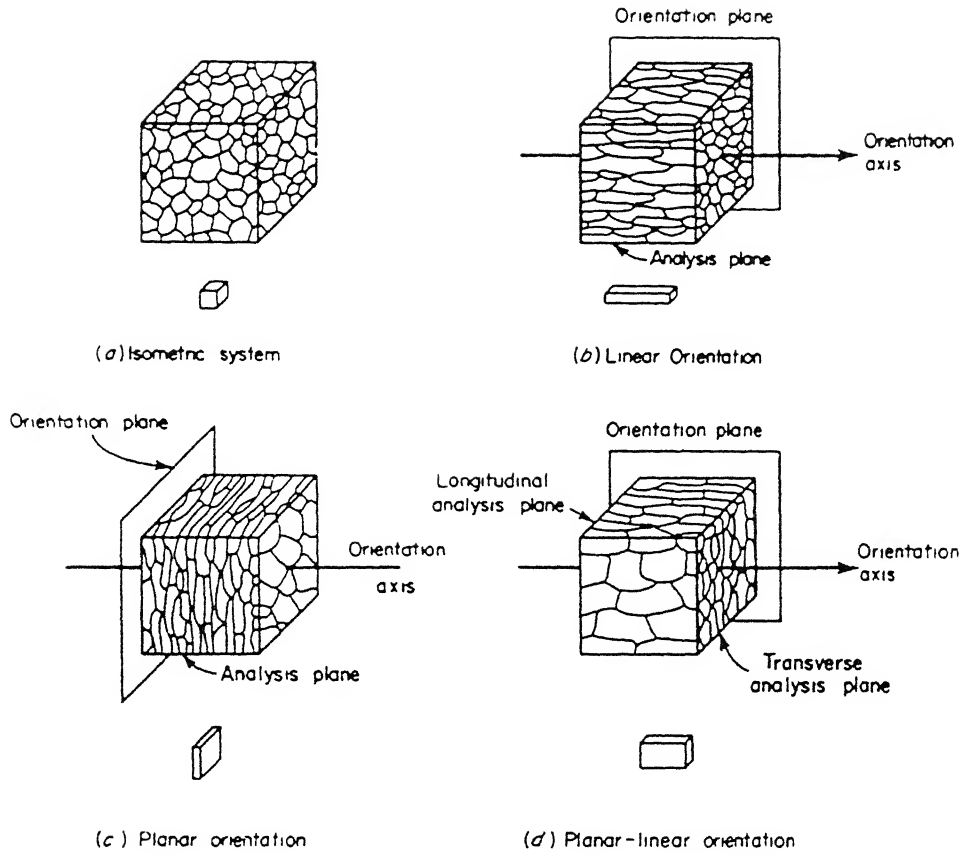

Figure 2.8: Classification of oriented boundary surfaces [17].

Table 2.1: Equations for surface areas and degree of orientation.

Type of orientation	Type of surface: Isometric $(S_V)_{Is}$	Linear $(S_V)_{IIa}$	Planar $(S_V)_{pl}$	Total surface S_V	Degree of orientation ω_{or}, %
Linear	$2(N_L)_{\parallel}$	$\frac{\pi}{2}[(N_L)_{\perp} - (N_L)_{\parallel}]$		$0.429(N_L)_{\parallel} + 1.571(N_L)_{\perp}$	$\omega_{IIa} = \frac{100[(N_L)_{\perp} - (N_L)_{\parallel}]}{0.273(N_L)_{\parallel} + (N_L)_{|}}$
Planar	$2(N_L)_{\parallel}$		$(N_L)_{\perp} - (N_L)_{\parallel}$	$(N_L)_{\perp} + (N_L)_{\parallel}$	$\omega_{pl} = \frac{100[(N_L)_{\perp} - (N_L)_{\parallel}]}{(N_L)_{|} + (N_L)_{\parallel}}$
Planar-linear	$2(N_L)_{\parallel}$*	$\frac{\pi}{2}[(N_L)_{\perp} - (N_L)_{\parallel}]$†	$(N_L)_{\perp} - (N_L)_{|}$‡	$0.429(N_L)_{\parallel} + 2.571(N_L)_{\perp} - (N_L)_{|}$	$\omega'_{IIa} = \frac{157.1[(N_L)_{\perp} - (N_L)_{\parallel}]}{0.429(N_L)_{\parallel} + 2.571(N_L)_{\perp} - (N_L)_{|}}$¶
					$\omega'_{pl} = \frac{100[(N_L)_{\perp} - (N_L)_{|}]}{0.429(N_L)_{\parallel} + 2.571(N_L)_{\perp} - (N_L)_{|}}$
					$\omega'_{IIa/pl} = \frac{100[2.571(N_L)_{\perp} - 1.571(N_L)_{\parallel} - (N_L)_{|}}{0.429(N_L)_{\parallel} + 2.571(N_L)_{\perp} - (N_L)_{|}}$

* The subscript $_{\parallel}$ here refers to secants drawn parallel to the orientation plane on the longitudinal analysis plane
† The subscript $_{\perp}$ here refers to secants drawn perpendicular to the orientation plane on the transverse analysis plane
‡ The subscript $_{|}$ here refers to secants drawn parallel to the orientation plane on the transverse analysis plane
¶ The primes in Ω'_{IIa}, Ω'_{pl}, and $\Omega'_{IIa/pl}$ specify the planar-linear system of surfaces.

2.2.3 Rose-of-the-number-of-intersections

These polar graphs were first plotted by Saltykov to give the flavour of the state of isometricity of the structure. These plots were obtained by drawing test secants on the micrographs, in all the directions and then plotting the number of intersections per unit length $N_L(\theta)$ against the angle, θ, between the considered orientation axis and the secant, on a polar graph paper.

It has been found [17] that for an isometric system of lines on a plane, the rose-of-the-number-of-intersections is the circumference of a circle, with its centre at the origin of the polar co-ordinates. But the shape of the curve changes with the presence of preferential orientation in the system. For a completely oriented system, the rose-of-the-number-of- intersections becomes circular, with the circle touching the origin of the co-ordinates. The curve, however, has a different shape in case of a partially oriented system (like the one obtained by controlled rolling).

For a partially oriented system, the shape of the rose-of-the-number-of-intersections can be approximated by that depicted in Fig.2.9 . An analytical method has also been proposed by Underwood, for the construction of the rose, for calculating the value of $N_L(\theta)$:

$$N_L(\theta) = \sin\theta (L_A)_{or} + \frac{2}{\Pi} (L_A)_{is} \qquad \ldots(2.10)$$

But this method requires the knowledge of the lengths of the oriented and isometric portions of lines in the system. Thus the graphical method is more popular.

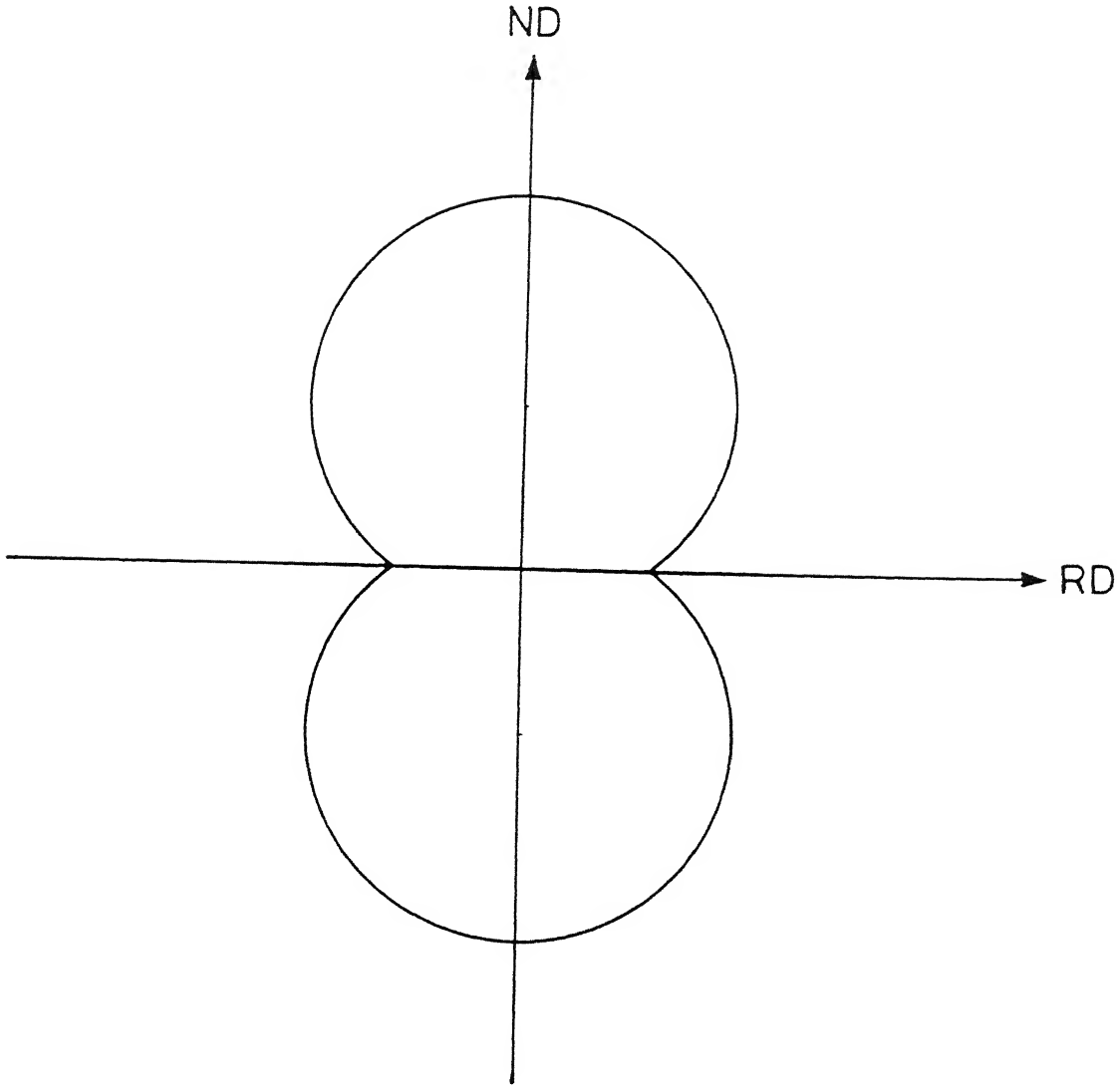

Figure 2.9: Shape of the rose-of-the-number-of-intersections for a partially oriented system (schematic) [17].

2.3. CORRELATION BETWEEN MICROSTRUCTURE AND TEXTURE

Although it is generally believed that there should be a correlation between the nature and sharpness of the crystallographic texture of a material and its microstructure, there has hardly been any attempt so far to bring out this correlation. Ray et al [15] have indicated a probable correlation between the microstructure and texture of plain C and Nb-microalloyed steels, but this study has been made in a qualitative manner. Hence an attempt is made in this investigation to make this correlation quantitative and more meaningful. In case a successful correlation is possible then in certain simple systems at least, an idea about the complicated texture data may be more easily obtained from a proper study of the microstructural aspects.

CHAPTER III

EXPERIMENTAL TECHNIQUES

As stated earlier in Chapter I, a plain C and a Nb-microalloyed steel have been selected for study. The composition of the two steels are given in Table 3.1. These steels were supplied in the form of transfer bars, out of which ingots (about 180 X 120 X 50 mm) were cut and subjected to controlled rolling. After that textural and microstructural studies were made on the controlled rolled samples.

3.1 CONTROLLED ROLLING

Five pieces each of the plain C and Nb-microalloyed steels were first soaked for two hours at 1250°C in an electric muffle furnace. Then controlled rolling was carried out upto 90% reduction in an instrumental reversing mill. The rolling was initiated in each case at1200°C,but finishing was done at five different temperatures viz., 1020°C (in the $\gamma_{recryst.}$ range), 870°C (in the $\gamma_{nonrecryst.}$ range), 770°C (in the upper $\gamma+\alpha$ range), 730°C(in the lower $\gamma+\alpha$ range) and 630°C (in the lower α range). These ten controlled rolled steels thus obtained, constitute the first set of samples.

Another set of samples was obtained by taking five pieces each of the two steels again and subjecting them to controlled rolling upto 75% reduction. The austenitizing temperature and the finish rolling temperatures were same as above.

A third set of samples was obtained by lowering

Table 3.1: Compositions of the two steels considered for study (wt%)

Steel	C	Mn	P	S	Si	Cu	Ni	Cr	Mo	V	Nb	ASA*	N
Plain C	0 20	1 24	0.011	0 004	0 185	0 012	0.013	0.030	0.006	0.004	0 002	0 044	0 0065
Nb microalloyed	0 18	1.35	0 005	0 008	0 244	0 014	0 009	0 018	0 002	0 003	0 034	0 048	0 0074

* Acid soluble aluminum

the austenitizing temperature to 1150°C. The two steels were soaked at 1150°C for two hours and then controlled rolled upto 90% reduction. In this case also, five different rolling schedules were carried out on the two steels, involving finishing at 1020°C, 870°C, 770°C, 730°C and 630°C.

The whole controlled rolling process was carried out at the CANMET Laboratories, Ottawa, Canada.

3.2 TEXTURAL STUDIES

The controlled rolled samples were subjected to texture measurement at the mid-thickness sections. Crystallographic textures of these samples were measured on an automatic texture goniometer, in the form of {200} pole figures. These measurements were carried out at the Department of Metallurgical Engineering, McGill University, Montreal, Canada.

The {200} pole figures of the thirty samples were analysed, to find out the predominant texture components. The corresponding texture intensities were also recorded from the pole figures.

3.3 MICROSTRUCTURAL STUDIES

3.3.1 Qualitative metallography

Three sections of the controlled rolled samples viz., the rolling plane section, the longitudinal section and the transverse section were prepared for optical metallography by using standard metallographic techniques. These were then etched using 5% Nital and observed under a metallograph.Using the

metallograph, photomicrographs of the three sections of all the thirty samples were taken (at 500 X).

The micrographs of all the three sections of each sample were, then cut into proper shapes and put together to give three dimensional views of the microstructures.

3.3.2 Quantitative metallography

A detailed measurement of the following metallographic parameters was done using the photomicrographs of the three sections of the steel samples considered.

(i) Grain shape parameter,

(ii) Degree of orientation,

(iii) Grain thickness along ND, and

(iv) Rose-of-the-number-of-intersections.

3.3.2.1 Grain shape parameter

As an attempt to find out the approximate shapes of the grains in the various steel samples considered, the following method was employed.

It was observed that on all the three section of each sample, the shape and size of the grains varied to some extent. Thus for simplicity, the grains representing the average shape and size, on each micrograph, were selected and measurements were done upon them. The dimensions of these grains along RD, TD and ND, namely d_1, d_2 and d_3 respectively, were measured by drawing tangents to the selected grains in directions perpendicular to the respective directions. An average of three

measurements was recorded as the value against each of the three dimensions mentioned above. The grain shape was then approximated by using eqn.2.1 to eqn.2.3.

3.3.2.2 Determination of degree of orientation

The linear, planar and overall(linear-planar) degrees of orientation were evaluated by using the following method. Two sections namely, the longitudinal section and the transverse section of all the samples were selected for study. Ten lines parallel to the RD were drawn on the longitudinal section of each sample and the corresponding values of N_L i.e. the number of intersections per unit length were counted. The mean of the ten values of N_L was recorded as the $(N_L)_{\parallel}$ value for every sample {where $(N_L)_{\parallel}$ is defined as the value of N_L counted on the lines parallel to RD [17]}. Similarly the values of $(N_L)_{\perp}$ and $(N_L)_{|}$ were recorded, where the former stands for N_L counted on lines parallel to the ND and the latter stands for that counted on lines parallel to TD.

After this, the linear, planar and the overall degrees of orientation were calculated for each sample by using the following formulae (already mentioned in section 2.2.2).

$$w'_{lin} = \frac{157.1[(N_L)_{\perp}-(N_L)_{\parallel}]}{0.429(N_L)_{\parallel}+2.571(N_L)_{\perp}-(N_L)_{|}} \qquad \ldots(3.1)$$

$$w'_{pl} = \frac{100[(N_L)_{\perp}-(N_L)_{|}]}{0.429(N_L)_{\parallel}+2.571(N_L)_{\perp}-(N_L)_{|}} \qquad \ldots(3.2)$$

$$w'_{lin/pl} = \frac{100[2.571(N_L)_{\perp} - 1.571(N_L)_{\parallel} - (N_L)_{I}]}{0.429(N_L)_{\parallel} + 2.571(N_L)_{\perp} - (N_L)_{I}} \quad \ldots(3.3)$$

3.3.2.3 Measurement of grain thickness along ND

The grain thickness of all the samples were measured by drawing lines on the longitudinal section, along the ND. The thickness was obtained by dividing the total length of the secant by the number of grains intersected by it. In case of the first set of samples a set of five secants was drawn on the longitudinal section of each sample and the mean of the five readings was recorded as the grain thickness in each case. However, in case of the latter two sets, a set of ten secants was drawn and the mean of the ten readings was recorded as the grain thickness.

3.3.2.4 Plotting of the rose-of-the-number-of-intersections

The rose-of-the-number-of-intersections is a polar plot of N_L, i.e. the number of intersections per unit length, as a function of some angle θ, where θ is the angle between the orientation axis and the secant. For plotting this, the data were recorded by drawing secants on the longitudinal section of each sample at angular intervals of 30°, from 0° to 180°. These data were then plotted on polar graph papers, with the N_L values plotted as the corresponding radius vectors. The ends of the radius vectors were then connected by a smooth curve.

CHAPTER IV

RESULTS

4.1 OPTICAL MICROSTRUCTURES

The optical micrographs taken from the rolling plane, the longitudinal as well as the transverse sections of each controlled rolled sample have been put together to give a three dimensional view. These are all shown in Fig 4.1 to Fig. 4.8. All these microstructures reveal that their major constituent phase is α-ferrite. In addition, there is pearlite present in the form of a minor constituent. In general, the structural features appear rather elongated in the longitudinal and transverse sections whereas they look more equiaxed in the rolling plane section. Fig 4.1 and Fig. 4.2 represent the microstructures of the as received plain C and Nb-microalloyed steels, respectively. The average ferrite grain size is much larger in the plain C steel than in the Nb-microalloyed steel.

rolled steels have been shown in Fig.4.3 to Fig.4.8. The total number of samples have been catagorized into three sets, of ten samples each. The first set corresponds to plain C and Nb-microalloyed steels austenitized at 1250°C (90% reduction), the second set is made up of the two steels, austenitized at the same temperature but controlled rolled upto 75% reduction and the third set corresponds those austenitized at 1150°C (90% reduction).

Figure 4.1: Three dimensional microstructural view of as received plain C steel.

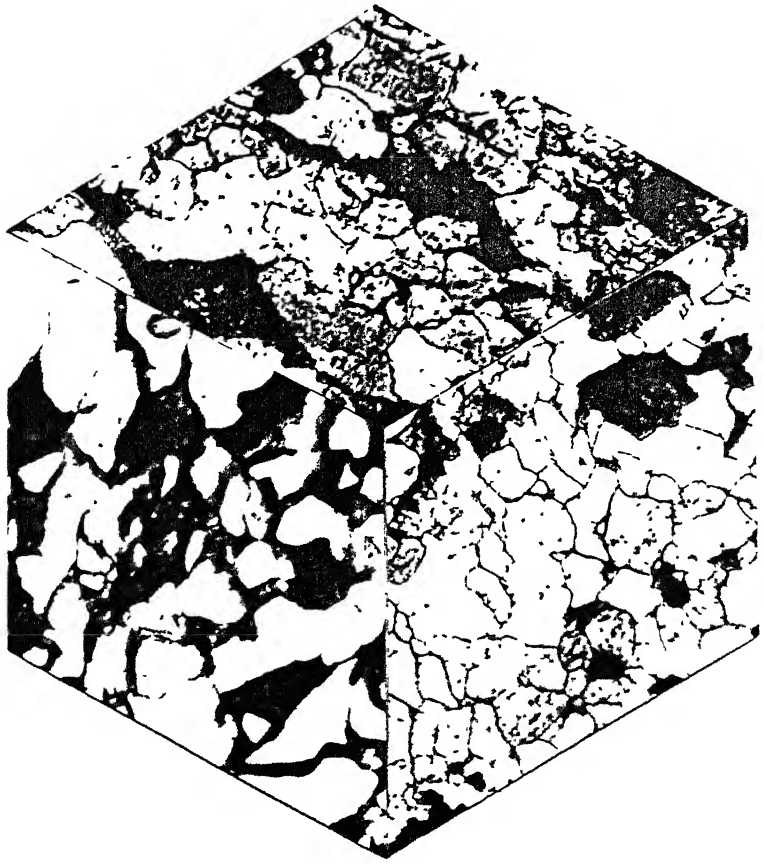

Figure 4.2: Three dimensional microstructural view of as received Nb-microalloyed steel.

4.1.1 Plain C and Nb-microalloyed steels austenitized at 1250°C (90% reduction)

The microstructures of the controlled rolled plain C steels are given in Fig.4.3. It is evident from these figures that the grains become more refined as well as more and more pancaked as the finish rolling temperature is decreased from 1020°C to 630°C. In the plain C steel, finish rolled at 1020°C and 870°C, the ferrite grains appear rather equiaxed in the rolling plane, the longitudinal as well as the transverse sections. In case of the steel finish rolled in the intercritical range, some of the microstructural features appear elongated (especially in the longitudinal and transverse sections), but some are equiaxed as before. In case of the steel finish rolled at 630°C (lower ferritic region), all the grains appear highly elongated in the longitudinal and transverse sections.

The microstructures of the controlled rolled Nb-microalloyed steel are presented in Fig.4.4. Although the structural features of Nb-steel, finish rolled at 1020°C, appear quite similar to the corresponding plain C steel sample, finish rolling at 870°C causes the microstructural features to assume a rather elongated shape in the Nb-steel as compared to the plain C steel. The evolution of the microstructure with the lowering of the finish rolling temperature seems to be rather similar in both the plain C and the Nb-microalloyed steel. The only noticeable difference is that the microstructure is finer in case of the Nb-steel as compared to the plain C steel, at comparable reductions.

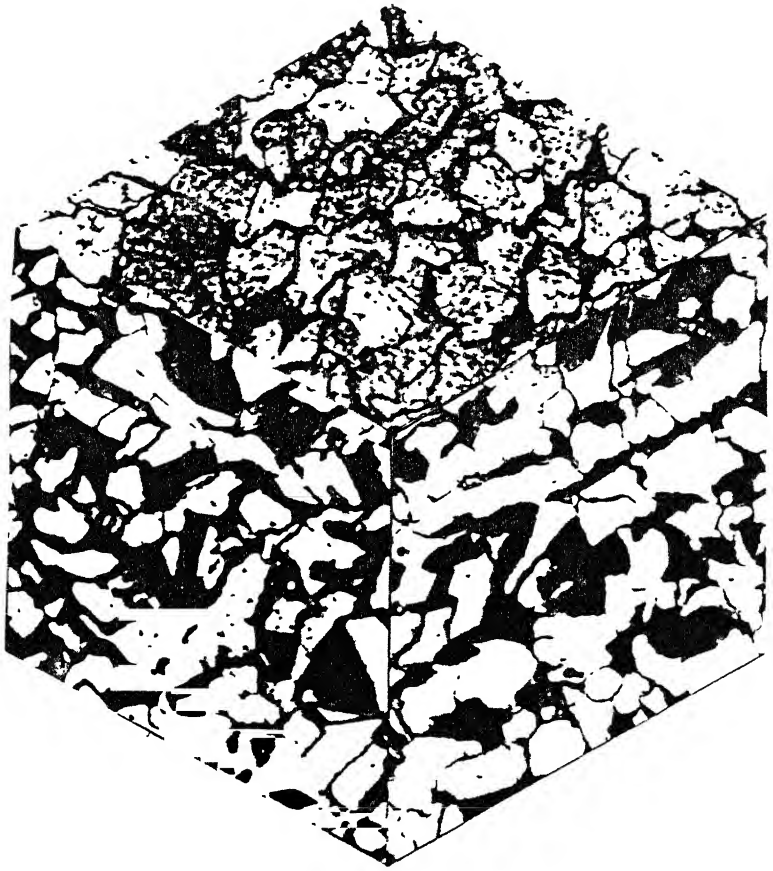

(a)

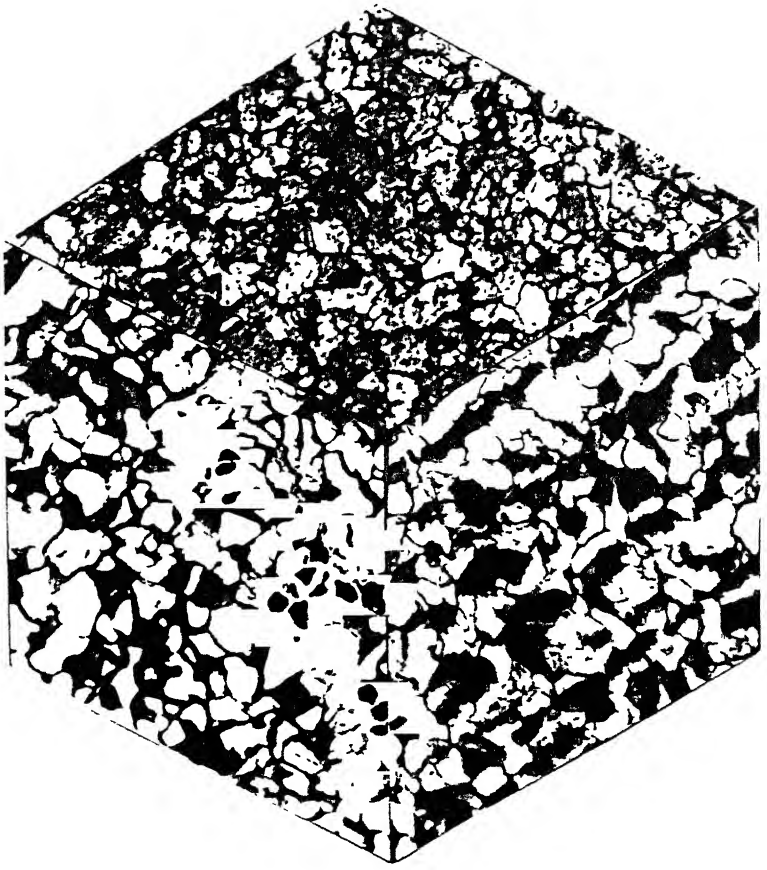

(b)

contd

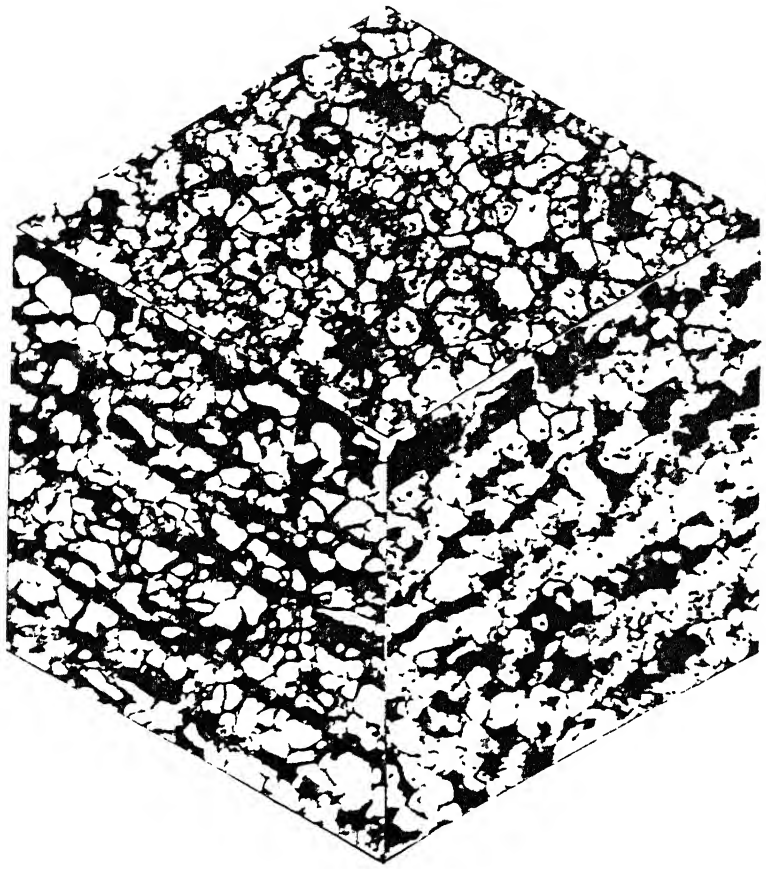

(c)

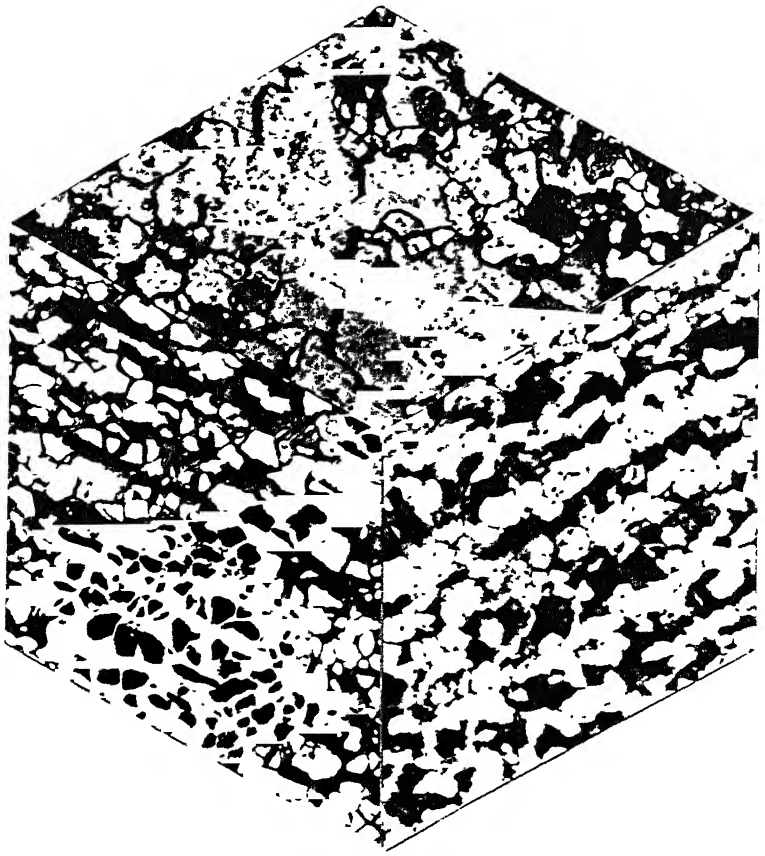

(d)

contd..

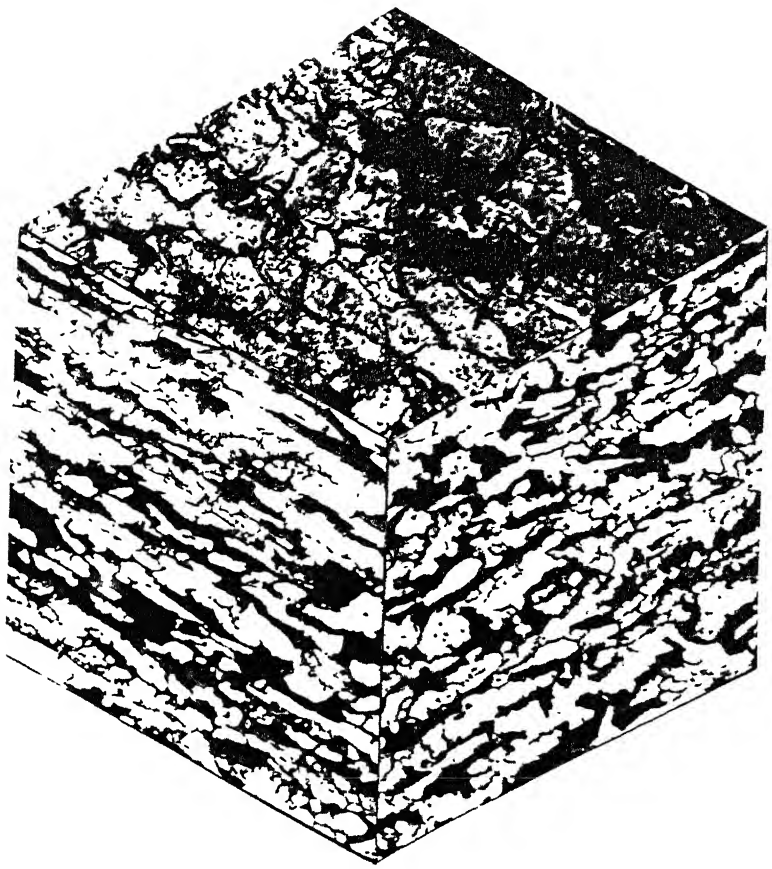

(e)

Figure 4.3: Microstructures of plain C steel finish rolled at five different temperatures, (a)1020°C, (b)870°C, (c)770°C, (d)730°C, and (e)630°C (austenitizing temperature 1250°C, 90% reduction).

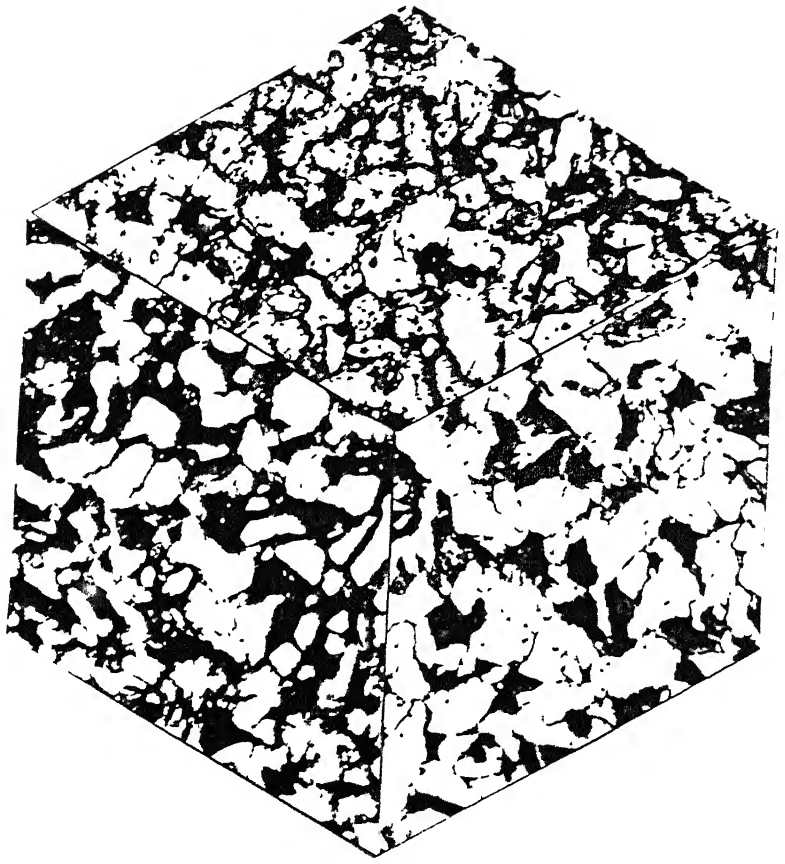

(a)

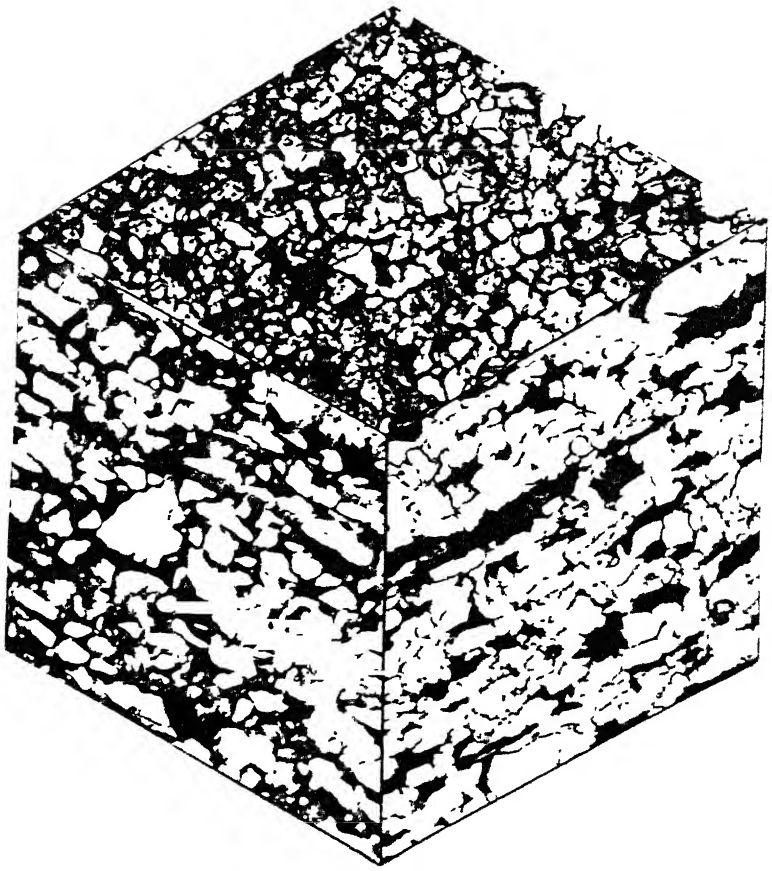

(b)

contd.

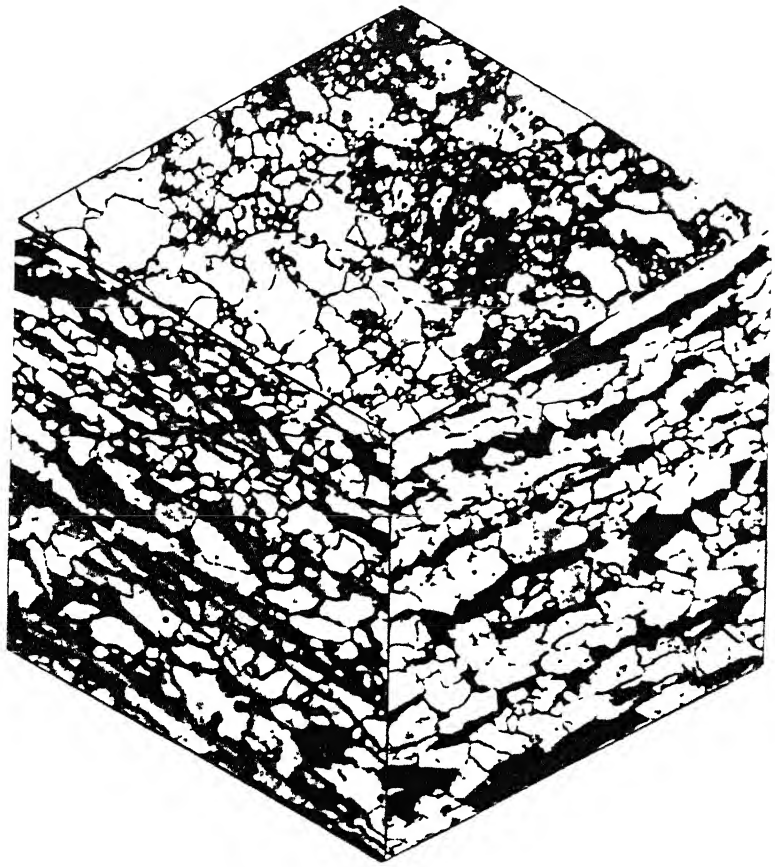

(c)

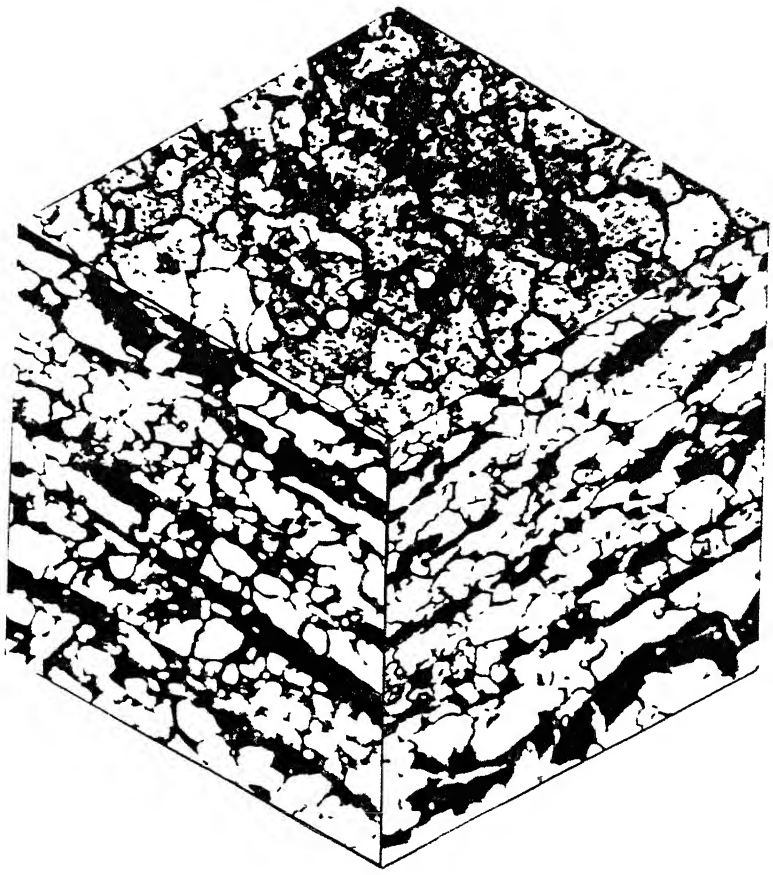

(d)

contd.

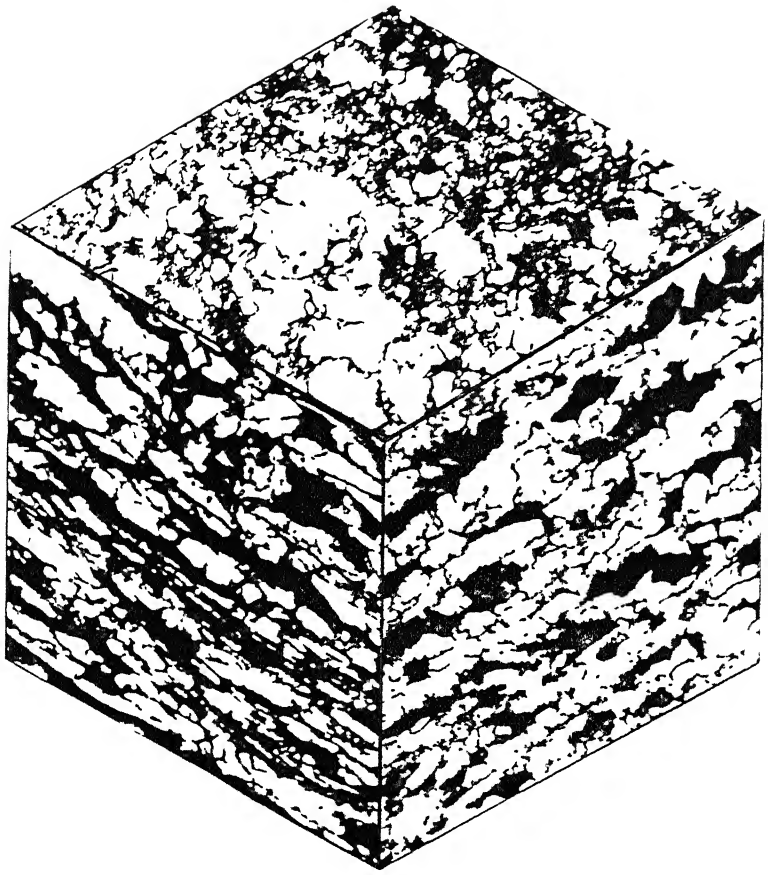

(e)

Figure 4.4: Microstructures of Nb-microalloyed steel finish rolled at five different temperatures, (a)1020°C, (b)870°C, (c)770°C, (d)730°C, and (e)630°C (austenitizing temperature 1250°C, 90% reduction).

4.1.2. Steels austenitized at 1250°C (75% reduction)

The relevant microstructures are shown in Fig 4.5 and Fig.4.6. Here, for both the steels, we observe a similar trend of grain refinement with decreasing finish rolling temperature, from 1020°C to 630°C. Equiaxed grains are obtained in the rolling plane sections as well as the other sections in case of almost all the finish rolling temperatures, for both the steels. Some elongation of the microstructural features are visible, in the longitudinal and transverse sections for both the steels, when the finishing temperature is lowered down to the intercritical and ferritic regions.

4.1.3 Steels austenitized at 1150°C (90% reduction)

The microstructural features of the samples in this set (Fig.4.7 and Fig.4.8) are similar to those of the first set. The only difference is that here the structure is somewhat finer as compared to the structures of the samples of the first set.

From the above it is quite clear that qualitatively not very significant difference is apparent between the microstructural features of the corresponding samples in the first and the third sets. The microstructures of the samples of the second set are, of course, little bit different from the other two. In order to quantify the microstructural features, so as to bring out the essential differences between the different steel samples, an attempt was made to measure a few parameters, quantitatively. The technique has been described in Chapter III

(a)

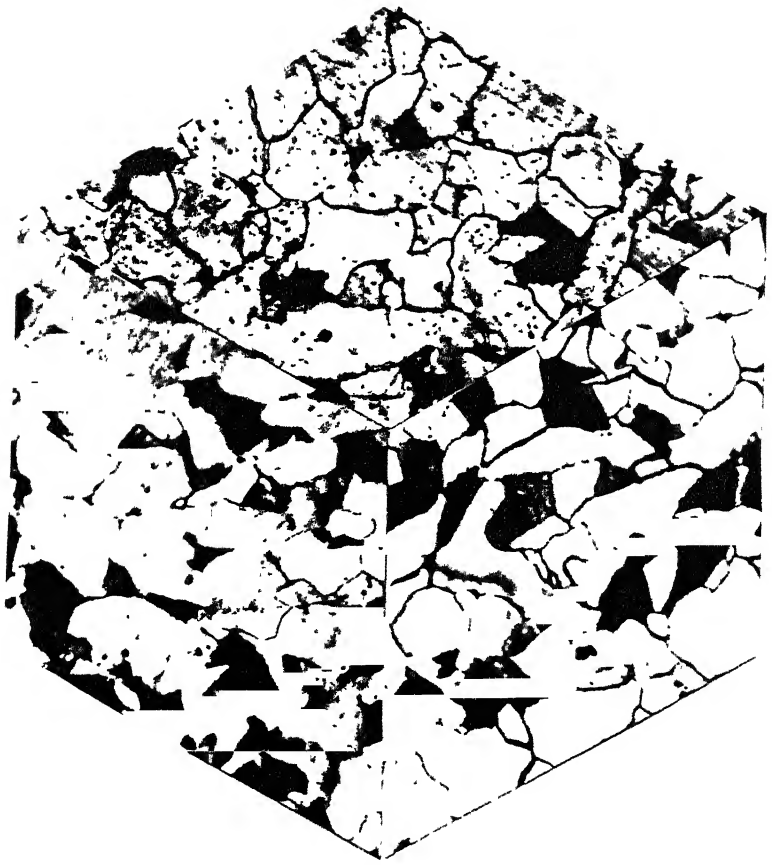

(b)

contd

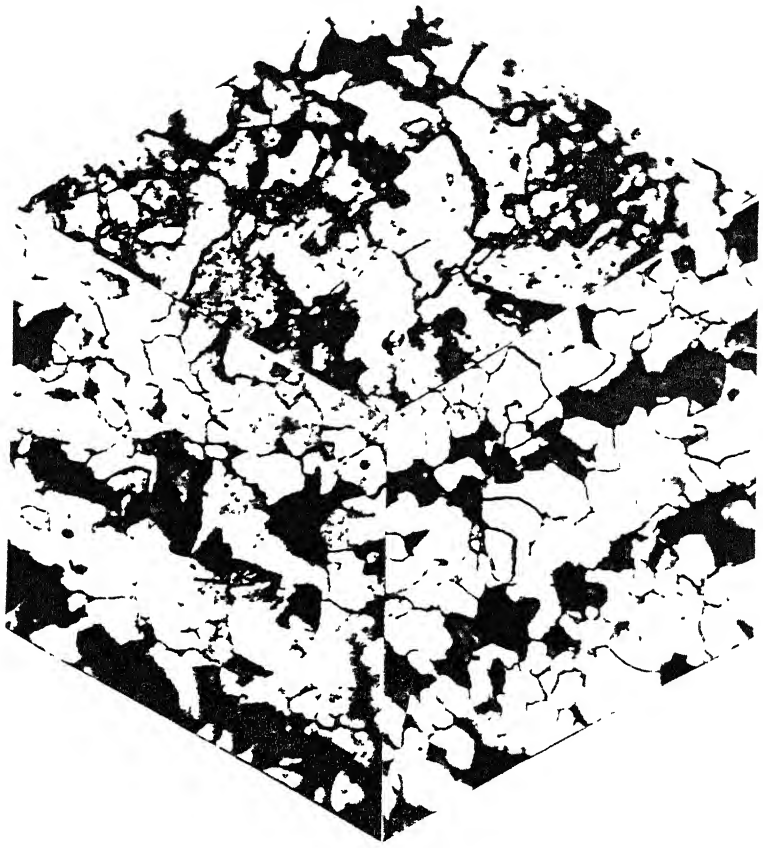

(c)

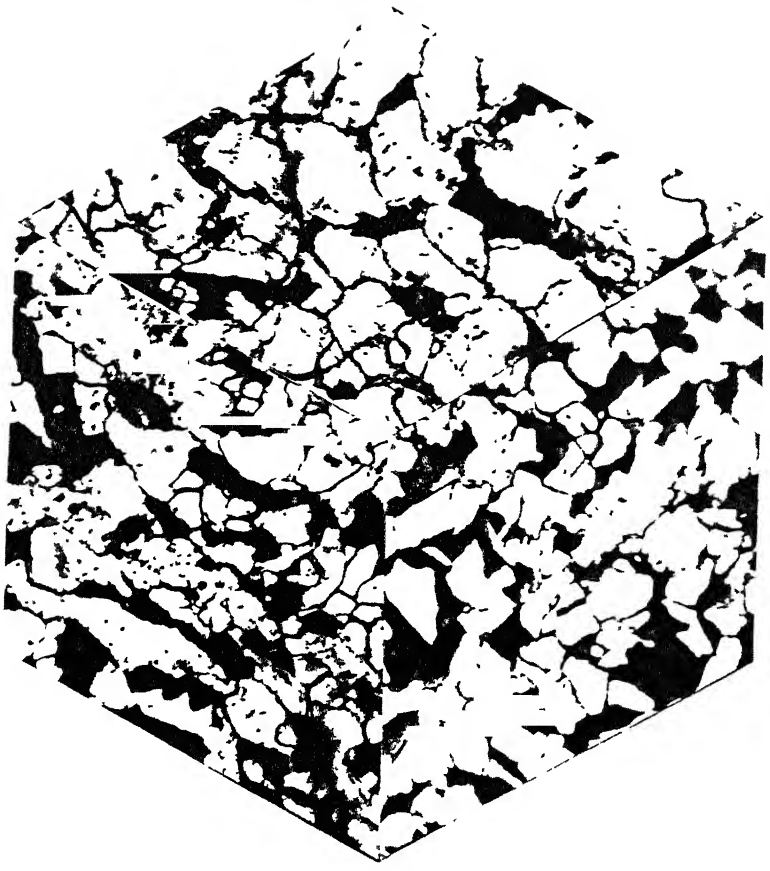

(d)

contd

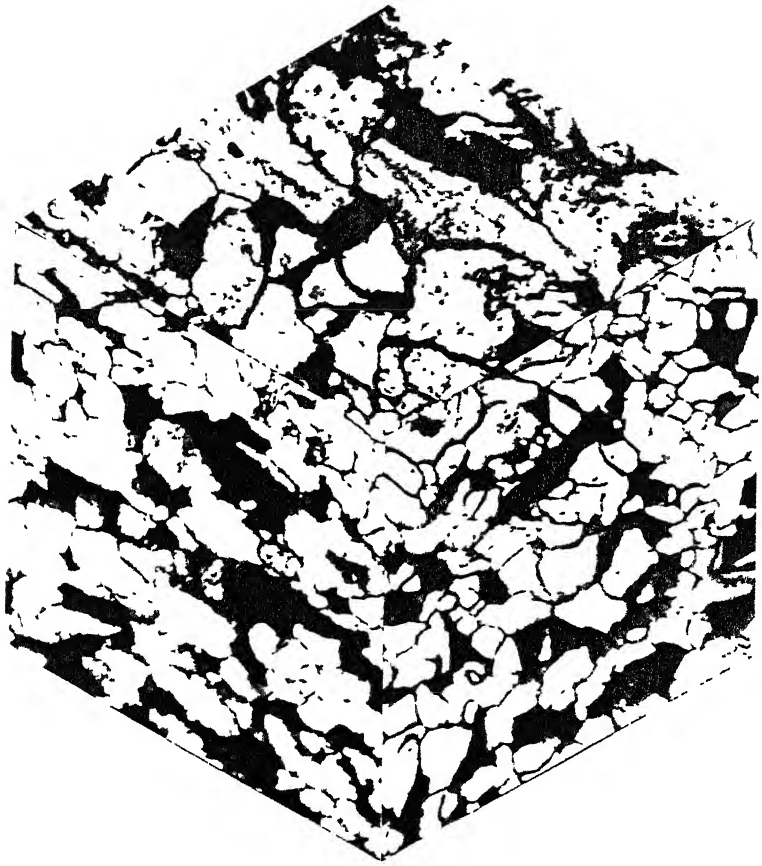

(e)

Figure 4.5: Microstructures of plain C steel finish rolled at five different temperatures, (a)1020°C, (b)870°C, (c)770°C, (d)730°C, and (e)630°C (austenitizing temperature 1250°C, 75% reduction).

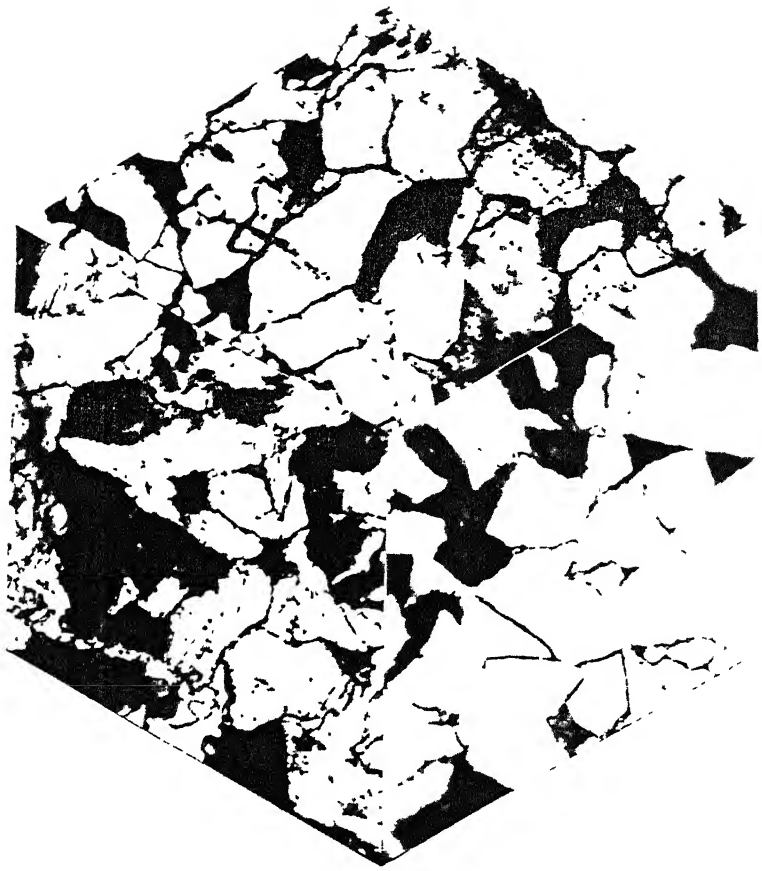

(a)

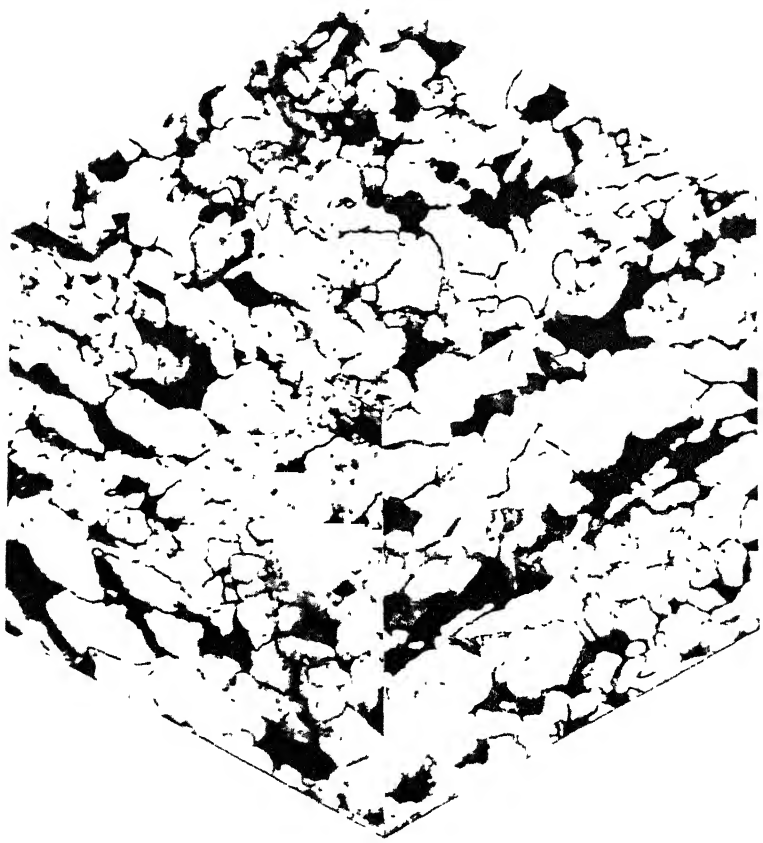

(b)

contd..

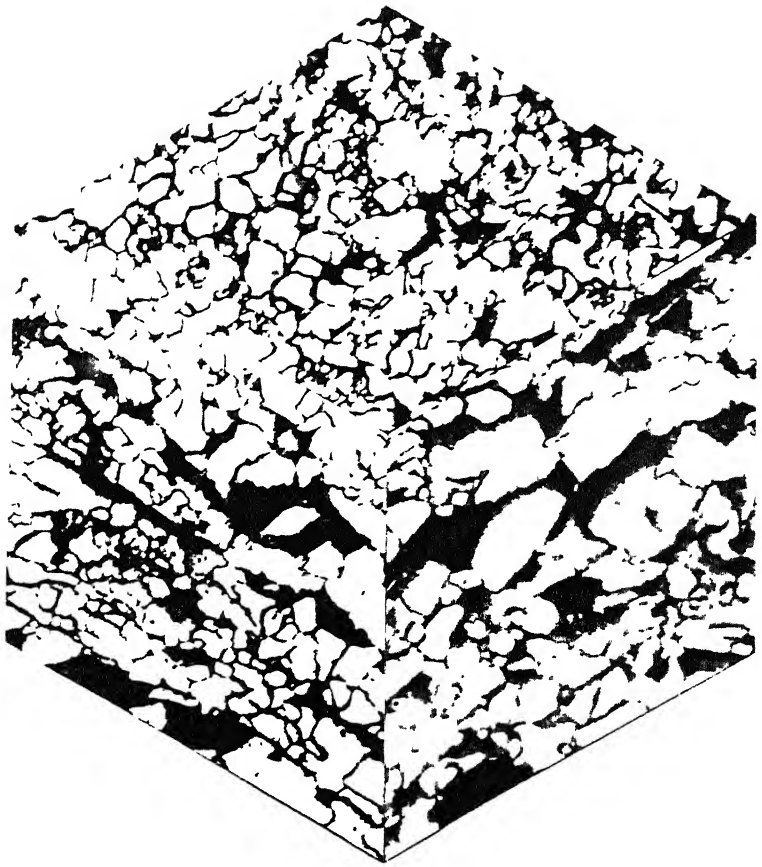

(c)

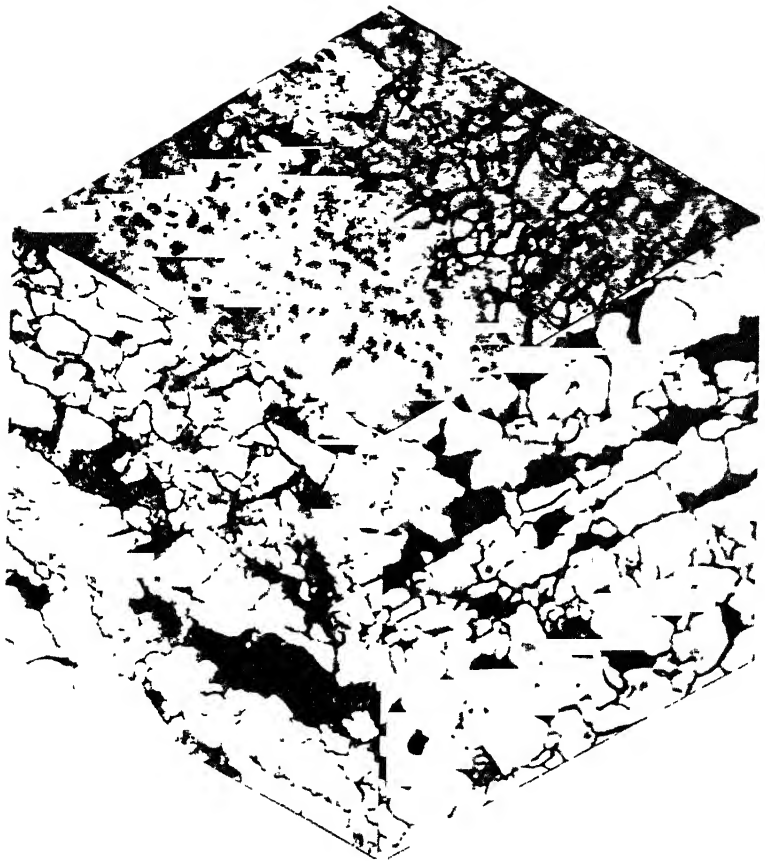

(d)

contd

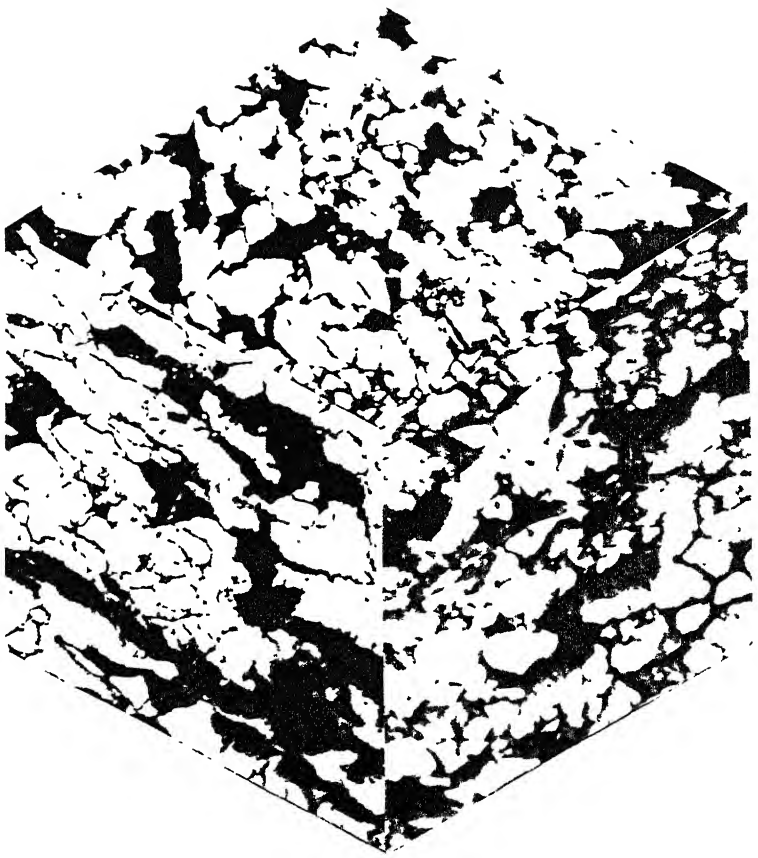

(e)

Figure 4.6: Microstructures of Nb-microalloyed steel finish rolled at five different temperatures, (a)1020°C, (b)870°C, (c)770°C, (d)730°C, and (e)630°C (austenitizing temperature 1250°C, 75% reduction).

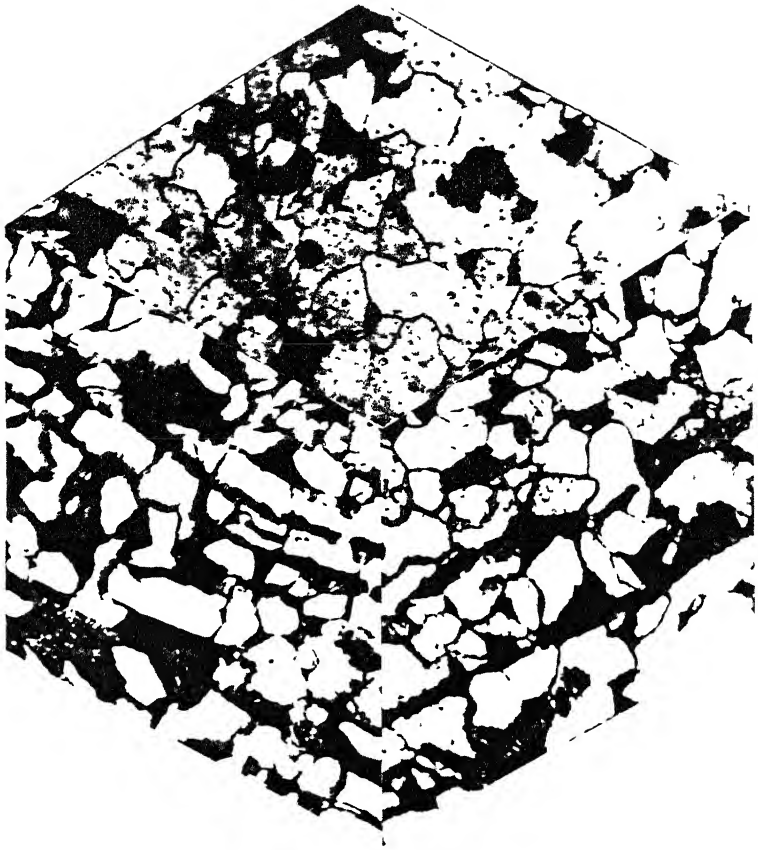

(a)

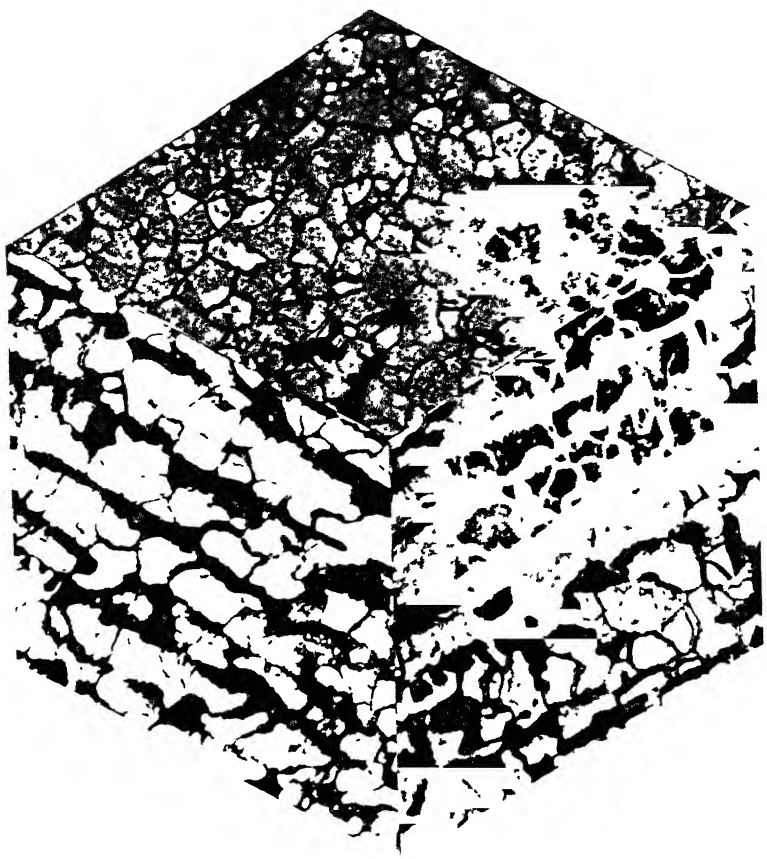

(b)

contd..

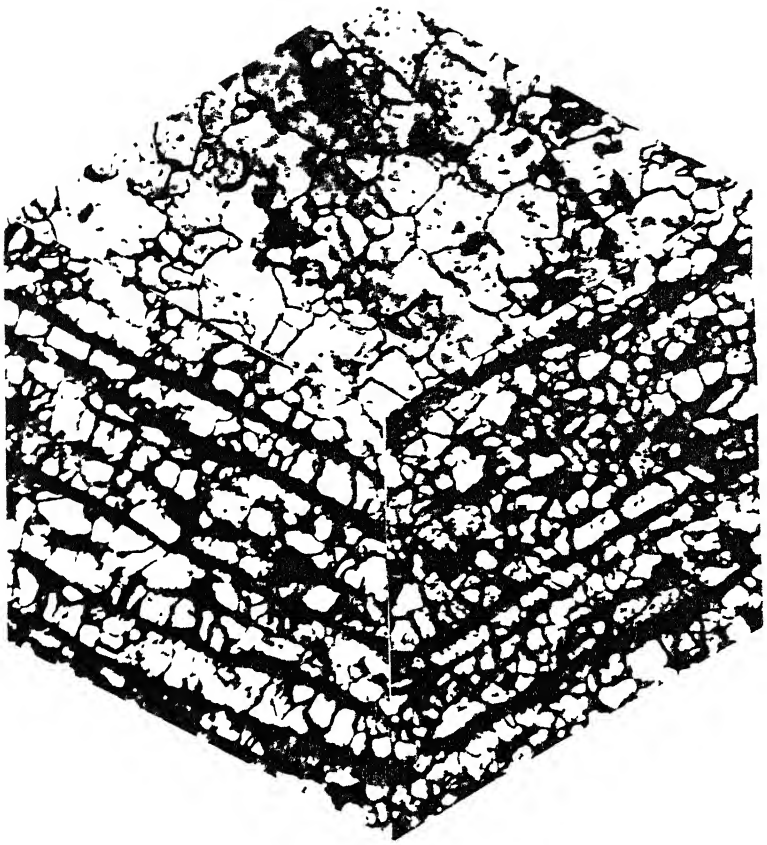

(c)

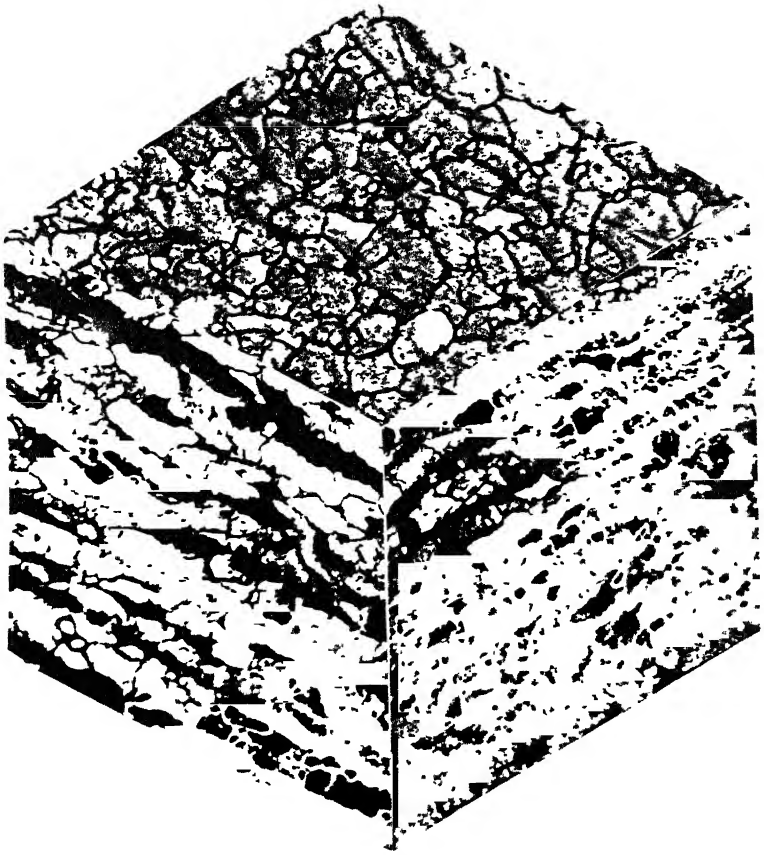

(d)

contd

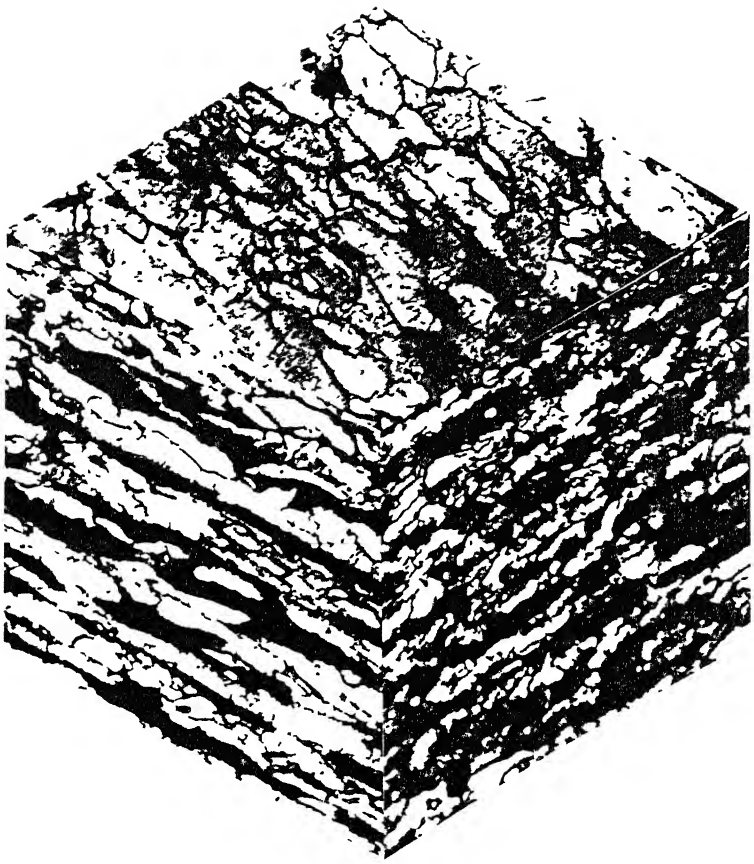

(e)

Figure 4.7: Microstructures of plain C steel finish rolled at five different temperatures, (a)1020°C, (b)870°C, (c)770°C, (d)730°C, and (e)630°C (austenitizing temperature 1150°C, 90% reduction).

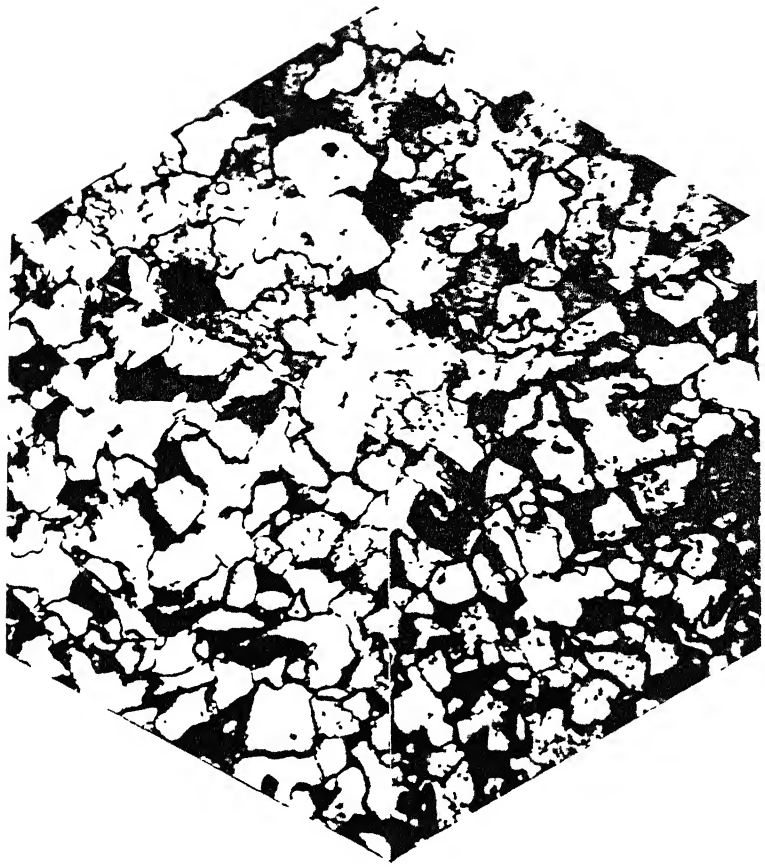

(a)

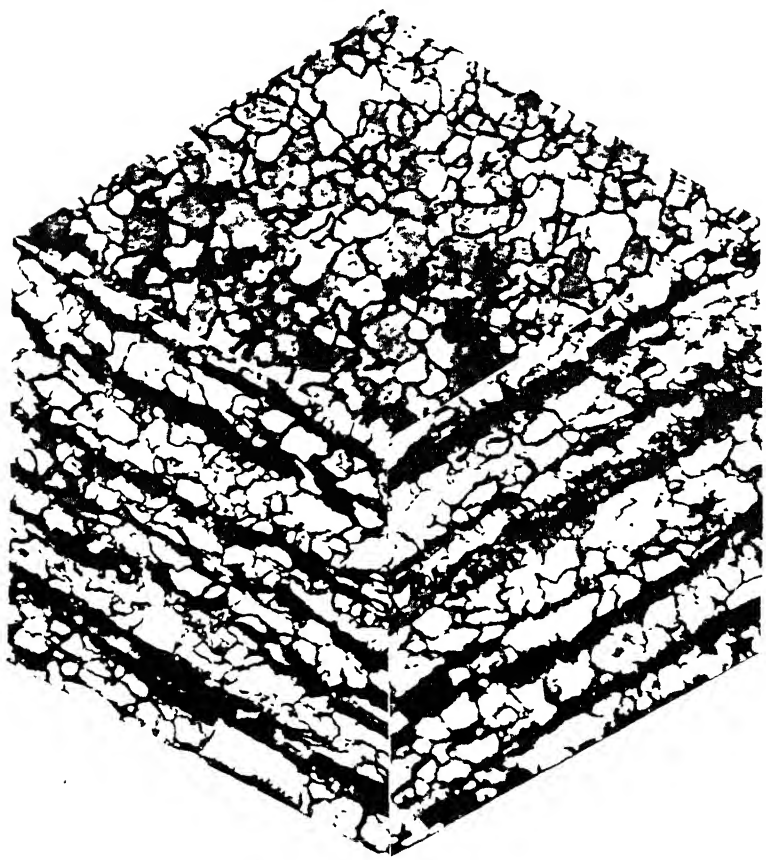

(b)

contd

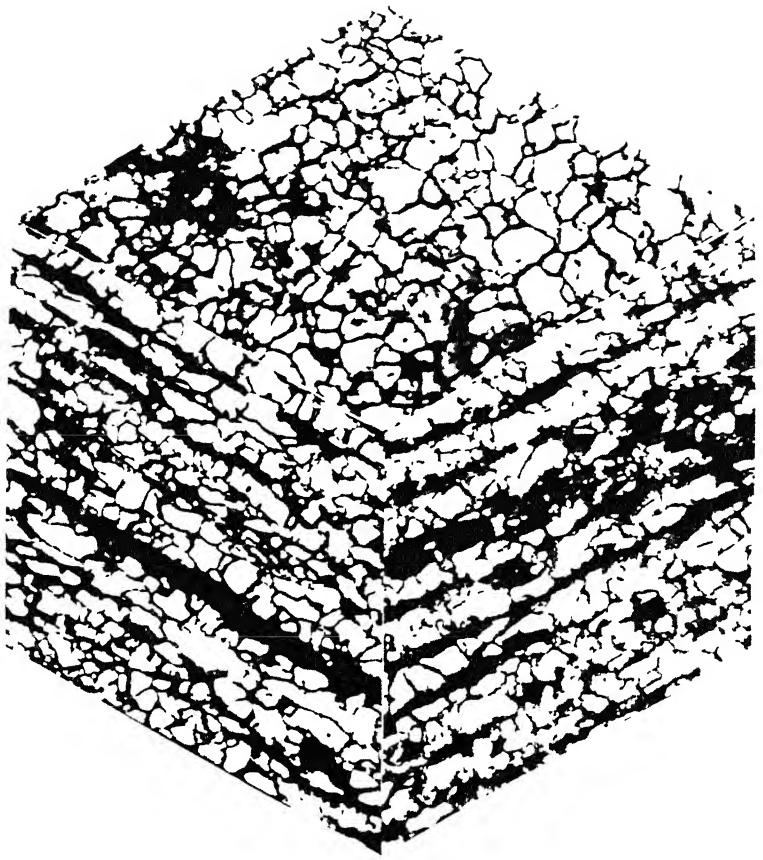

(c)

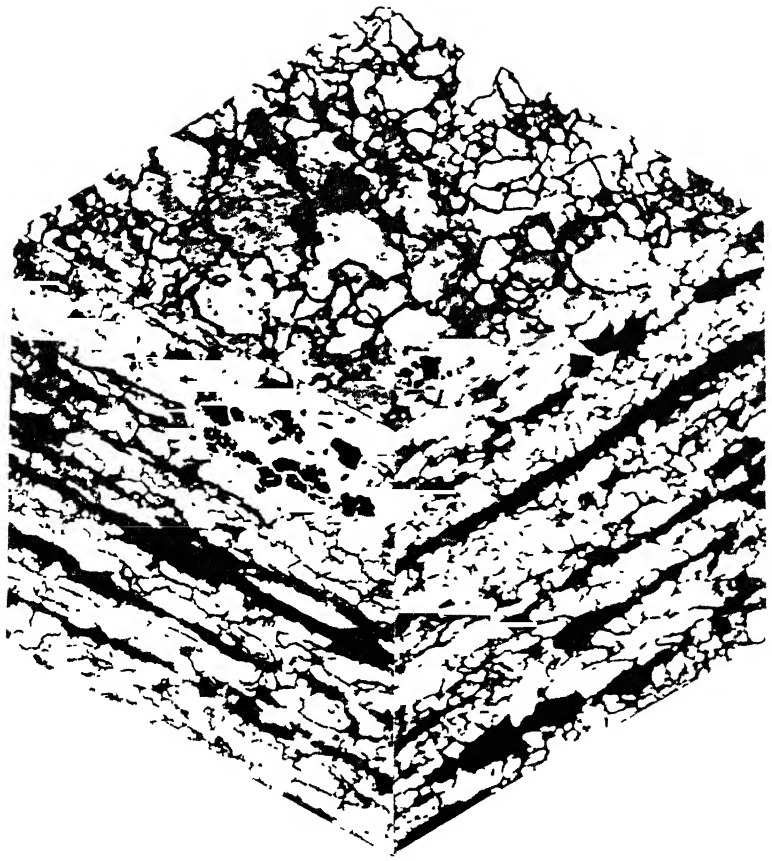

(d)

contd

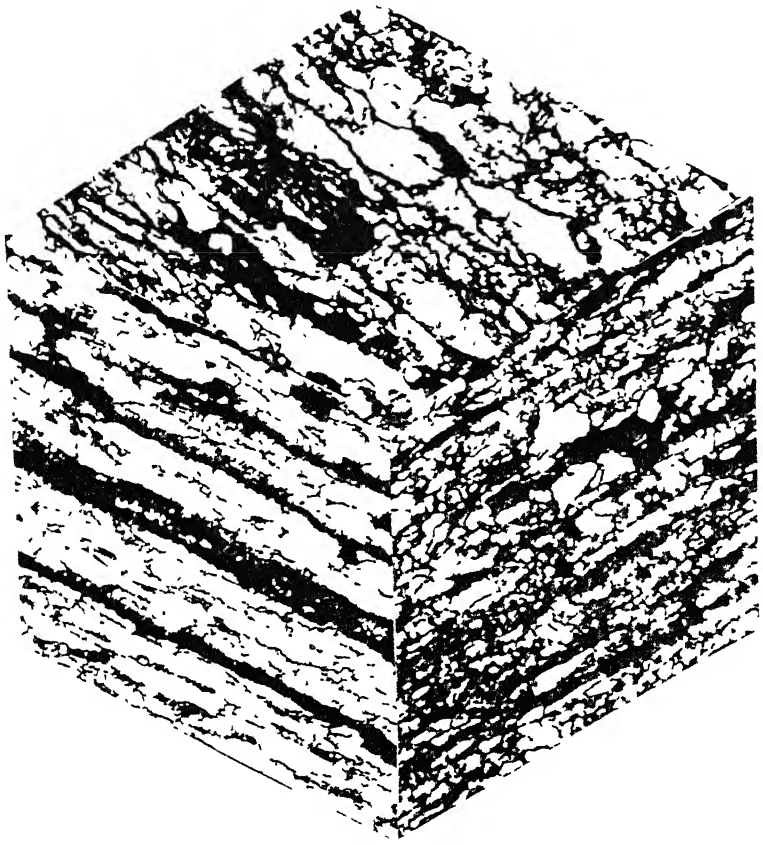

(e)

Figure 4.8: Microstructures of Nb-microalloyed steel finish rolled at five different temperatures, (a)1020°C, (b)870°C, (c)770°C, (d)730°C, and (e)630°C (austenitizing temperature 1150°C, 90% reduction).

and the results are depicted below.

4.2 MEASUREMENT OF VARIOUS MICROSTRUCTURAL PARAMETERS

The parameters studied to quantify the microstructural features of the thirty samples are,

(i) grain shape parameter,

(ii) degree of orientation,

(iii) grain thickness along ND and

(iv) rose-of-the-number-of-intersections.

The results of these measurements have been given in a tabular form in Table 4.1 to Table 4.3. These have also been depicted graphically in Fig.4.9 to Fig.4.23. The detailed data of the actual measurements and various calculations leading to the results shown in the above tables have been given in the Appendix.

4.2.1 Grain shape parameter

As evident from Table 4.1, the grain diameter ratios g_{12}, g_{23} and g_{13} follow a consistent trend of increasing value with decreasing finish rolling temperature in all the cases.

In case of set 1, the g_{12} and g_{23} values for the Nb-microalloyed steel are found to be somewhat higher than the corresponding values for the plain C steel. However, these values are nearly equal (excepting g_{23}) in both the steels for the lowest finishing temperature i.e 630°C. The g_{13} values also show a similar trend. Furthermore, the change in g_{13} values with

Table 4.1

Variation of grain shape parameter with finishing tempearture

SET 1

Steel	Finishing Temperature °C	g_{12}	g_{13}	g_{23}
Plain Carbon Steel	1020	0.72	0.69	0.96
	870	0.80	1.20	1.50
	770	0.92	1.37	1.50
	730	1.00	1.33	1.33
	630	1.45	5.33	3.36
Nb-micro-alloyed Steel	1020	0.88	0.93	1.07
	870	0.80	0.88	1.11
	770	1.23	1.78	1.44
	730	1.14	2.78	2.44
	630	1.42	5.67	4.00

SET 2

Steel	Finishing Temperature °C	g_{12}	g_{13}	g_{23}
Plain Carbon Steel	1020	1.10	1.05	0.95
	870	0.74	1.25	1.69
	770	1.17	1.68	1.44
	730	2.07	2.00	0.96
	630	2.43	3.78	1.55
Nb-micro-alloyed Steel	1020	1.00	1.40	1.40
	870	1.12	1.50	1.33
	770	1.14	1.50	1.30
	730	1.40	1.89	1.35
	630	1.81	3.03	1.68

SET 3

Steel	Finishing Temperature °C	g_{12}	g_{13}	g_{23}
Plain Carbon Steel	1020	1.30	1.50	1.15
	870	0.92	1.60	1.75
	770	1.30	3.20	2.50
	730	1.90	4.20	2.20
	630	2.54	6.20	2.40
Nb-micro-alloyed Steel	1020	1.20	1.30	1.06
	870	1.06	1.90	1.70
	770	1.00	2.06	2.06
	730	1.44	3.70	2.50
	630	2.30	8.60	3.70

finish rolling temperature has been found to be more drastic as compared to g_{12} and g_{23}. This is obvious from the fact that reduction in thickness of a steel billet is very large compared to increase in its length and breadth during the controlled rolling process.

The values of g_{12} and g_{23} for the samples belonging to sets 2 and 3 show somewhat different behaviour. In these cases, the g_{12} and g_{13} values of the plain C steel are higher than those of the corresponding Nb-microalloyed samples. In case of set 2, both the steels show nearly same values of g_{12} and g_{13} at higher finishing temperatures. The same is observed in case of the g_{12} values of set 3, however the variation of g_{13} with temperature in this case is different. Here the g_{13}values remain somewhat similar for both plain C and Nb-microalloyed steels, except at the lowest finishing temperature at which the difference between the g_{13} values of the two steels is quite large. In these cases too, the variation of g_{13} with finishing temperature is more drastic than that of g_{12}. So far as the g_{23} values are concerned, for any one of the steels, g_{23} has an increasing trend with the lowering of the finishing temperature. Between the two steels, the value of this parameter is larger in the Nb-steel as compared to the corresponding plain C steel.

The nature of the variations in g_{12},g_{23} and g_{13} has been shown graphically in Fig.4.9 to Fig.4.11.

4.2.2 Degree of orientation

As explained in Chapter III, by looking at the

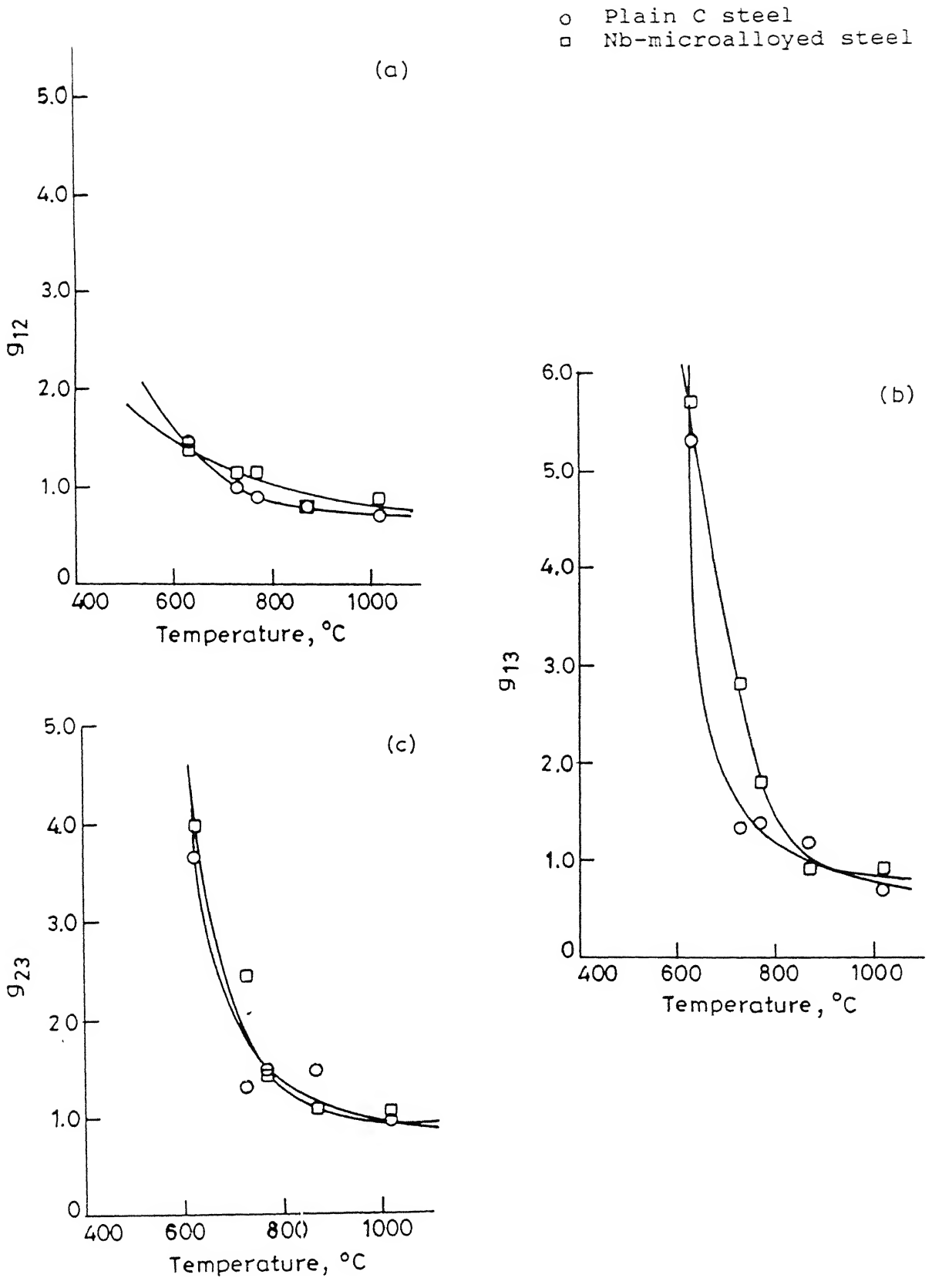

Figure 4.9: Variation of (a)g_{12}, (b)g_{13}, and (c)g_{23} values of steels austenitized at 1250°C and rolled upto 90% reduction, with finish rolling temperature.

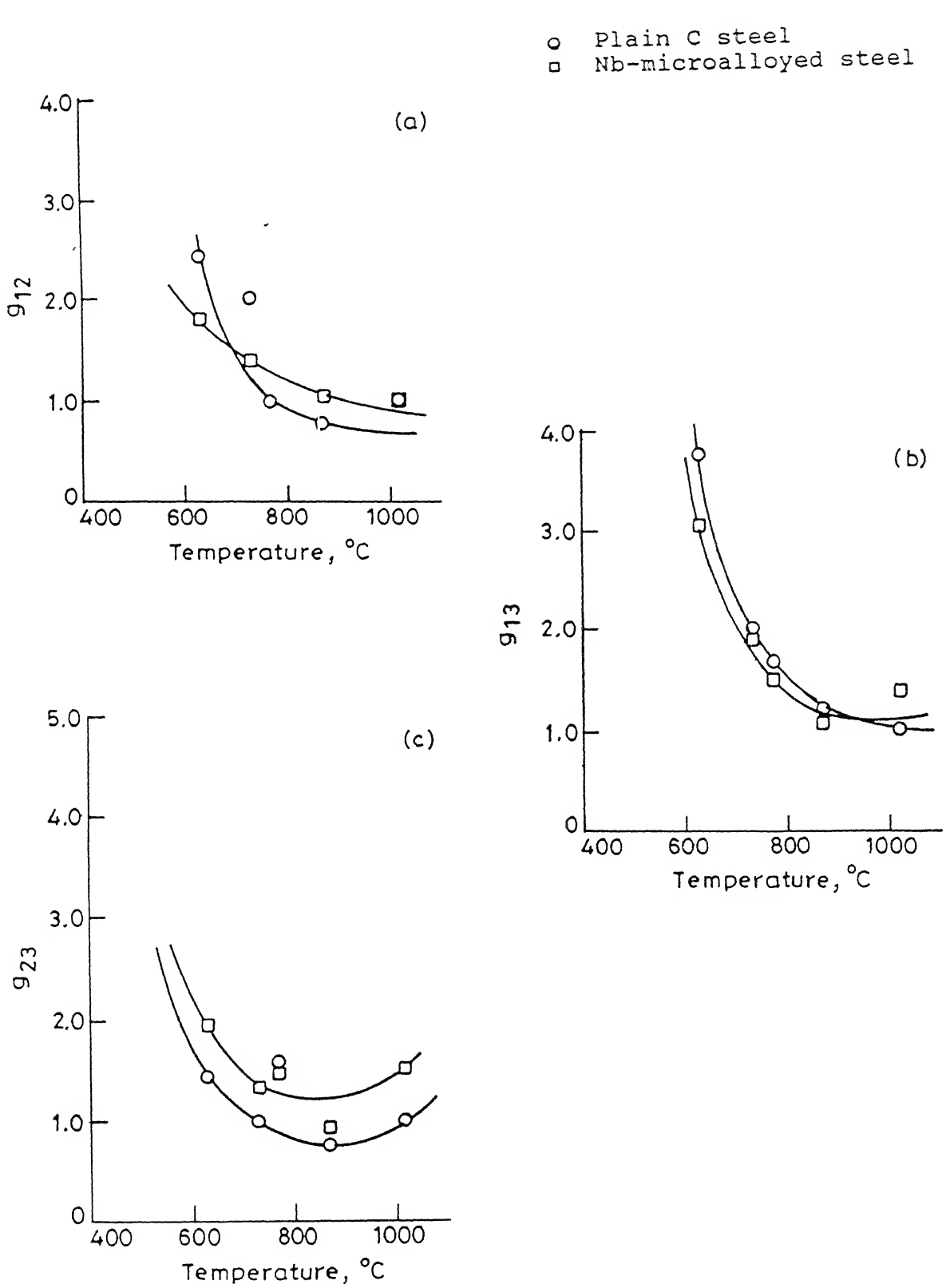

Figure 4.10: Variation of (a)g_{12}, (b)g_{13}, and (c)g_{23} values of steels austenitized at 1250°C and rolled upto 75% reduction, with finish rolling temperature.

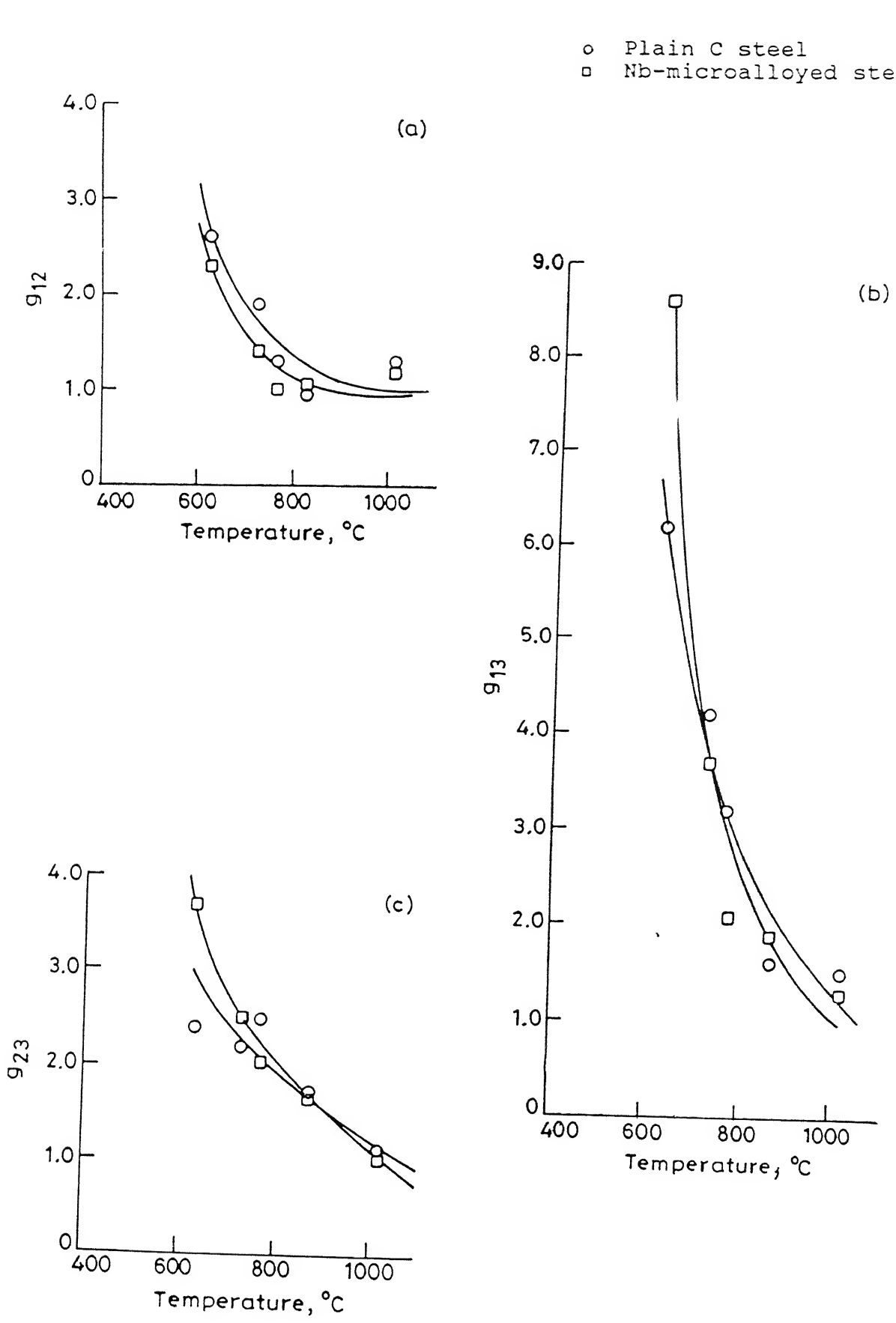

Figure 4.11: Variation of (a)g_{12}, (b)g_{13}, and (c)g_{23} values of steels austenitized at 1150°C and rolled upto 90% reduction, with finish rolling temperature.

microstructure of the three sections of the samples, it can be said that after controlled rolling the grains appear to be oriented along the RD and along the rolling plane as well. This means that the controlled rolled steels exhibit both linear and planar orientations. Table 4.2 gives the numerical values calculated for the degrees of orientation of the two steels (ref. Appendix).

For all the three sets of samples considered, the degree of orientation exhibits more or less an increasing trend with decreasing finish rolling temperatures (Table 4.2), except the discrepancy found at a particular value in each case. For example, in set 1, this happens at the temperature corresponding to the finish rolling in the $\gamma_{nonrecryst}$ range. This is also evident from the graphical representations of these values in Fig.4.12 to Fig.4.14. It has also been observed that the values of degree of orientation of Nb-microalloyed steel in each set, are somewhat higher than those of plain C steel, although this is not strictly true for the samples of set 2.

In the first set of samples, all the three degrees of orientaion of the plain C steel have been observed to first decrease for a finishing temperature of 870°C followed by a continous increase as the finishing temperature goes down right upto 630°C. However, in case of Nb-microalloyed steel, the values first increase and then drop at the finishing temperature of 770°C. After that the degrees of orientation increase in a manner similar to those for plain C steel. These trends have also been shown in Fig. 4.12.

Table 4.2

Variation of degrees of orientation with finishing temperature

SET 1

Steel	Finishing Temperature °C	W'_{lin} %	W'_{pl} %	$W'_{lin/pl}$ %
Plain Carbon Steel	1020	7.4	6.4	13.8
	870	2.2	1.4	6.8
	770	2.6	11.8	14.5
	730	7.5	13.3	20.8
	630	29.1	13.7	42.8
Nb-micro-alloyed Steel	1020	5.1	6.2	11.5
	870	19.1	16.6	35.7
	770	8.2	14.3	22.5
	730	17.9	15.5	33.4
	630	33.8	17.4	51.2

SET 2

Steel	Finishing Temperature °C	W'_{lin} %	W'_{pl} %	$W'_{lin/pl}$ %
Plain Carbon Steel	1020	3.7	7.5	11.3
	870	22.1	13.3	35.4
	770	19.2	8.5	27.6
	730	24.9	10.4	35.4
	630	29.3	14.7	44.0
Nb-micro-alloyed Steel	1020	4.05	4.5	8.5
	870	19.6	6.2	25.9
	770	5.4	9.05	14.5
	730	17.7	13.05	30.8
	630	44.1	16.6	60.8

SET 3

Steel	Finishing Temperature °C	W'_{lin} %	W'_{pl} %	$W'_{lin/pl}$ %
Plain Carbon Steel	1020	11.6	8.9	20.5
	870	18.9	10.9	29.8
	770	13.8	7.9	21.8
	730	28.5	18.0	46.5
	630	42.5	17.2	59.7
Nb-micro-alloyed Steel	1020	7.3	3.3	10.6
	870	20.7	13.3	34.0
	770	24.7	14.6	39.3
	730	33.7	14.8	48.6
	630	38.8	18.8	57.6

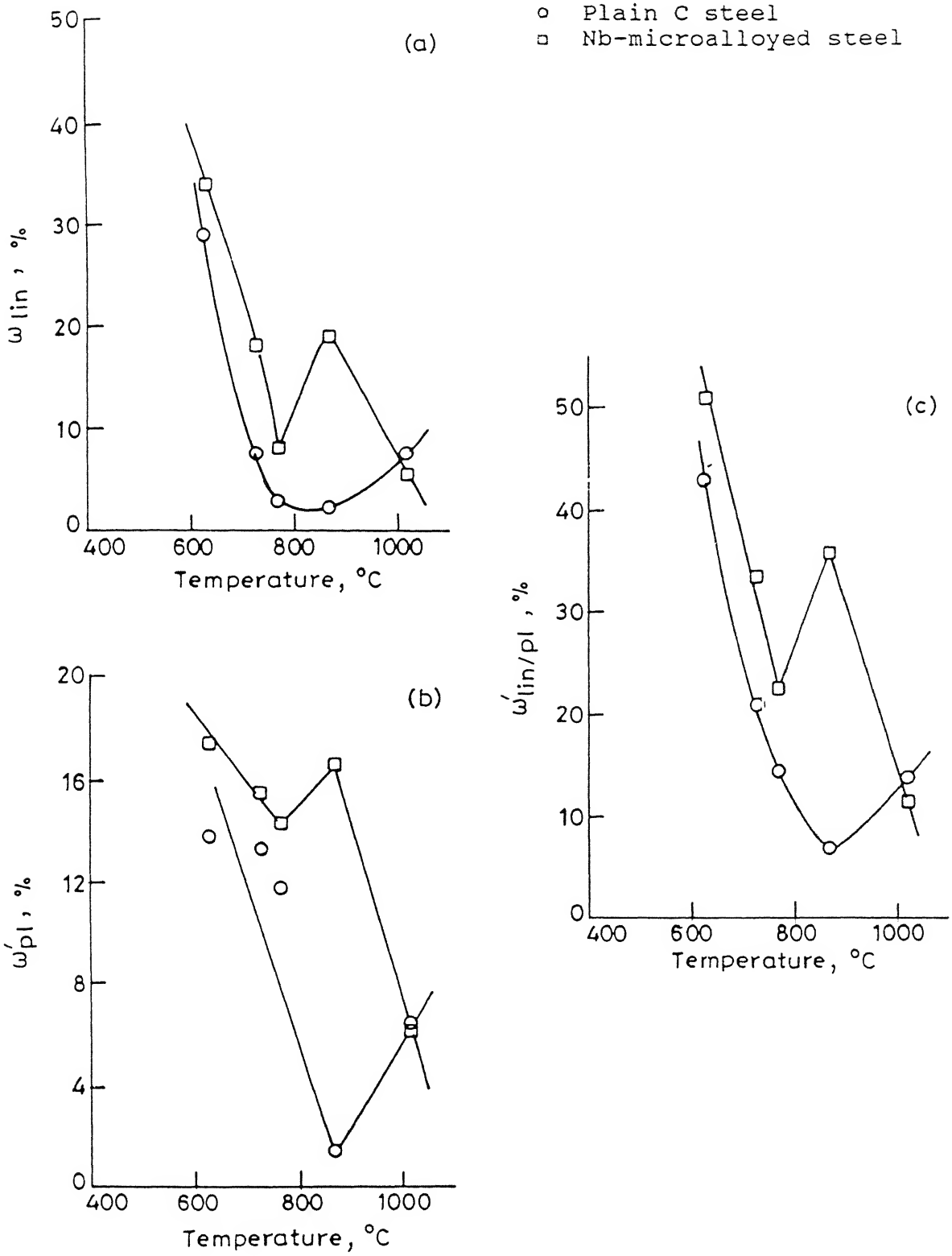

Figure 4.12: Variation of (a)degree of linear orientation, w'_{lin} , (b) degree of planar orientation, w'_{pl} , and (c)degree of linear-planar orientation, $w'_{lin/pl}$, of steels austenitized at 1250°C and rolled upto 90% reduction, with finish rolling temperature.

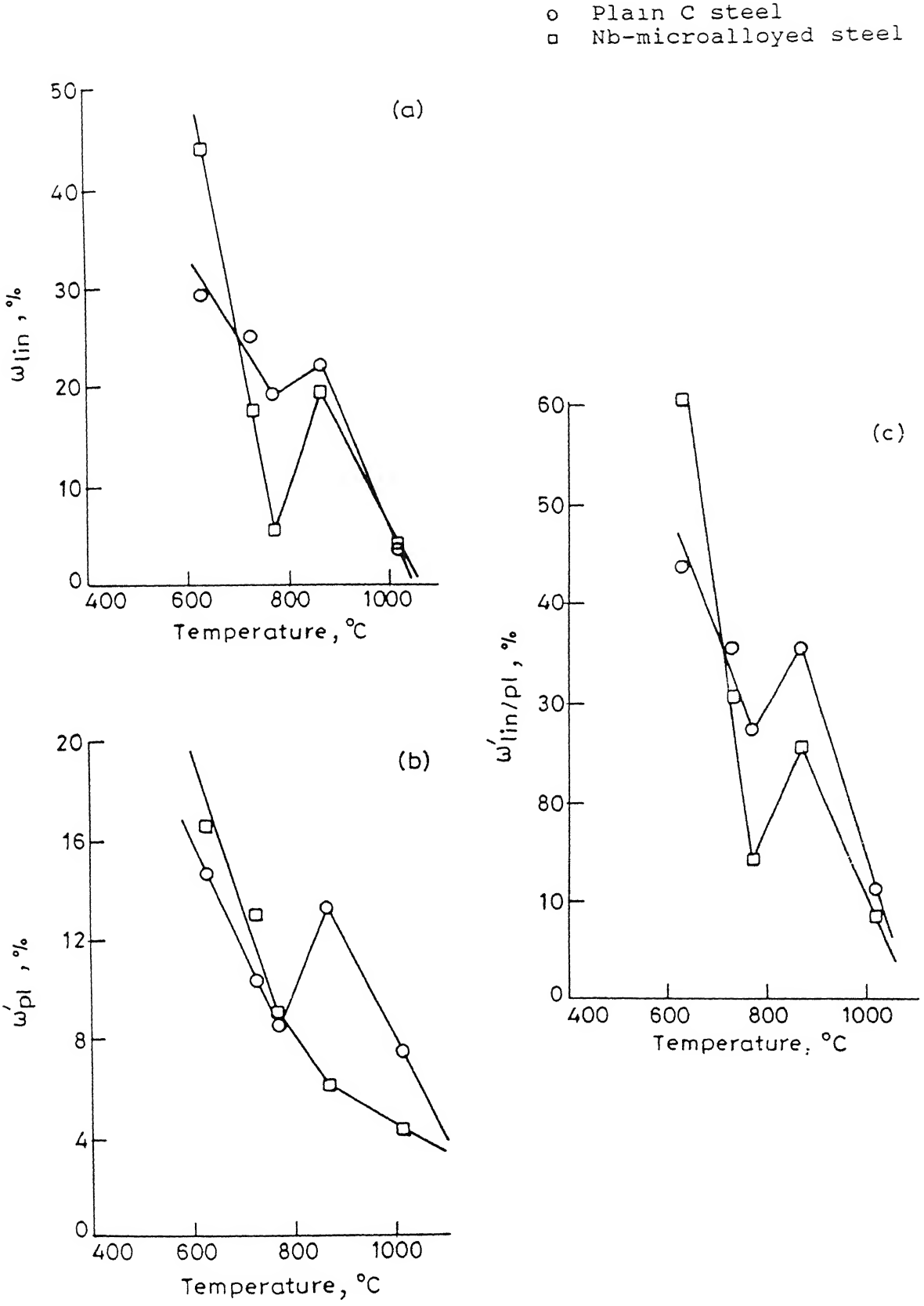

Figure 4.13: Variation of (a) degree of linear orientation, W'_{lin} , (b) degree of planar orientation, W'_{pl} , and (c) degree of linear-planar orientation, $W'_{lin/pl}$, of steels austenitized at 1250°C and rolled upto 75% reduction, with finish rolling temperature.

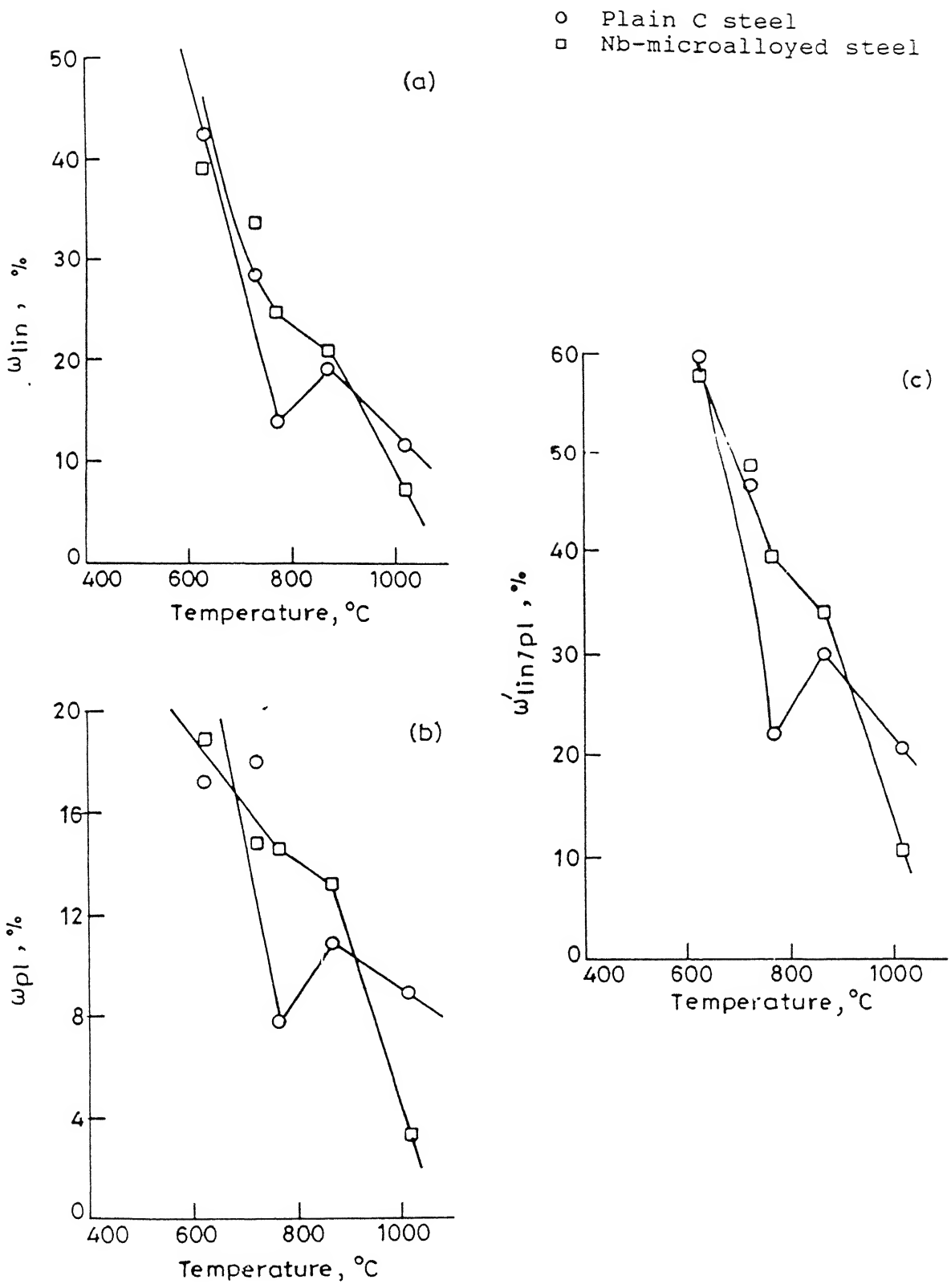

Figure 4.14: Variation of (a)degree of linear orientation, w'_{lin} , (b) degree of planar orientation, w'_{pl} , and (c)degree of linear-planar orientation, $w'_{lin/pl}$, of steels austenitized at 1150°C and rolled upto 90% reduction, with finish rolling temperature.

In the samples belonging to set 2, the value of the degree of orientation initially goes up, for both the steels, then decreases at the finishing temperature of 770°C, beyond which it increases again. At the lowest finishing temperature, i.e. 630°C, the value of the degree of orientation is much larger for the Nb-microalloyed steel as compared to the plain C steel, although this parameter appears to have a lower value in the Nb-microalloyed steel for every other finishing temperature employed. These have been shown graphically in Fig.4.13.

In the third set of steels, the degree of orientation for the plain C steel is found to first increase and then drop for the finishing temperature of 770°C followed by a continuous increase with the lowering of the finishing temperature. In contrast, in the Nb-microalloyed steel, the values of the degree of orientation increases throughout with decreasing finishing temperature. These trends have been depicted graphically in Fig.4.14.

4.2.3 Grain thickness along ND.

As explained in Chapter III, this parameter shows the extent of flattening of grains with decreasing finishing temperature. The results of the measurements done on the micrographs are given in Table 4.3 and the variation of this parameters with finish rolling temperature has been shown graphically in Fig.4.15 to Fig.4.17.

It has been observed that the grain thickness decreases in both the steels as finishing temperature is

Table 4.3

Variation of grain thickness (along ND) with finishing temperature

	Steel	Finishing Temperature °C	Grain thickness mm (at 500 X)
Set 1	Plain Carbon Steel	1020	4.01
		870	2.86
		770	2.66
		730	2.63
		630	1.50
	Nb-micro-alloyed Steel	1020	3.00
		870	2.32
		770	2.25
		730	2.09
		630	1.45
Set 2	Plain Carbon Steel	1020	9.30
		870	6.30
		770	4.20
		730	3.50
		630	2.99
	Nb-micro-alloyed Steel	1020	6.30
		870	3.50
		770	2.54
		730	2.44
		630	2.09
Set 3	Plain Carbon Steel	1020	3.31
		870	3.02
		770	2.12
		730	1.75
		630	1.48
	Nb-micro-alloyed Steel	1020	2.82
		870	1.92
		770	1.62
		730	1.43
		630	1.27

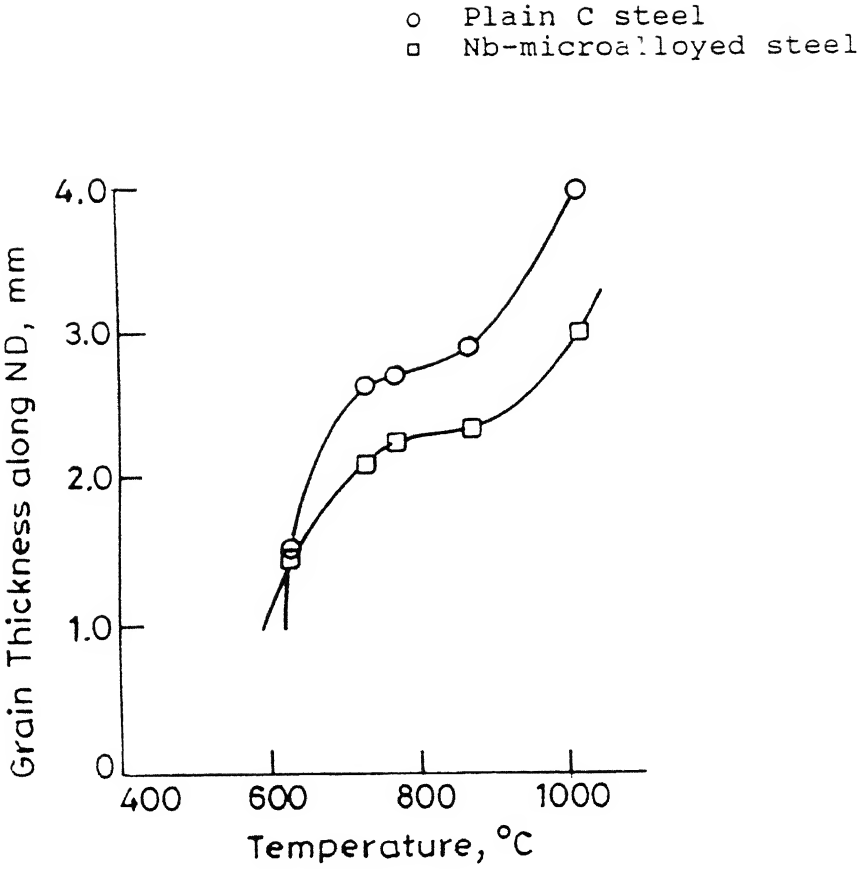

Figure 4.15: Variation of grain thickness along ND, of the steels austenitized at 1250°C (90% reduction), with finish rolling temperature.

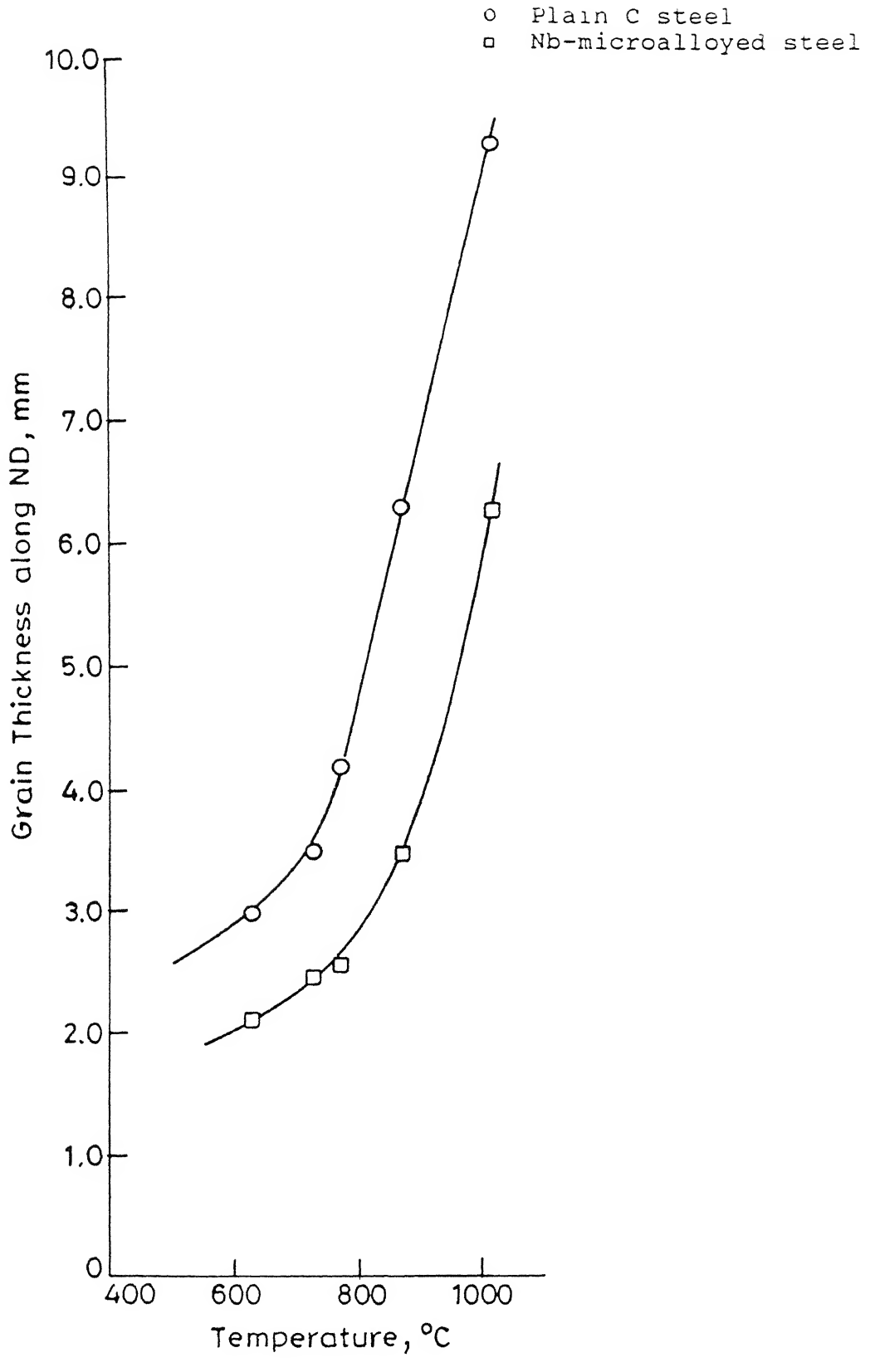

Figure 4.16 Variation of grain thickness along ND, of the steels austenitized at 1250°C (75% reduction), with finish rolling temperature.

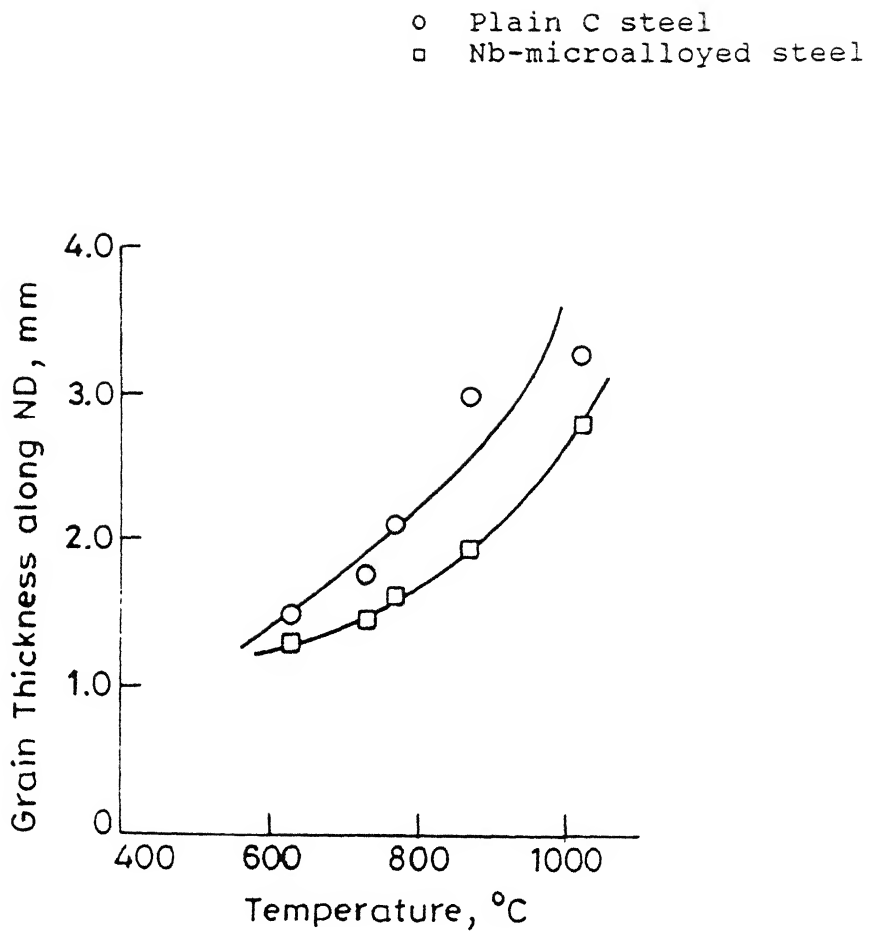

Figure 4.17: Variation of grain thickness along ND, of the steels austenitized at 1150°C (90% reduction), with finish rolling temperature.

decreased. At every temperature the grain thicknesses of the Nb-microalloyed steel are much smaller than those of the plain C steel. The difference between the grain thickness values of the two steels gradually decrease with decrease in finish rolling temperature (for the samples in set 1 and set 3). It has also been observed that the grain thickness of both the steels is nearly the same at the lowest finishing temperature, when the steels are rolled upto 90%, irrespective of the austenitizing temperature. On the other hand, in case of 75% rolled steels, the difference between the grain thicknesses of plain C and Nb-microalloyed steels is much larger for all finishing temperatures right upto 630°C. For a particular finishing temperature, the grain thickness is much larger for the 75% rolled material as compared to the 90% rolled material, in case of both the steels considered.

4.2.4 Rose-of-the-number-of-intersections

The rose-of-the-number-of-intersections for all the thirty samples have been shown in Fig.4.18 to Fig.4.23, and the data used for plotting them are given in the Appendix. In all the three sets of samples the curves have been found to be symmetrical to only one axis i.e. the rolling direction. It has also been observed that the peak value of N_L corresponds to that measured along ND and it increases as the finish rolling temperature is decreased. This is obvious from the fact that the grain thickness along ND decreases with finishing temperature (ref. section 4.2.3). In each set of samples, the peak value of

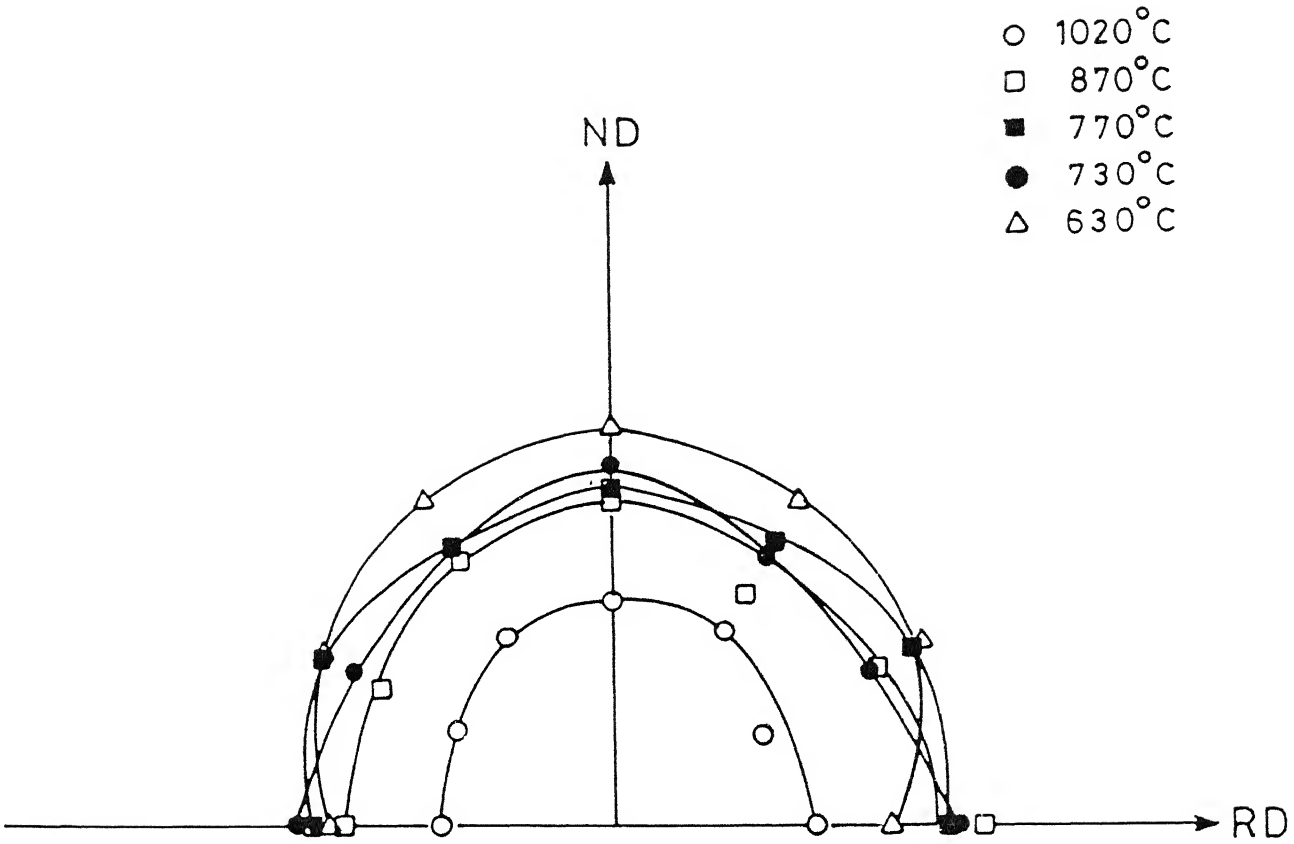

Figure 4.18: The roses-of-the-number-of-intersections of plain C steel, (austenitized at 1250°C, 90% reduction) finish rolled at five different temperatures.

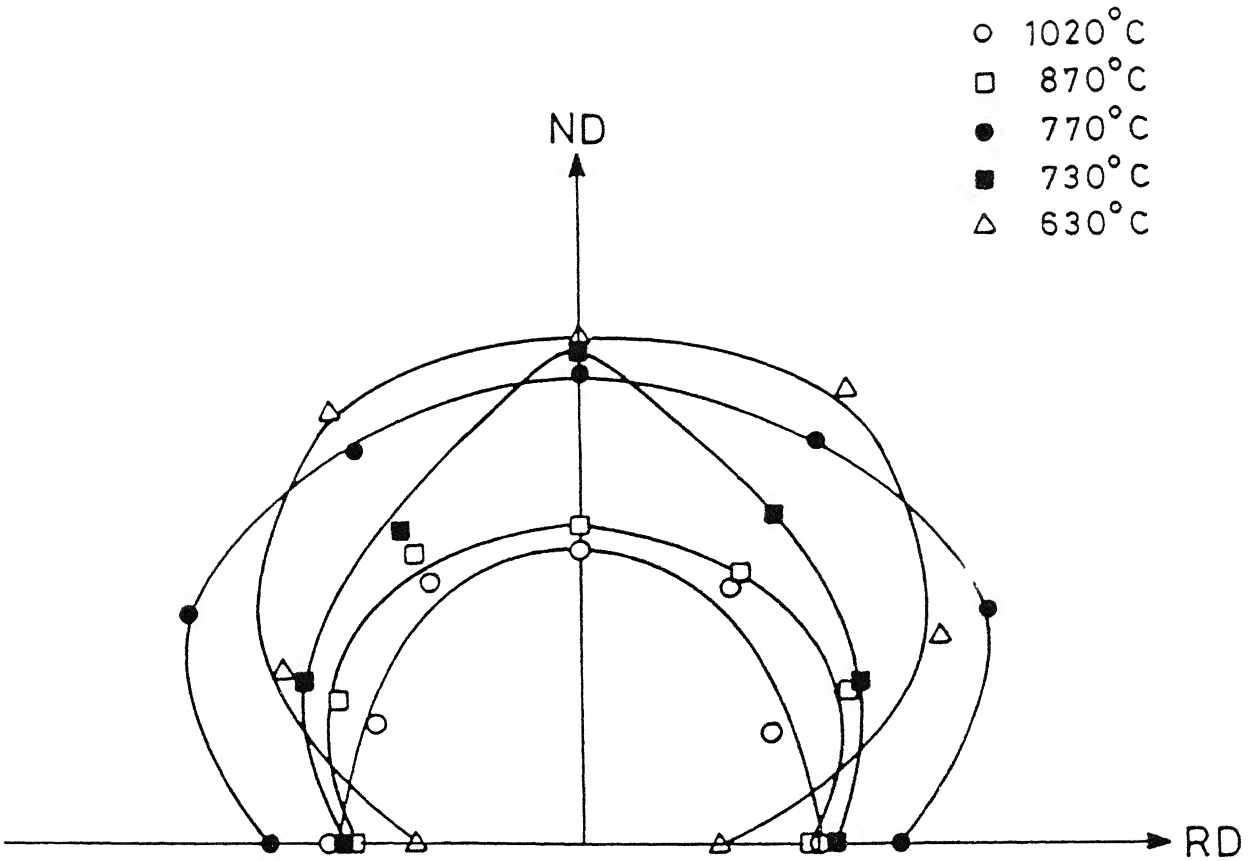

Figure 4.19: The roses-of-the-number-of-intersections of Nb-microalloyed steel, (austenitized at 1250°C, 90% reduction) finish rolled at five different temperatures.

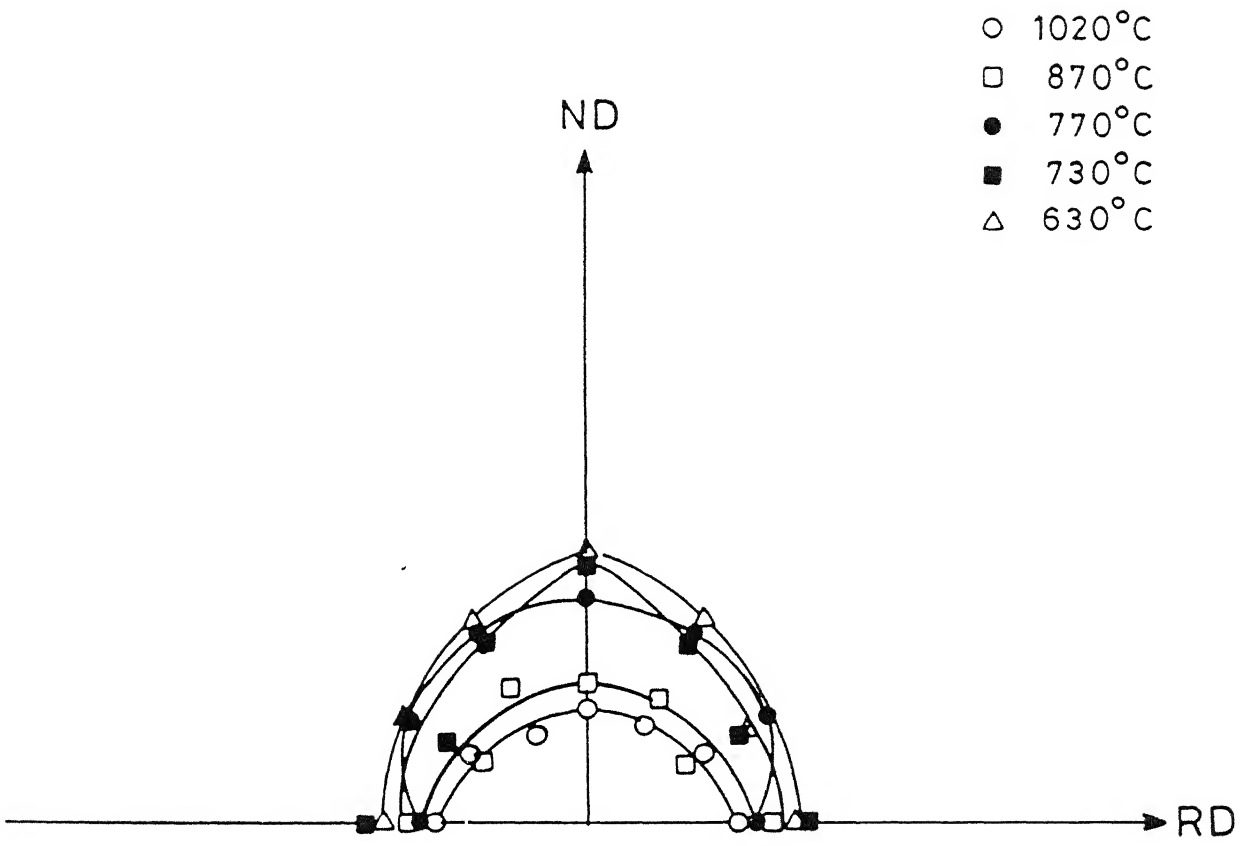

Figure 4.20: The roses-of-the-number-of-intersections of plain C steel, (austenitized at 1250°C, 75% reduction) finish rolled at five different temperatures.

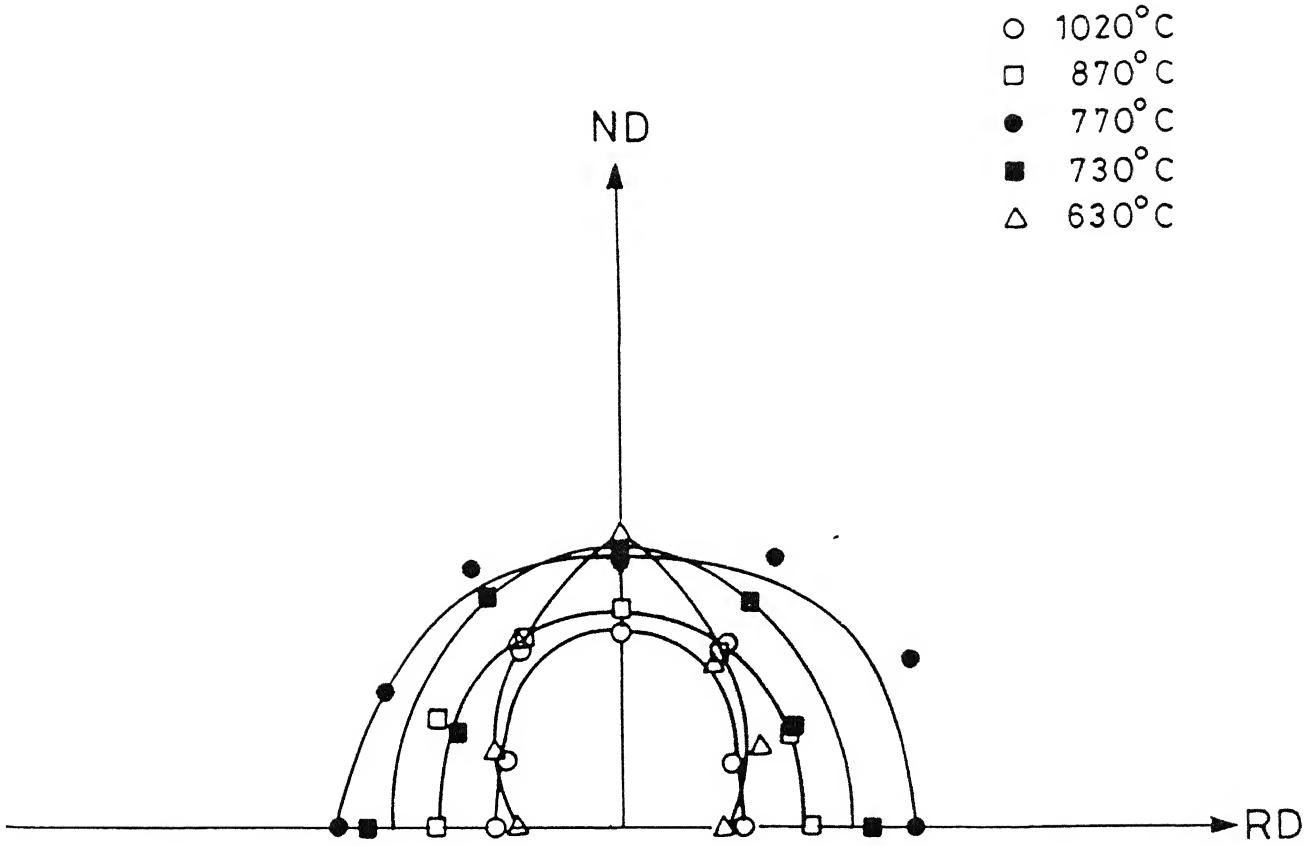

Figure 4.21: The roses-of-the-number-of-intersections of Nb-microalloyed steel, (austenitized at 1250°C, 75% reduction) finish rolled at five different temperatures.

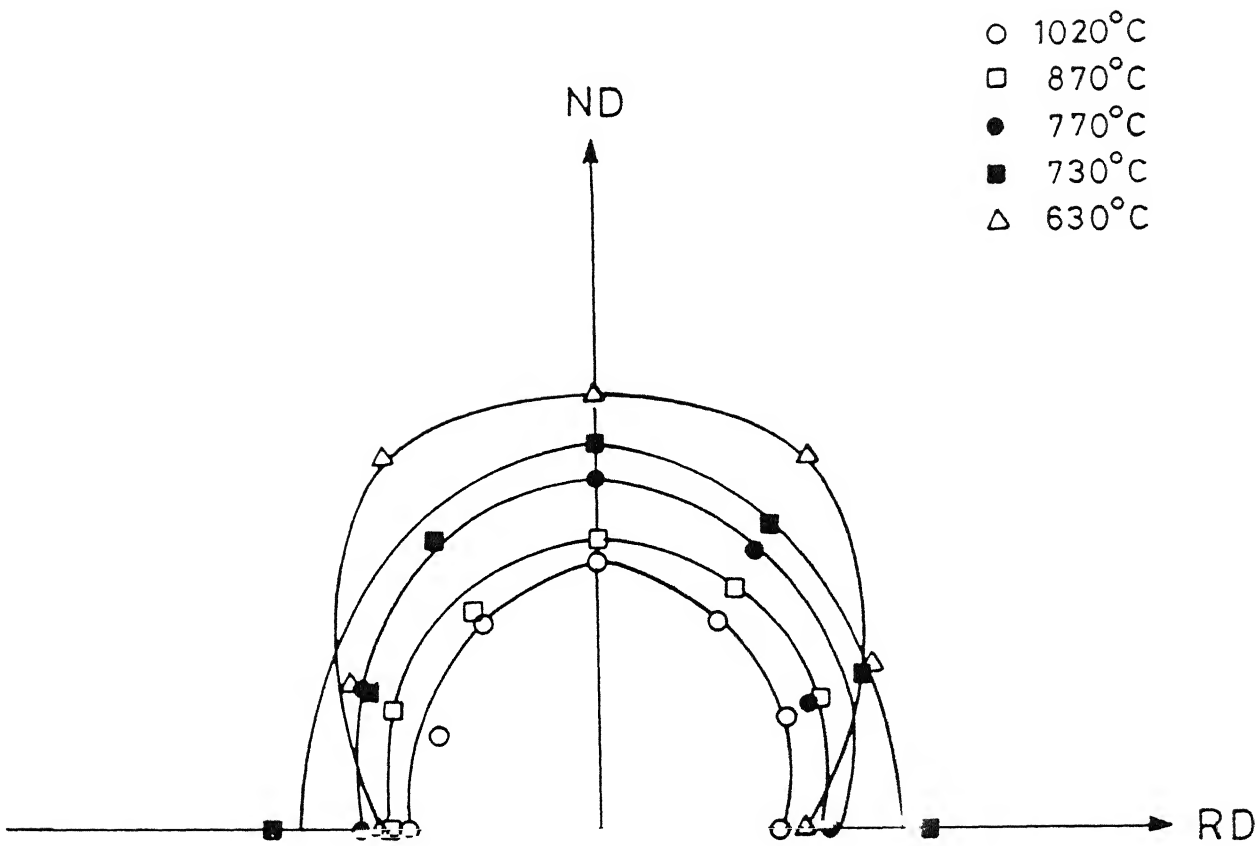

Figure 4.22: The roses-of-the-number-of-intersections of plain C steel, (austenitized at 1150°C, 90% reduction) finish rolled at five different temperatures,

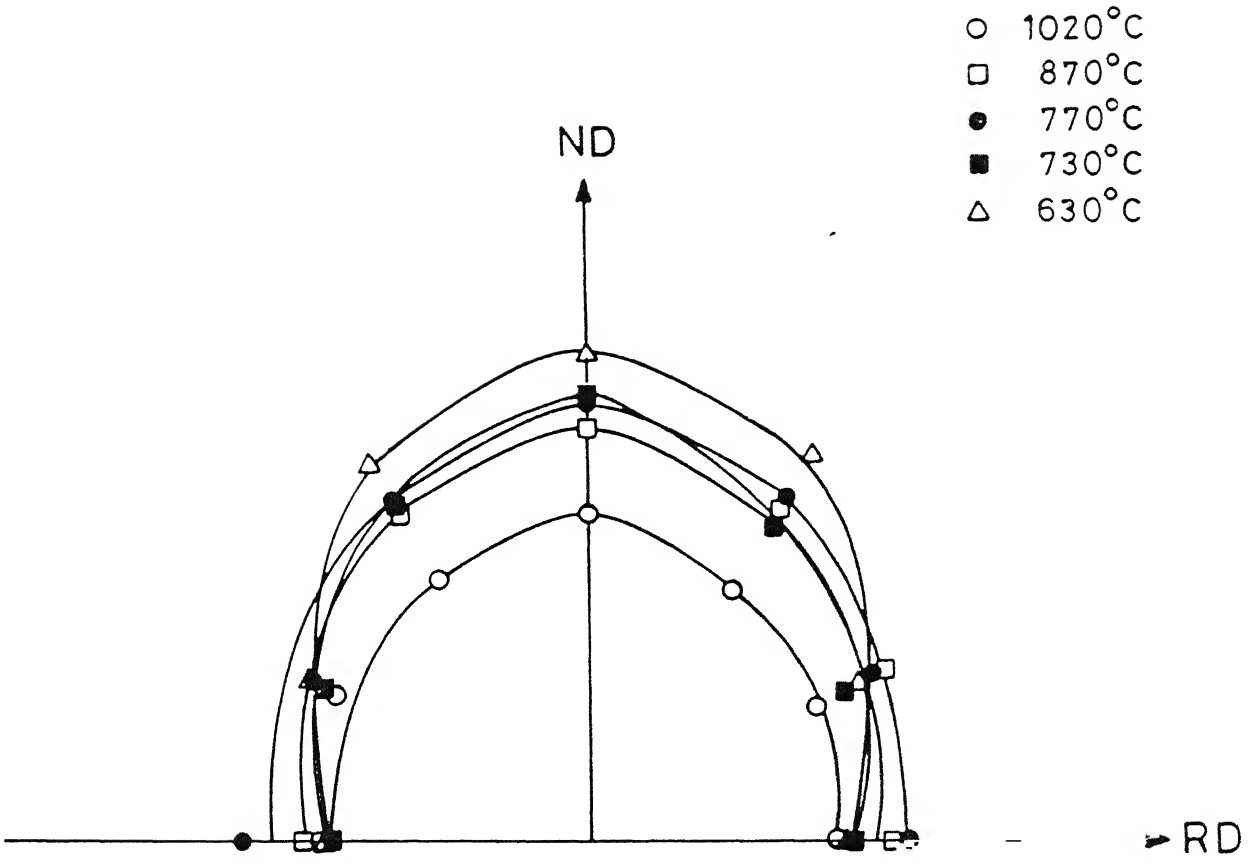

Figure 4.23: The roses-of-the-number-of-intersections of, Nb-microalloyed steel, (austenitized at 1150°C, 90% reduction) finish rolled at five different temperatures.

N_L is found to be higher for the Nb-microalloyed steel than that for the plain C steel.

In all the three sets of samples, the shape of the curve has been observed to change with finish rolling temperature. In the first set, the plain C steel samples finish rolled at 1020°C and 870°C yield semicircular curves, and beyond that the curve becomes somewhat dumbell shaped (elongated towards the ND axis). In case of the Nb-microalloyed steel, however, the latter trend is observed right from the finish rolling temperature of 870°C. The curve corresponding to the finishing temperature of 1020°C is semicircular in this case also.

In the second set of samples also, the shape of the curve follows a similar trend. The N_L values however, are found to be much smaller than the corresponding values in the first set of samples.

In the third set of samples the trend is somewhat different. In this case, the curves corresponding to the first three finishing temperatures i.e. 1020°C, 870°C and 770°C, are more or less semicircular in case of the plain C steel. The curve gets a bit elongated towards ND at 730°C, and becomes dumbell shaped at the lowest finishing temperature i.e. 630°C. In case of the Nb-microalloyed steel, the curves are found to be elongated right from the finishing temperature of 1020°C to 730°C. Beyond this, the curve becomes dumbell shaped. The N_L values of all the samples in this set have been found to be larger than the corresponding N_L values of the samples belonging to the previous two sets.

4.3 TEXTURE STUDIES

Results of the texture studies carried out on the thirty samples have been given in Table 4.4 to Table 4.6, in which the predominant texture components, their corresponding intensity values and the maximum texture intensity for each sample have been shown. The pole figures from which these data have been obtained are shown in Fig.4.24 to Fig.4.29.

In the first set of samples (Table 4.4), the maximum texture intensity for the plain C steel first decreases to a minimum value at the finishing temperature of 870°C and increases gradually beyond that as the finish rolling temperature is decreased. However, in case of the Nb-microalloyed steel, the maximum texture intensity first increases to a high value for the same finishing temperature at the finishing temperature of 770°C. Beyond this, the maximum intensity follows the usual increasing trend. Furthermore, the maximum texture intensity of plain C steel (3.3 times random) at the lowest finishing temperature, has been found to be higher than that of Nb-microalloyed steel (3.0 times random) at the same finishing temperature. It has also been observed that the maximum texture intensity corresponds to the {100}<011> component for both the steels.

Table 4.5 shows the texture results for the second set of samples. It has been observed that the maximum texture intensity for the plain C steel drops to a minimum value at the finishing temperature of 770°C and then increases again, with decreasing finish rolling temperature. In case of the Nb-microalloyed steel, the maximum intensity drops at the

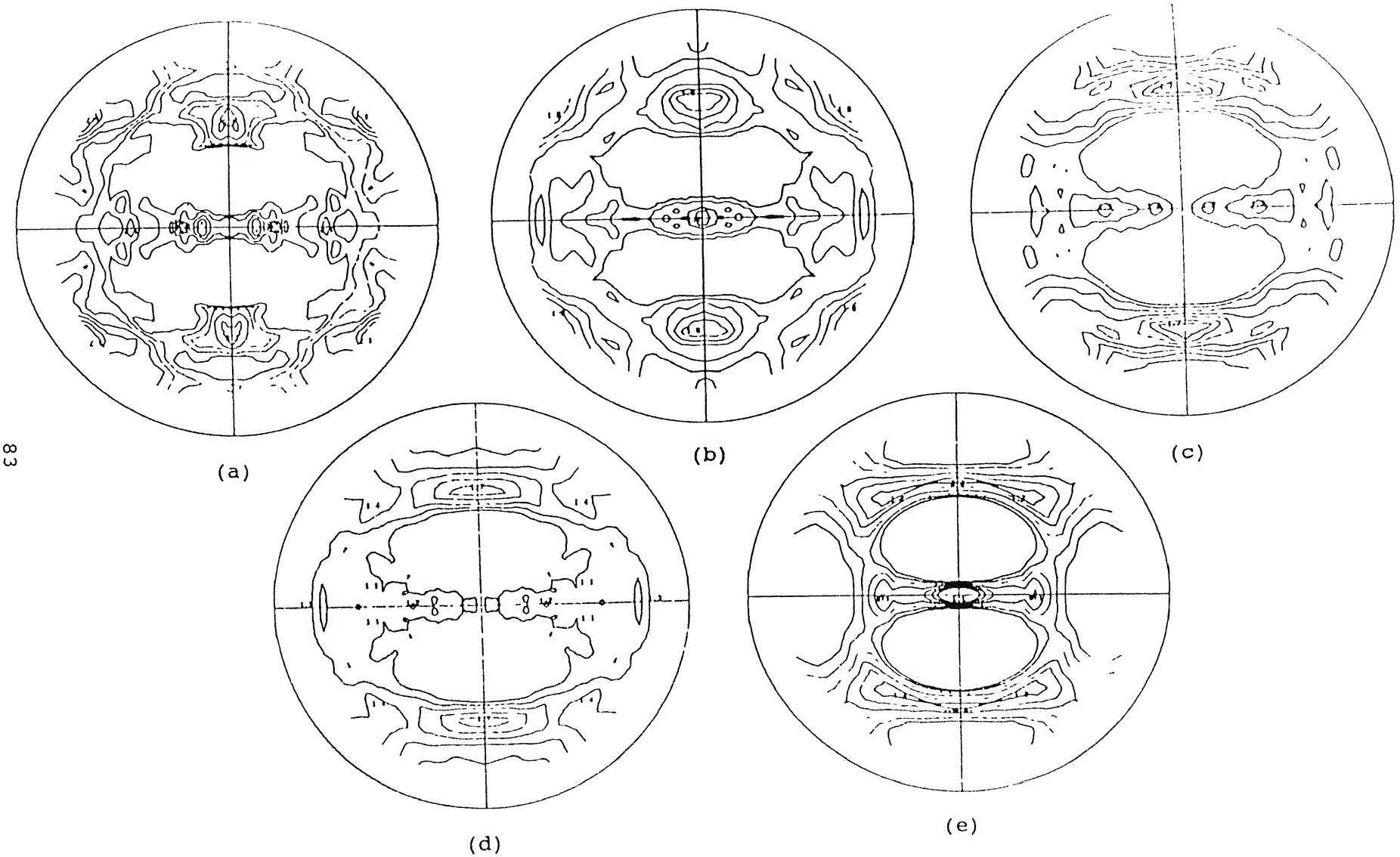

Figure 4.24: Pole figures corresponding to the plain C steel (austenitizing temperature 1250°C, 90% reduction,) finish rolled at five different temperatures (a)1020°C, (b)870°C, (c)770°C, (d)730°C, and (e)630°C.

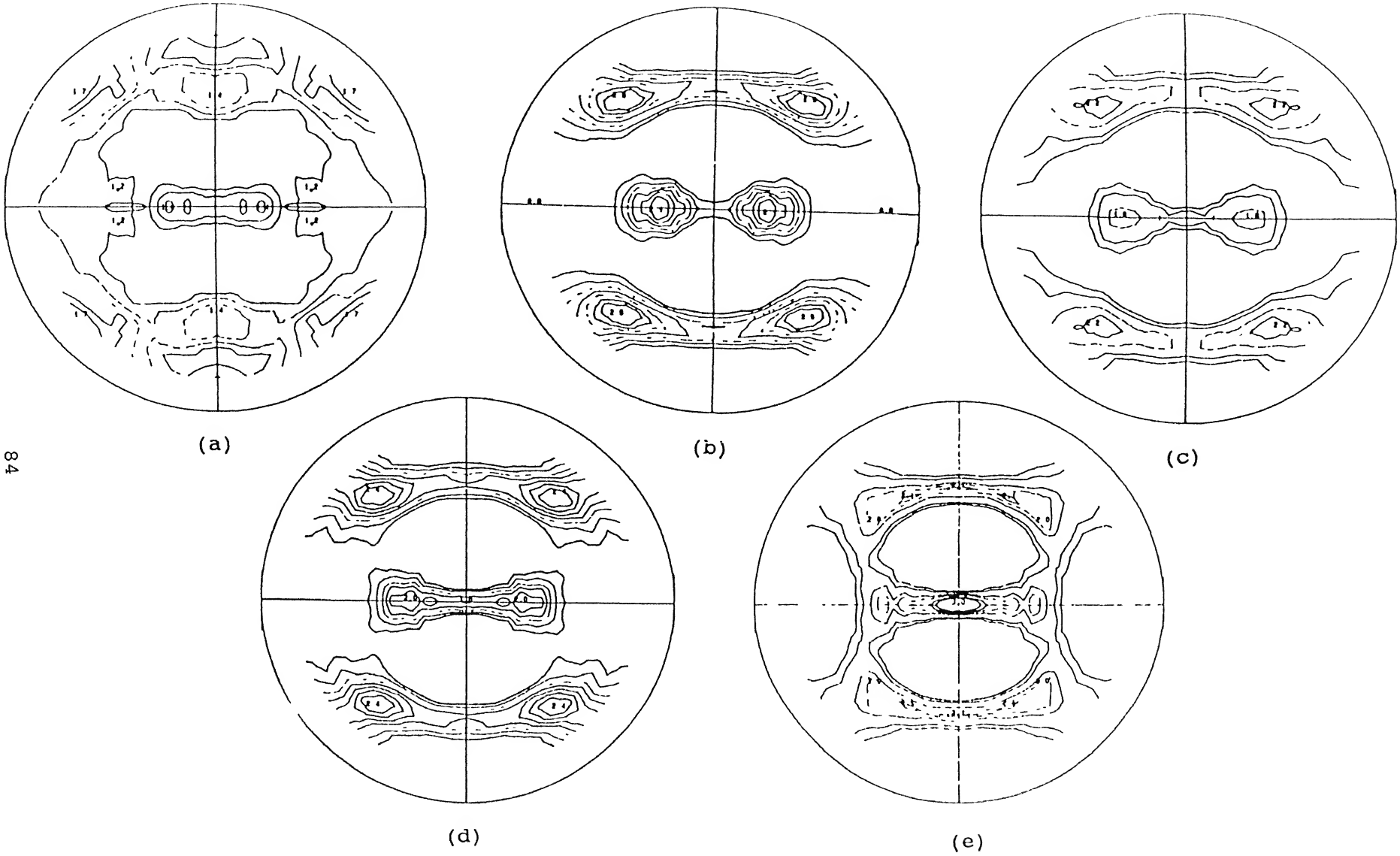

Figure 4.25: Pole figures corresponding to the Nb-microalloyed steel (austenitizing temperature 1250°C, 90% reduction,) finish rolled at five different temperatures (a)1020°C, (b)870°C, (c)770°C, (d)730°C, and (e)630°C.

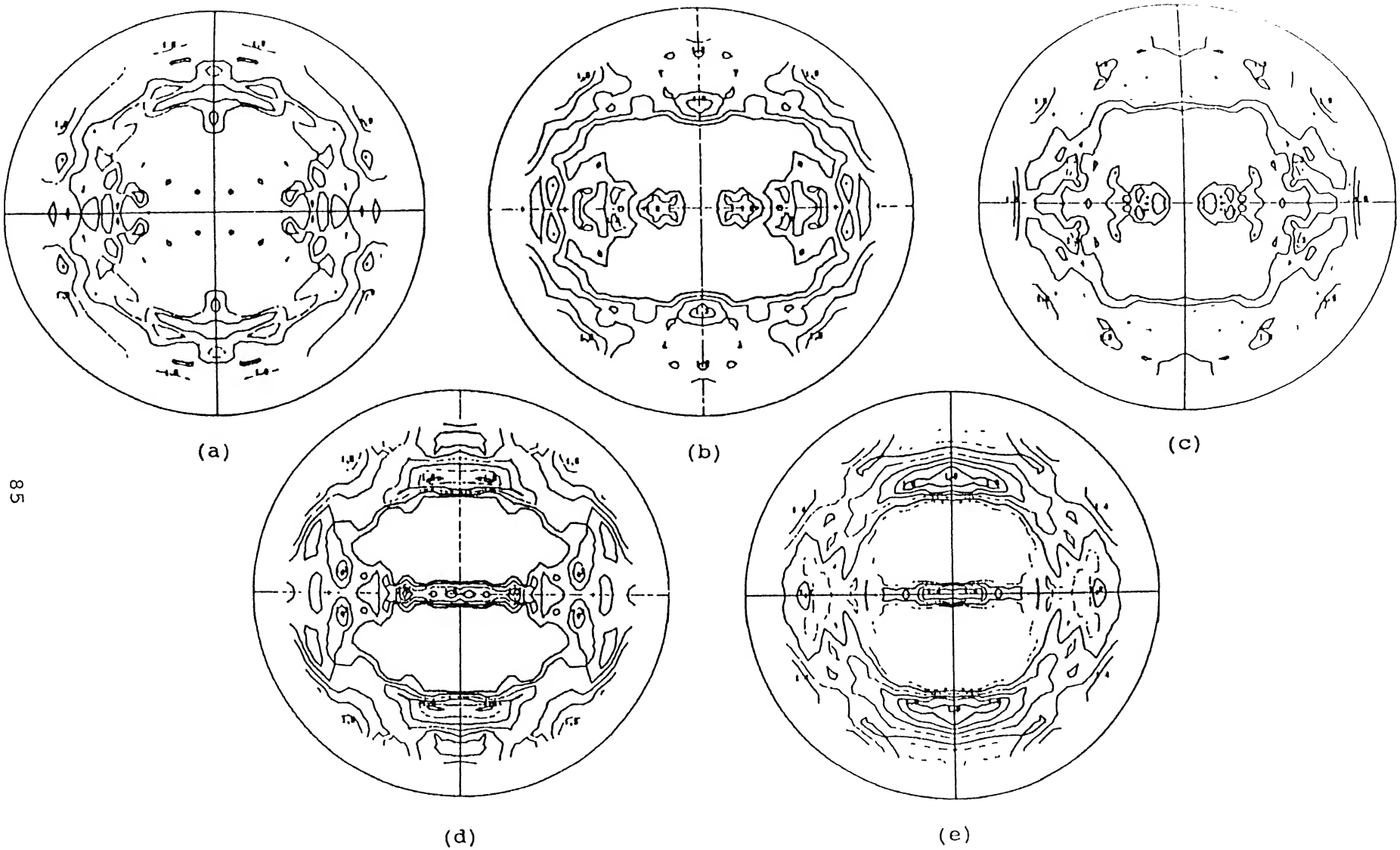

Figure 4.26: Pole figures corresponding to the plain C steel (austenitizing temperature 1250°C, 75% reduction,) finish rolled at five different temperatures (a) 1020°C, (b) 870°C, (c) 770°C, (d) 730°C, and (e) 630°C.

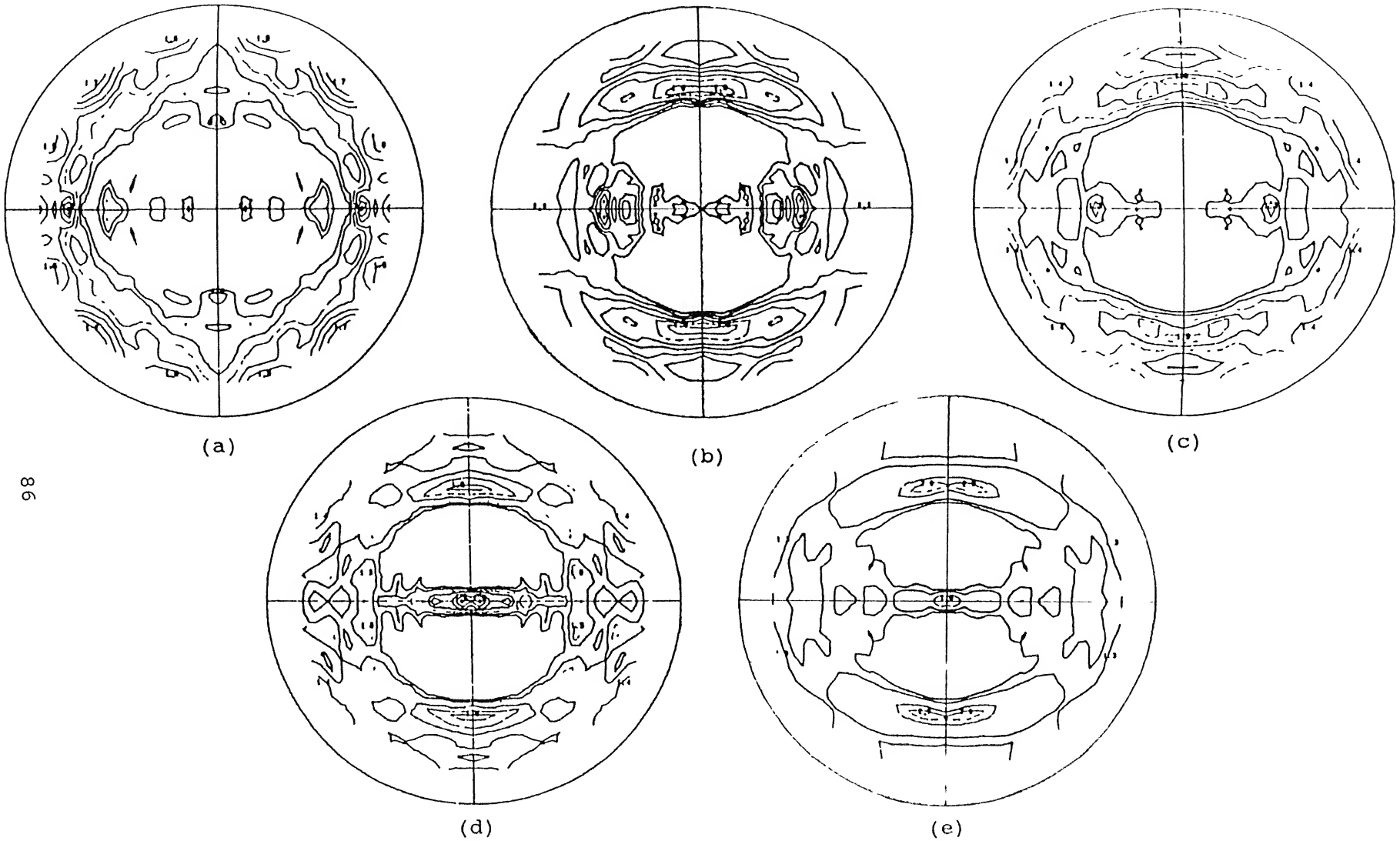

Figure 4.27: Pole figures corresponding to the Nb-microalloyed steel (austenitizing temperature 1250°C, 75% reduction,) finish rolled at five different temperatures (a)1020°C, (b)870°C, (c)770°C, (d)730°C, and (e)630°C.

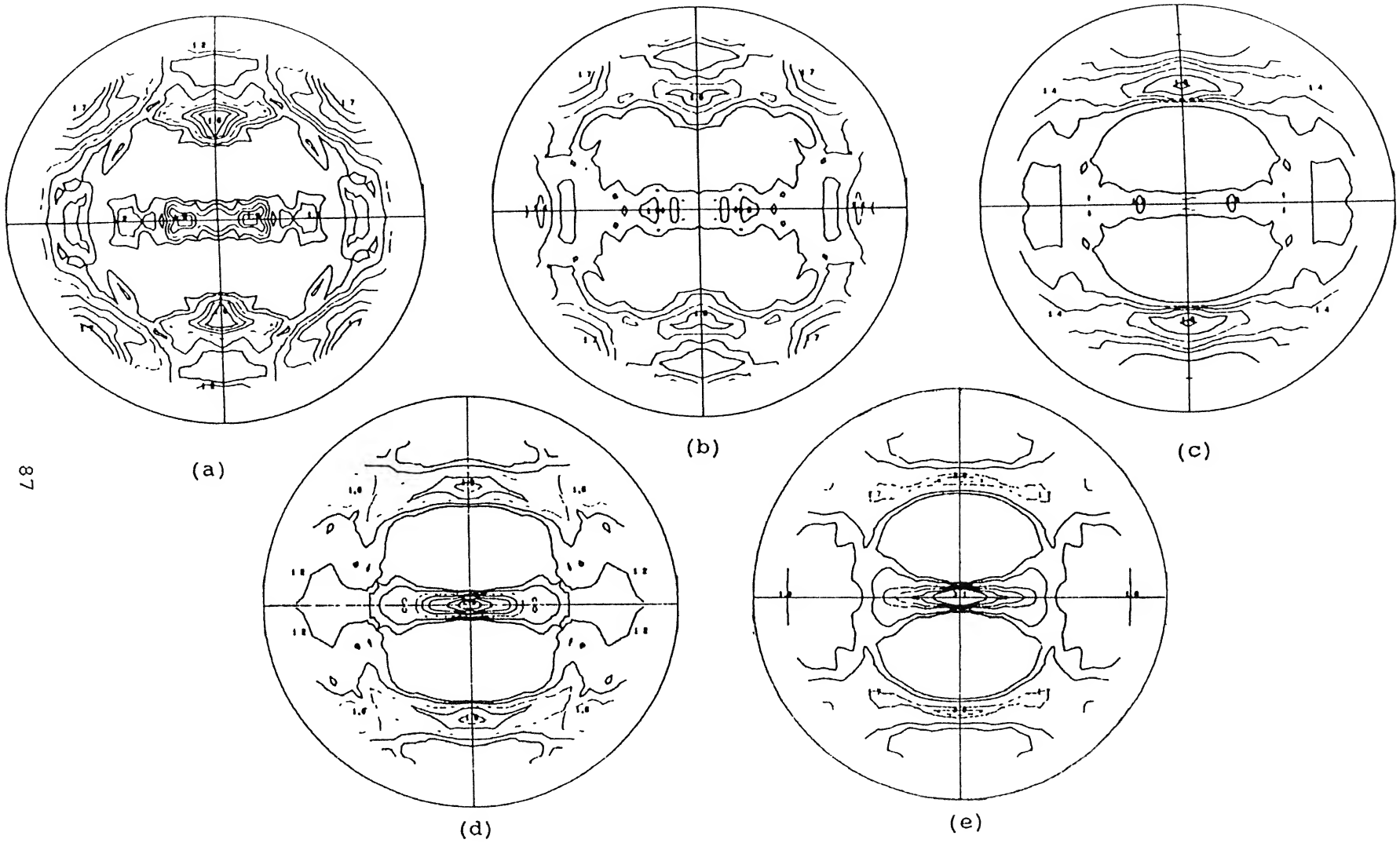

Figure 4.28: Pole figures corresponding to the plain C steel (austenitizing temperature 1150°C, 90% reduction,) finish rolled at five different temperatures (a) 1020°C, (b) 870°C, (c) 770°C, (d) 730°C, and (e) 630°C.

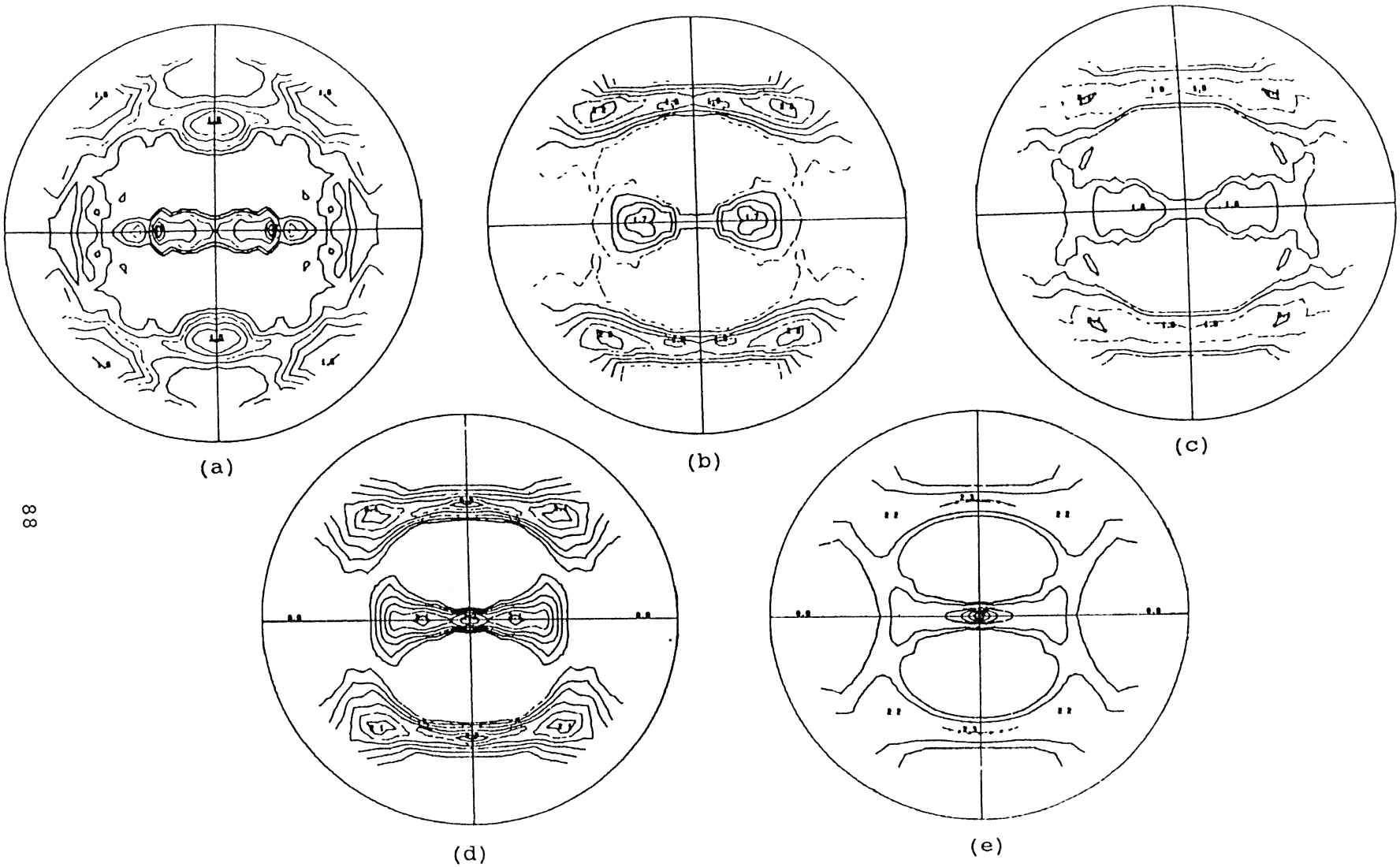

Figure 4.29: Pole figures corresponding to the Nb-microalloyed steel (austenitizing temperature 1150°C, 90% reduction,) finish rolled at five different temperatures (a)1020°C, (b)870°C, (c)770°C, (d)730°C, and (e)630°C.

Table 4.4

Texture results (Set 1)

Steel	Finishing Temperature °C	Texture Component	Intensity (x Random)	Maximum Intensity (x Random)
Plain Carbon Steel	1020	{111}<112> {113}<110>	1.5 1.7	1.7
	870	{113}<110> {111}<112> {100}<011>	1.5 1.5 weak	1.6
	770	{111}<112> {113}<110>	1.7 1.2	1.7
	730	{111}<112> {113}<110>	1.7 1.4	1.9
	630	{100}<011> {112}<110>	3.3 2.1	3.3
Nb-micro-alloyed Steel	1020	{113}<110> {111}<112>	1.7 1.2	1.9
	870	{113}<110>	2.5	2.5
	770	{113}<110>	2.2	2.2
	730	{113}<110>	2.4	2.4
	630	{100}<011> {112}<110> {111}<112>	3.0 2.0 2.1	3.0

Table 4.5

Texture results (Set 2)

Steel	Finishing Temperature °C	Texture Component	Inten ity (x Random)	Maximum Intensity (x Random)
Plain Carbon Steel	1020	A number of orientations of low intensity		1.9
	870	{113}<110> {111}<112>	1.6 1.2	1.6
	770	{113}<110>	1.5	1.5
	730	{113}<110> {111}<112>	1.5 1.5	1.6
	630	{113}<110> {111}<112>	1.3 1.6	1.6
Nb-micro-alloyed Steel	1020	{113}<110> and a number of minor orientations	1.7	1.7
	870	{113}<110> {111}<112>	1.2 1.3	1.6
	770	{113}<110> {111}<112>	1.4 1.5	1.6
	730	{100}<011> {113}<110> {111}<112>	1.5 1.2 1.5	1.6
	630	{100}<011> {113}<110> {111}<112>	1.8 1.2 2.0	2.2

Table 4.6

Texture results (Set 3)

Steel	Finishing Temperature °C	Texture Component	Intensity (x Random)	Maximum Intensity (x Random)
Plain Carbon Steel	1020	{113}<110> {111}<112>	Weak Very weak	1.6
	870	{113}<110> {332}<113>	1.7 Weak	1.9
	770	{113}<110> {332}<113>	1.4 1.6	1.6
	730	{100}<011> {113}<110> {111}<112>	2.2 1.6 1.9	2.2
	630	{100}<011> {111}<112>	3.1 2.0	3.1
Nb-micro-alloyed Steel	1020	{113}<110> {111}<112>	1.5 1.5	1.6
	870	{113}<110>	2.2	2.2
	770	{113}<110>	2.1	2.2
	730	{113}<110> {111}<112> {100}<011>	2.1 2.2 Weak	2.2
	630	{100}<011> {113}<110>	3.4 2.2	3.4

finishing temperature of 870°C, increases with decreasing finishing temperature, and gives a maxima at the lowest finishing temperature i.e. 630°C. In both the steels the strongest texture component is {111}<112>, having intensity of 1.6 times random in case of plain C steel and 2.2 times random in case of Nb-microalloyed steel.

The texture results of the third set of samples have been shown in Table 4.6. The maximum texture intensity of plain C steel in this case is found to first increase to a high value at the finishing temperature of 870°C and then drop to a low value at the finishing temperature of 770°C. After this, the value shows an increasing trend with decreasing finish rolling temperature. In case of the Nb-microalloyed steel, however, the maximum intensity is found to increase and give a maxima at the lowest finishing temperature. The strongest texture component in this case is found to be {100}<011> for both the steels, the intensity being 3.1 for plain C steel and 3.4 for Nb-microalloyed steel.

The trends of variation of the maximum texture intensity with decreasing finish rolling temperature for all the three cases have been depicted graphically in Fig.4.30 to Fig.4.32.

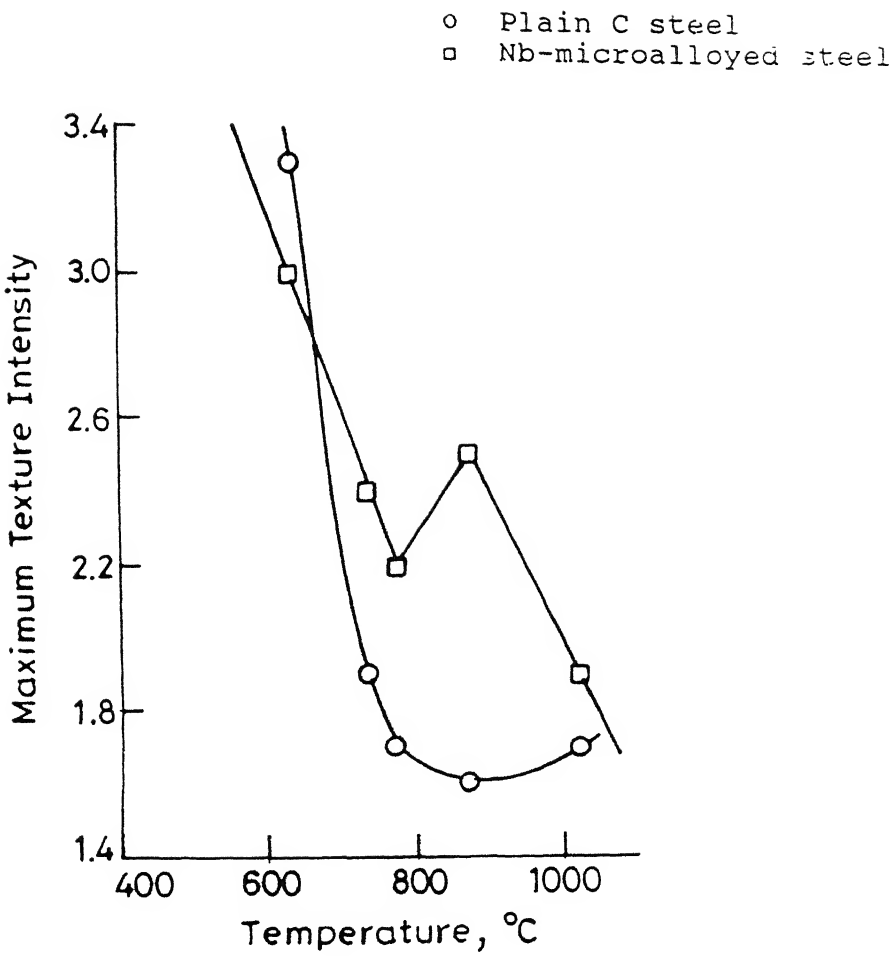

Figure 4.30: Variation of the maximum texture intensity of steels, austenitized at 1250°C and rolled upto 90%, with finish rolling temperature.

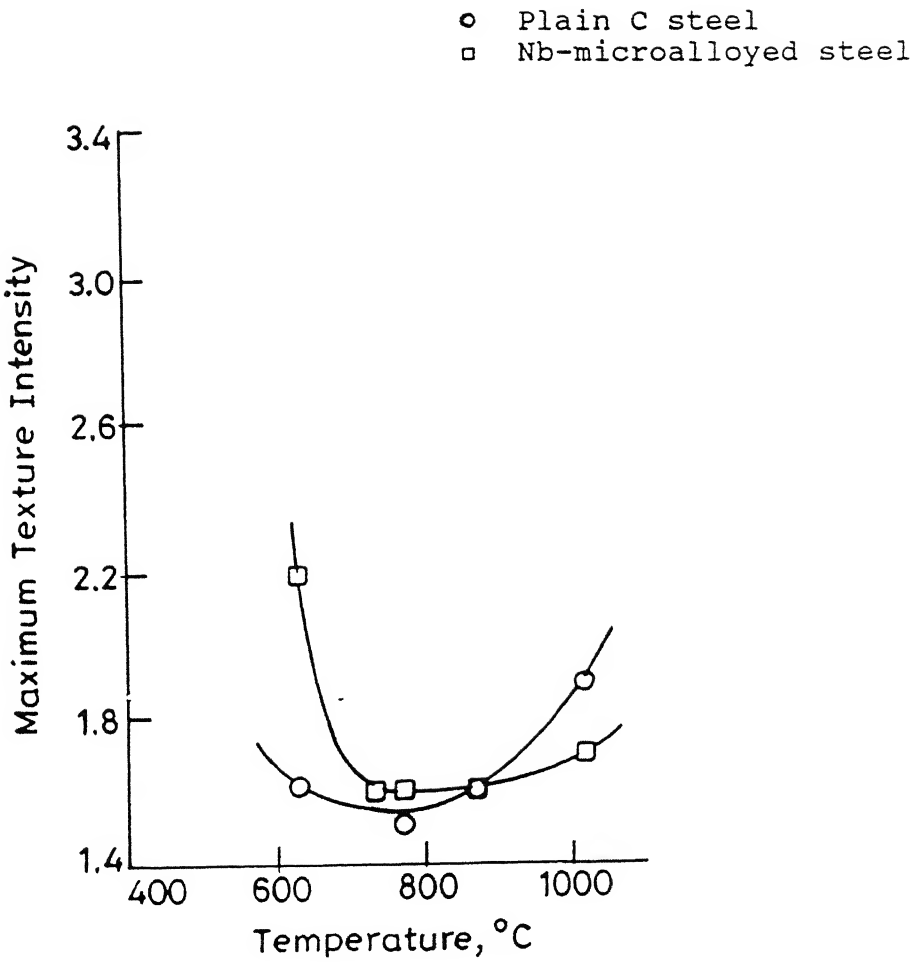

Figure 4.31: Variation of the maximum texture intensity of steels, austenitized at 1250°C and rolled upto 75%, with finish rolling temperature.

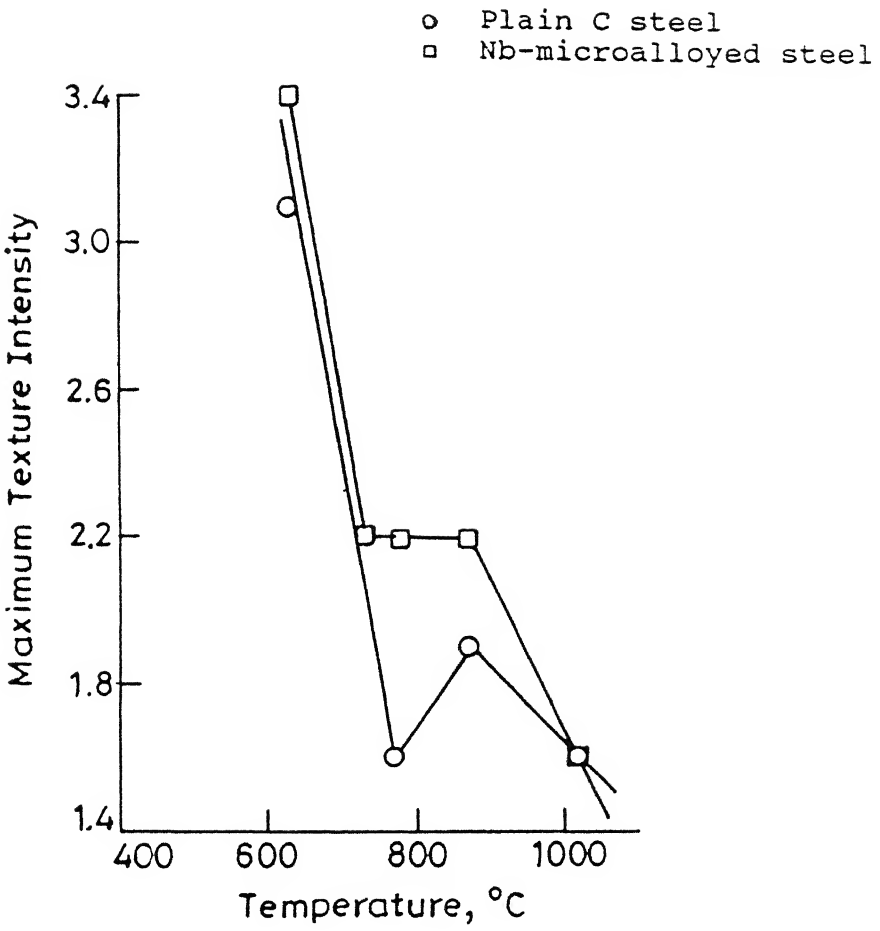

Figure 4.32: Variation of the maximum texture intensity of steels, austenitized at 1150°C and rolled upto 90%, with finish rolling temperature.

CHAPTER V

DISCUSSION

5.1 MICROSTRUCTURAL CHARACTERISTICS

5.1.1 Effect of finishing temperature

It is known that as the finishing temperature is lowered during controlled rolling, the grains become more and more flattened. When rolling takes place above T_{nr}, i.e. the γ-no recrystallization temperature, the austenite grains deform subsequently recrystallize, giving equiaxed grains. On the other hand, when deformation takes place below T_{nr}, the γ grains are essentially pancaked. The equiaxed γ grains, on transformation lead to an equiaxed ferrite grain structure, as was seen in the case of the steels, when finish rolled at 1020°C(i.e.above T_{nr}).

The ferrite structure obtained after finish rolling in the $\gamma_{nonrecryst.}$ range, i.e. at 870°C, is expected to be obtained from pancaked austenite. Profuse nucleation of the α grains at γ grain boundaries and on deformation bands inside, and their growth during transformation is also expected to produce equiaxed ferrite, but with a smaller grain size.

The existence of some elongated grains alongwith equiaxed ferrite grains in the steels finish rolled at 770°C and 730°C ($\gamma+\alpha$ interciritical range), can be explained by the fact that the proeutectoid ferrite grains get warm worked and hence get elongated. However, the temperature should be high enough for them to recrystallize at least partly. This seems to explain the presence of the elongated ferrite grains. Further, the increase in the amount of elongated grains with lowering of finishing temperature in the ($\gamma+\alpha$) range, can be explained by corresponding increase in the amount of proeutectoid ferrite. The fact, that

the ferrite grains obtained after finishing at 630°C are fully elongated, indicates that ferrite recrystallization takes place well above this temperature.

The structural features are more or less smeared along the rolling plane and, therefore the effect of rolling can be seen more clearly only along the longitudinal and the transverse sections of the specimens. A close observation shows that the grains show a preferential extension along the rolling direction, that is why they appear more elongated in the longitudinal sections than in the transverse section.

5.1.2 Effect of composition

The effect of Nb as microalloying element on the development of microstructure has been well documented [3,10,11]. Nb is known to suppress the γ as well as α recrystallization and subsequent grain growth during interpass intervals. This is the main reason why a much finer ferrite grain size is achieved in case of the Nb-microalloyed steel than in the plain C steel. This is true for all the finish rolling temperatures considered, especially those in the γ-region.

In case of finish rolling in the $\gamma+\alpha$ region, it is observed that the ferrite grains are more elongated in the Nb-microalloyed steel than in the plain C steel. Reasons similar to that given above are responsible for this behaviour. The effect of Nb on the steel finish rolled at 630°C, however, is not very significant because this temperature is much below the usual $\alpha_{recryst}$ temperature.

5.1.3 Effect of the amount of deformation

It is known that increasing amount of deformation increases the pearlite pancaking. This is also evident from the observation that pearlite bands are wider in case of steels rolled upto 75% reduction than those rolled upto 90% reduction. Furthermore, the ferrite grains in the former have been found to be larger than those in the latter steels especially in case of finish rolling in $\gamma_{recryst.}$ range. This is supported by the explanation given by Tanaka et al [3], that the recrystallized γ grain size decreases with increasing amount of deformation. This gives rise to smaller ferrite grains by subsequent transformation.

In the unrecrystallized γ, more and more subgrains are formed due to increasing deformation and hence, more ferrite nuclei are generated, as a result of which ferrite grains become finer. The same reason can be given to explain away the refinement of grains in case of finish rolling at 770°C and 730°C i.e. in the $\gamma+\alpha$ range. In case of steels finished at 630°C, the grains are essentially of cold worked ferrite.

5.1.4 Effect of austenite grain size

Towle and Gladman [5], and others [1,4] have shown that, if the amount of reduction is constant, the recrystallized γ grain size increases linearly with the initial grain size. This explains why, the grains obtained by finish rolling the two steels at 1020°C (austenitizing Temperature 1150°C, 90% reduction) are smaller than those obtained in case of steels austenitized at 1250°C (90% reduction) and finished at the same temperature.

When the conditions during rolling are such that γ

recrystallization is suppressed (i.e., when finish rolled below the $\gamma_{recryst.}$ range or micro-alloyed with Nb), the above reason will not hold good to explain the observed refinement of grain structure due to the decrease of the parent austenite grain size. The increase in the austenite surface area, and hence, the ferrite nucleation sites (due to decrease in the austenite grain size) is the probable reason behind the ferrite grain refinement in these cases.

5.2 VARIATION OF MICROSTRUCTURAL PARAMETERS

5.2.1 Grain shape parameters

The g_{12} value gives the ratio of grain dimensions along RD to that along TD, g_{13} gives that along RD to ND and g_{23} gives the same along TD to ND. Now, since the average grains get more and more elongated as the finishing temperature is decreased from 1020°C to 630°C, it is obvious that an increasing trend (with decreasing finishing temperature) will be observed in all the three above ratios.

Further, since the volume of each grain remains constant, the dimension along TD as well as ND will decrease with increasing elongation along RD. This explains why the increase in the values of g_{13} values exhibit a very large increase because the reduction in thickness is much more drastic than the increase in either width or length of the billet, during the rolling operation. Furthermore, it becomes apparent from the results that increase in length, during rolling is more than that of the width of the billet, due to anisotropic flow.

The effect of microalloying with Nb, on the grain

shape parameter, is not very clear. The probable reason is that the effect itself is sensitive to various other factors such as, temperature and amount of deformation, austenitizing temperature, the rolling schedule, etc. These factors influence the precipitation of Nb(C,N) in the matrix, which in turn influences the extent of deformation of individual grains in the three orthogonal directions RD, TD and ND. The pattern of precipitation of Nb(C,N) particles in the rolled material needs to be carefully examined in order to come to a definite conclusion in this matter. This is, however, beyond the scope of the present work.

5.2.2 Degree of orientation

Although the ferrite grains obtained after finish rolling in the γ-range are fully equiaxed, the structures exhibit a significant degree of physical orientation, when evaluated quantitatively. As the finishing temperature is lowered from 770°C to 630°C, these values follow a consistently increasing trend, apparently because of the increase in the extent of elongation of the ferrite grains.

Furthermore, the apparent contribution of the degree of planar orientation to the overall degree of orientation is much less than that of the degree of linear orientation, especially at the lowest finishing temperature. It may, hence, be inferred that due to ferrite cold working, the orientation of grains is affected more by their elongation along the RD that their stacking along the ND. This effect is less at the higher finishing temperatures.

As evident from the results, values of the degrees of orientation of the Nb-microalloyed steel are higher than the

corresponding values in case of plain C steel. This can be explained from the fact that the degree of elongation is more in case of the former (ref. section 5.1). However, there is a discrepancy in case of 75% rolled steels where the Nb steel, finish rolled at 770°C and 730°C exhibits lower degrees of orientation than the plain C steel. The most probable reason is the presence of Nb(C,N) particles in the matrix [13] of the Nb steel which may impede the movement of dislocations inside the proeutectoid ferrite grains, at 75% reduction, and hence prevent the deformation of these grains along the RD. But this can be a conjecture only, in the absence of any concrete evidence.

The effect of decreasing austenitizing temperature or, in other words, decreasing parent austenite grain size, has been known to increase the amount of elongated ferrite grains, especially at finishing temperatures below Ar_3. This explains the presence of higher degrees of orientation in case of steels austenitized at 1150°C, than those in case of steels austenitized at 1250°C.

5.2.3 Grain thickness along ND

As stated in the previous sections, the ferrite grain size decreases with decreasing finish rolling temperature, and the grain size corresponding to each finishing temperature is finer in case of Nb-microalloyed steel than increase of the plain C steel. This explains the observed decreasing trend in the grain thickness, with decreasing finishing temperature, for both the steels and the lower values of the grain thickness in case of Nb-microalloyed steel. However, at the lowest finishing

temperature this difference is very small because the influence of Nb(C,N) precipitation is not very significant in this case. It has been known (ref. section 2.1.4) that the grain size decreases with increasing amount of deformation and decreasing initial austenite grain size. This is also evident from the observed grain thickness values; e.g. the grain thickness values corresponding to the steels austenitized at 1250°C (75% reduction) are larger than those corresponding to the respective values of both the steels austenitized at 1250°C (90% reduction) and steels austenitized at 1150°C (90% reduction).

5.2.4 Rose-of-the-number-of-intersections

The nearly semicircular shape of the rose-of-the-number-of-intersections in case of the plain C steel finish rolled at 1020°C in all the three sets of samples, can be explained by the rather equiaxed nature of the ferrite grains, due to which very little orientation is observed in these samples (ref. section 5.2.2). Similarly, as the grains appear more and more elongated, the corresponding curves become more and more dumbbell shaped (extreme case of which is a circle touching the RD axis, which represents a completely oriented structure [17]). This shows that higher the degree of orientation, more will be the tendency of the curve to be of dumbbell shape.

As explained earlier, microalloying with Nb results in the suppression of recrystallization and hence the corresponding structures in Nb-steel are much more elongated than those in plain C steel. This explains the departure from the semicircular shape of the curves for the Nb microalloyed steel in

contrast to the behaviour of the corresponding sample in the plain C steel.

In case of the steels austenitized at 1150°C and rolled upto 90%, the roses-of-the-number-of-intersections appear somewhat elongated towards ND, right from the finishing temperature of 1020°C. This results from the fact that the grains are oriented more in this case than those in the other two sets. Similar explanation can be given for such small deviation from semicircular nature of curves in case of steels rolled upto 75%.

5.3 TEXTURE RESULTS

It has now been well established that if γ recrystallization takes place during controlled rolling, a weak {100}<001> cube texture develops in γ which is later on inherited by α as {100}<011>, after transformation. However, if γ recrystallization does not take place then sharp γ-rolling texture components, {110}<112> and {112}<111> are formed in the parent austenite which get transformed into {332}<113> and {113}<110> respectively in the resulting ferrite. When controlled rolling is finished in the intercritical temperature range, these texture components get sharpened because of additional contribution of ferrite rolling to these orientation. Steels finished in the ferritic range, however, contain the strongest texture components because most of the rolling passes are given in the ferritic range due to which existing ferrite {100}<011>, {332}<113> and {113}<110> texture components get sharpened. The reason of this sharpening is that more and more ferrite grains rotate to acquire these orientations due to cold rolling.

The maximum texture intensity of the Nb-microalloyed steel has generally been found to be higher than that of the plain C steel, at the respective finish rolling temperatures. This is because of early suppression of γ-recrystallization, due to which γ-rolling texture forms much earlier in a rolling schedule and thus, gets ample chance to get sharpened.

It has been observed that {100}<011> is the strongest ferrite texture component in case of the steels rolled upto 90% reduction. This is because the fraction of deformation given to the billet in the γ-range is large enough to produce strong cube {100}<001> texture in it, which later on transforms to {100}<011> in ferrite. This is not the case, however, with steels rolled upto 75% reduction. The probable reason for this is the inability of the extent of deformation, in this case, to produce a strong {100}<001> cube texture in austenite. These steels, instead, contain {111}<112> as the major texture component. The {332}<113> component is not very far away from {111}<112>. Therefore, the former changes its orientation to the latter, during cold deformation, because {111}<112> is a more stable component of texture. This phenomenon adds to the intensity of the {111}<112> component in these steels.

5.4 CORRELATION BETWEEN MICROSTRUCTURES AND TEXTURES

5.4.1 Correlation between microstructural features and textures

A striking correlation is apparent between the state of microstructure and the corresponding texture of the steel samples. This is supported by the fact that weak textures

correspond to lesser pancaked structures while more pancaking produces stronger textures. For example, the samples rolled upto 75% reduction exhibit less pancaked structures than those rolled upto 90% reduction, at corresponding finishing temperatures. This correlates well with weaker textures in the former case than in the latter. Further, in each set of samples, it is observed that the texture severity increases with decreasing finish rolling temperature (from 1020°C to 730°C), which corresponds well to the increasing degree of pancaking. The correlation between the most intense textures, produced by warm rolling at 630°C, and the corresponding microstructures is also readily perceptible [15].

An attempt has also been made towards achieving a more meaningful correlation of texture with quantitative characterization of the microstructures. The following section describes an attempt to correlate the microstructures and corresponding textures in the different samples with respect to the various microstructural parameters mentioned earlier.

5.4.2 Correlation between microstructures and textures with respect to various microstructural parameters

The change in the grain shape parameter form $\gamma+\alpha$ to α rolling temperature, follows a trend similar to that of the maximum texture intensity, in case of the steels rolled upto 90% reduction as well as upto 75% reduction, irrespective of the austenitizing temperature. The percentage change is less in the Nb steel than that in plain C steel when the austenitizing temperature in 1250°C and deformation is upto 90%. This tallies well with the corresponding change in the maximum texture intensities.

The grain thickness along ND shows an inverse correspondence with the maximum texture intensity, in case of steels rolled upto 90% (except a discrepancy at the finishing temperature of 870°C). There is no correlation, however, with the texture intensities of the steels rolled upto 75%.

It can thus be inferred that not much correlation is visible between the microstructures and textures of the two steels, when compared with respect to the grain shape parameter and the grain thickness along ND. However, the following discussion shows that a striking correlation exists, when the microstructures and textures are compared with respect to the degree of orientation of grains and the rose-of-the-number-of-intersections.

In case of the first set of samples, it has been observed that the highest and lowest values of degrees of orientation fall at the finishing temperatures corresponding to the highest and lowest values of the maximum texture intensity. For example, in case of plain C steel, both the parameters give a minima at the finishing temperature of 870°C which the values start increasing and reach a maximum value at the lowest finishing temperature i.e., 630°C. In case of the Nb-microalloyed steel also, the highest and lowest values of the degrees of orientation as well as the maximum texture intensity fall at the same finishing temperatures (ref. Figures 4.12 and 4.30). Similar trends are observed in the third set of samples too (ref. Figures 4.14 and 4.32). In case of the second set, however, no similarity is observed between the variations of the two parameters with finishing temperature.

It can be inferred, therefore, that the variation of the degree of orientation with finishing temperature, is similar to that of the corresponding maximum texture intensity with finishing temperature, in case of the steels rolled upto 90%. This means that a one-to-one correlation exists between the maximum texture intensity and the degree of orientation in steels which have been rolled upto 90%.

This is not the case with the steels rolled upto 75%. Furthermore, it has been observed that the strongest texture component, in case of the steels rolled upto 90%, is the rotated cube {100}<011> (which is obtained by transformation from the cube {100}<011> in γ). This component is weak in the samples, rolled upto 75%, and there the {111}<112> component is the strongest. It may be suggested on this basis, that correlation between microstructures and textures is possible only in case of steels having the rotated cube texture as a major component; i.e., in case of a large amount of deformation in the γ-range.

It has already been shown in section 5.2.4, that a direct correlation exists between the degree of orientation of grains and the rose-of-the-number-of-intersections. Therefore, these curves can also be used to correlate the microstructures and textures of controlled rolled steels. Further, when the roses-of-the-number-of-intersections, for the steels rolled upto 75%, are compared with their corresponding maximum texture intensity values, it is found that the shape of these curves exhibit a striking relation with the corresponding maximum texture intensity values, the only exceptions being the curve corresponding to plain C steel finish rolled at 1020°C and 770°C.

In case of the plain C steel, the roses corresponding to the samples finish rolled at 870°C, 730°C and 630°C have similar nature, which tallies well with their corresponding maximum texture intensity values being equal. Similarly in case of the Nb-steel, the more or less semicircular curves, corresponding to the samples finished at 870°C, 770°C and 730°C tally well with the equal and low values of the corresponding maximum texture intensity. The curve corresponding to finish rolling at 1020°C is somewhat elongated towards ND which is obvious since the corresponding maximum texture intensity is higher than those of the above three samples. The curve for the lowest finishing temperature i.e., 630°C, is dumbbell shaped which shows that the degree of orientation is quite high. The texture intensity is also found to be quite high in this case.

From this discussion, it may be concluded that the microstructures and textures can be correlated with respect to rose-of-the-number-of-intersections, even if the amount of deformation is as low as 75%.

CHAPTER VI

CONCLUSIONS

1. Controlled rolling of the plain C steel in the $\gamma_{recryst}$ range produces a coarse and fully equiaxed structure whereas in case of Nb-microalloyed steel, the corresponding structure in fine as well as pancaked because of the suppression of γ - recrystallization due to the presence of Nb(C,N).

2. The microstructures of the plain C steel finish rolled at various temperatures below the $\gamma_{recryst.}$ temperature, exhibit an increasing trend in pancaking as well as in grain refinement, with decreasing finish rolling temperature.

   Similar trend is there in case of Nb-microalloyed steel also, but the pancaking and grain refinement is more in this steel as compared to those in plain C steel, finish rolled at the corresponding temperatures.

3. Nb-microalloying does not influence the ferrite structure significantly when the steel is finished in the ferritic range, since this temperature is below the $\alpha_{recryst.}$ temperature.

4. The final grain size of both the steels varies inversely with the amount of deformation and directly with the initial γ grain size. The extent of pancaking, however, varies directly with the amount of deformation and inversely with the initial γ grain size.

5. The ratios of the grain diameters, along RD, TD and

ND, g_{12}, g_{13} and g_{23}, show in general, an increasing trend with the decrease in finish rolling temperatures, the change in g_{13} being the most drastic.

6. The degree of orientation, of plain C as well as Nb-microalloyed steel, generally increases with the decrease in the finish rolling temperature from 770°C to 630°C. The maximum degree of orientation is thus, observed at the finishing temperature of 630°C. This value is usually higher in case of Nb-microalloyed steel than that in case of plain C steel.

7. The overall degree of orientation of grain is influenced greatly by the degree of linear orientation whereas it is much less affected by the planar orientation of grains.

8. The average grain thickness, measured along ND, decreases consistently with decreasing finish rolling temperature. The grain thickness of Nb-microalloyed steel is always less than the corresponding grain thickness value of the plain C steel.

9. The roses-of-the-number-of-intersections reveal that the structures of the two steels are partially oriented along the RD.

10. The major texture component in the steels rolled upto 90% in {100}<011> and that in the steels rolled upto 75% is {111}<112>.

11. The maximum texture intensity of the plain C and Nb-microalloyed steel, increases with decreasing finish

rolling temperature. The values are generally higher in case of the Nb-microalloyed steel as compared to those in case of plain C steel, at the respective finishing temperatures.

12. The degrees of orientation and the roses-of-the-number-of-intersections correlate well with the maximum texture intensity at different finishing temperatures in case of steels rolled upto 90%. Further, correlation is also present, between the roses-of-the-number-of-intersections and the maximum texture intensities of the two steels, rolled upto 75%.

REFERENCES

1. T. Tanaka: Int. Met. Rev., 4, (1981)185.

2. R. K. Ray and J. J. Jonas: Int. Mater. Rev., 35,(1990)1.

3. T. Tanaka, N. Tabata, T. Hatomura, and C. Shiga: "Microalloying '75'", (1977)107.

4. C. Ouchi, T. Okita, T. Sanpei and I. Kozasu: Tetsu-to-Hangane, 63(1977)A53.

5. D. J. Towle and T. Gladman: Met. Sci., 13, (1979)246.

6. C. Ouchi, T. Sanpei, T. Okita and I. Kozasu: Am. Inst. of Min., Met. and Petro. Eng., New York, (1977)316.

7. T. Tanaka, T. Hatomura and N. Tabata: Tetsu-to-Hagane', 62,(1976)S206.

8. J. D. Jones and A. B. Rothwell: Iron and Steel Inst., London, (1968)78.

9. H. Sekine and T. Maruyama: Seitetsu Kenkyu, 289, (1976)11920.

10. K. J. Irvine, T. Gladman, J. Orr, and F. B. Pickering: J. Iron and Steel Inst., 208, (1970)717.

11. I. Kozasu: Trans. Iron Steel Inst. Jpn., 12, (1972)241.

12. R. Coladas, J. Masunave, and J. P. Bailon: Am. Inst. of Min., Met. and Petro. Eng., New York, (1977)341.

13. R. Priestner and E. de los Rios: The Met. Soc., London, 76, (1976)129.

14. H. Inagaki: Z. Metallkd., 74, (1983)716.

15. R. K. Ray, M. P. Butron-Guillen, J. J. Jonas and G. E. Ruddle: ISIJ Int., 32, (1992)203.

16. R. DeHoff: Quantitative Microscopy, ed. R. T. DeHoff and F. N. Rhines, McGraw-Hill, NY, (1968).

17. E. E. Underwood: Quantitative Microscopy, ed. R. T. DeHoff and F. N. Rhines, McGraw-Hill, NY, (1968)77.

APPENDIX

Details of the controlled rolled samples used for study:

(i) Set 1 (Austenitizing temperature 1250°C, 90% reduction):

Steel	Plain C Steel					Nb Microalloyed steel				
Sample	1RC	1C	1TCA	1TC	1FC	1RN	1N	1TNA	1TN	1FN
Finishing Temp. °C	1020	870	770	730	630	1020	870	770	730	630

(ii) Set 2 (Austenitizing temperature 1250°C, 75% reduction):

Steel	Plain C Steel					Nb Microalloyed steel				
Sample	3RC	3C	2TCA	2TC	2FC	3RN	3N	2TNA	2TN	2FN
Finishing Temp. °C	1020	870	770	730	630	1020	870	770	730	630

(iii) Set 3 (Austenitizing temperature 1150°C, 90% reduction):

Steel	Plain C Steel					Nb Microalloyed steel				
Sample	L1RC	L1C	1TCAL	L1TC	L1FC	L1RN	L1N	1TNAL	L1TN	L1FN
Finishing Temp. °C	1020	870	770	730	630	1020	870	770	730	630

TABLE I : Data for the Grain Shape Parameter

Sample	Sl. No.	d_1 cm	$\bar{d}_1$	d_2 cm	$\bar{d}_2$	d_3 cm	$\bar{d}_3$
1RC	1 2 3	0.90 0.90 0.95	0.90	1.25 1.20 1.30	1.25	1.30 1.15 1.30	1.3
1C	1 2 3	0.60 0.55 0.60	0.60	0.75 0.70 0.80	0.75	0.55 0.50 0.45	0.5
1TCA	1 2 3	0.55 0.50 0.50	0.55	0.65 0.60 0.60	0.6	0.45 0.40 0.40	0.4
1TC	1 2 3	0.70 0.60 0.60	0.60	0.60 0.65 0.55	0.6	0.45 0.40 0.45	0.45
1FC	1 2 3	1.65 1.60 1.50	1.60	1.00 1.10 1.20	1.1	0.30 0.35 0.30	0.3
1RN	1 2 3	0.75 0.70 0.65	0.70	0.75 0.85 0.85	0.8	0.80 0.75 0.70	0.75
1N	1 2 3	0.40 0.45 0.40	0.40	0.55 0.50 0.50	0.5	0.45 0.45 0.45	0.45
1TNA	1 2 3	0.80 0.85 0.80	0.80	0.60 0.65 0.70	0.65	0.45 0.45 0.40	0.45
1TN	1 2 3	1.20 1.25 1.30	1.25	1.05 1.10 1.15	1.1	0.45 0.45 0.40	0.45
1FN	1 2 3	0.80 0.85 0.90	0.85	0.65 0.60 0.55	0.6	0.15 0.15 0.20	0.15

Contd.

Sample	Sl. No.	d_1 cm	$\bar{d}_1$	d_2 cm	$\bar{d}_2$	d_3 cm	$\bar{d}_3$
3RC	1 2 3	2.05 2.20 2.40	2.20	1.50 2.00 2.05	2.0	2.25 2.15 1.85	2.1
3C	1 2 3	1.15 1.15 1.15	1.15	1.60 1.65 1.45	1.56	0.95 0.90 0.90	0.92
2TCA	1 2 3	1.25 1.20 1.25	1.25	1.00 1.05 1.00	1.05	0.70 0.75 0.75	0.73
2TC	1 2 3	1.70 1.75 1.85	1.76	0.90 0.90 0.75	0.85	0.90 0.85 0.90	0.88
2FC	1 2 3	1.65 1.60 1.85	1.70	0.70 0.75 0.65	0.70	0.40 0.50 0.45	0.45
3RN	1 2 3	1.55 1.55 1.40	1.50	1.55 1.50 1.45	1.50	1.05 1.10 1.10	1.08
3N	1 2 3	0.95 0.90 0.85	0.90	0.85 0.70 0.85	0.80	0.85 0.60 0.60	0.60
2TNA	1 2 3	0.55 0.60 0.55	0.57	0.55 0.50 0.45	0.50	0.40 0.40 0.35	0.38
2TN	1 2 3	0.75 0.70 0.65	0.70	0.50 0.50 0.50	0.50	0.35 0.40 0.35	0.37
2FN	1 2 3	0.80 0.80 0.95	0.85	0.50 0.50 0.40	0.47	0.25 0.30 0.30	0.28

Contd.

Sample	Sl. No.	d_1 cm	$\bar{d}_1$	d_2 cm	$\bar{d}_2$	d_3 cm	$\bar{d}_3$
L1RC	1 2 3	1.25 1.15 1.10	1.17	0.90 0.95 0.85	0.90	0.75 0.80 0.80	0.78
L1C	1 2 3	0.75 0.70 0.80	0.75	0.80 0.80 0.85	0.82	0.50 0.45 0.45	0.47
1TCAL	1 2 3	0.95 0.95 1.00	0.97	0.75 0.75 0.80	0.77	0.35 0.30 0.25	0.30
L1TC	1 2 3	1.70 1.60 1.75	0.68	0.85 0.85 0.95	0.88	0.45 0.40 0.35	0.40
L1FC	1 2 3	1.80 1.70 1.70	1.73	0.70 0.70 0.65	0.68	0.30 0.25 0.30	0.28
L1RN	1 2 3	1.20 1.30 1.10	1.20	1.00 0.95 1.00	0.98	0.90 0.95 0.90	0.92
L1N	1 2 3	0.85 0.80 0.75	0.80	0.75 0.75 0.75	0.75	0.40 0.45 0.45	0.42
1TNAL	1 2 3	0.60 0.60 0.65	0.62	0.60 0.60 0.65	0.62	0.30 0.30 0.30	0.30
L1TN	1 2 3	1.00 1.00 0.95	0.98	0.70 0.70 0.65	0.68	0.25 0.25 0.30	0.27
L1FN	1 2 3	1.45 1.50 1.35	1.43	0.70 0.60 0.55	0.62	0.15 0.15 0.20	0.17

TABLE II : Data for the Degrees of Orientation

Set 1 : (a) 1RC

Sl. No. s	Length of Secant					
	105 mm		71 mm		107.5 mm	
	$(N_L)_{\parallel}$	$(\bar{N}_L)_{\parallel}$	$(N_L)_{\perp}$	$(\bar{N}_L)_{\perp}$	$(N_L)_{I}$	$(\bar{N}_L)_{I}$
1	0.286		0.282		0.232	
2	0.286		0.239		0.325	
3	0.295		0.296		0.251	
4	0.276		0.282		0.251	
5	0.229	0.264	0.296	0.293	0.232	0.254
6	0.200		0.366		0.223	
7	0.314		0.282		0.232	
8	0.248		0.267		0.242	
9	0.257		0.296		0.307	
10	0.247		0.324		0.242	

(b) 1C

Sl. No.	Length of Secant					
	105.5mm		65 mm		98.0 mm	
	$(N_L)_{\parallel}$	$(\bar{N}_L)_{\parallel}$	$(N_L)_{\perp}$	$(\bar{N}_L)_{\perp}$	$(N_L)_{I}$	$(\bar{N}_L)_{I}$
1	0.351		0.400		0.357	
2	0.360		0.354		0.326	
3	0.417		0.338		0.306	
4	0.360		0.385		0.306	
5	0.322	0.3733	0.400	0.3845	0.398	0.3471
6	0.369		0.369		0.377	
7	0.369		0.369		0.398	
8	0.379		0.400		0.347	
9	0.417		0.461		0.357	
10	0.389		0.369		0.306	

(c) 1TCA

Sl. No.	Length of Secant					
	103 mm		69.5 mm		103.0 mm	
	$(N_L)_{\parallel}$	$(\bar{N}_L)_{\parallel}$	$(N_L)_{\perp}$	$(\bar{N}_L)_{\perp}$	$(N_L)_{I}$	$(\bar{N}_L)_{I}$
1	0.359		0.417		0.291	
2	0.456		0.432		0.349	
3	0.434		0.489		0.320	
4	0.434		0.460		0.340	
5	0.437	0.434	0.446	0.451	0.320	0.331
6	0.476		0.460		0.320	
7	0.456		0.446		0.349	
8	0.456		0.432		0.330	
9	0.379		0.460		0.359	
10	0.456		0.460		0.330	

(d) 1TC

Sl. No.	Length of Secant					
	105 mm		70 mm		85 mm	
	$(N_L)_{\parallel}$	$(\bar{N}_L)_{\parallel}$	$(N_L)_{\perp}$	$(\bar{N}_L)_{\perp}$	$(N_L)_{I}$	$(\bar{N}_L)_{I}$
1	0.504		0.557		0.294	
2	0.428		0.457		0.353	
3	0.371		0.543		0.318	
4	0.438		0.429		0.318	
5	0.409	0.417	0.471	0.467	0.294	0.327
6	0.447		0.486		0.318	
7	0.362		0.443		0.376	
8	0.409		0.428		0.306	
9	0.438		0.443		0.341	
10	0.362		0.414		0.353	

(e) 1FC

Sl. No.	Length of Secant					
	104.5 mm		70.5 mm		80.5 mm	
	$(N_L)_{\parallel}$	$(\bar{N}_L)_{\parallel}$	$(N_L)_{\perp}$	$(\bar{N}_L)_{\perp}$	$(N_L)_{I}$	$(\bar{N}_L)_{I}$
1	0.364		0.468		0.397	
2	0.344		0.511		0.373	
3	0.249		0.539		0.360	
4	0.258		0.496		0.362	
5	0.201	0.264	0.481	0.481	0.314	0.341
6	0.306		0.486		0.339	
7	0.249		0.517		0.316	
8	0.268		0.417		0.365	
9	0.335		0.446		0.278	
10	0.344		0.478		0.306	

(f) 1RN

Sl. No.	Length of Secant					
	105 mm		70.0 mm		85 mm	
	$(N_L)_{\parallel}$	$(\bar{N}_L)_{\parallel}$	$(N_L)_{\perp}$	$(\bar{N}_L)_{\perp}$	$(N_L)_{I}$	$(\bar{N}_L)_{I}$
1	0.371		0.357		0.317	
2	0.390		0.328		0.341	
3	0.343		0.371		0.435	
4	0.352		0.414		0.306	
5	0.362	0.350	0.386	0.377	0.259	0.328
6	0.286		0.400		0.353	
7	0.371		0.443		0.306	
8	0.390		0.371		0.353	
9	0.343		0.400		0.282	
10	0.295		0.300		0.329	

(g) 1N

Sl. No.	Length of Secant					
	105 mm		69.5 mm		103.5 mm	
	$(N_L)_{\parallel}$	$(\bar{N}_L)_{\parallel}$	$(N_L)_{\perp}$	$(\bar{N}_L)_{\perp}$	$(N_L)_{I}$	$(\bar{N}_L)_{I}$
1	0.314		0.475		0.317	
2	0.342		0.503		0.341	
3	0.305		0.460		0.435	
4	0.343		0.446		0.306	
5	0.295	0.334	0.460	0.460	0.259	0.287
6	0.305		0.475		0.353	
7	0.371		0.475		0.306	
8	0.362		0.432		0.353	
9	0.333		0.417		0.282	
10	0.371		0.460		0.329	

(h) 1TNA

Sl. No.	Length of Secant					
	106.5 mm		69.5 mm		103.0 mm	
	$(N_L)_{\parallel}$	$(\bar{N}_L)_{\parallel}$	$(N_L)_{\perp}$	$(\bar{N}_L)_{\perp}$	$(N_L)_{I}$	$(\bar{N}_L)_{I}$
1	0.413		0.547		0.349	
2	0.446		0.460		0.369	
3	0.488		0.504		0.320	
4	0.446		0.547		0.349	
5	0.478	0.446	0.518	0.506	0.300	0.342
6	0.478		0.504		0.349	
7	0.385		0.517		0.349	
8	0.451		0.532		0.369	
9	0.460		0.489		0.339	
10	0.413		0.446		0.330	

(i) 1TN

Sl. No.	Length of Secant					
	103 mm		69 mm		85 mm	
	$(N_L)_{\parallel}$	$(\bar{N}_L)_{\parallel}$	$(N_L)_{\perp}$	$(\bar{N}_L)_{\perp}$	$(N_L)_{I}$	$(\bar{N}_L)_{I}$
1	0.320		0.478		0.341	
2	0.388		0.493		0.329	
3	0.427		0.493		0.353	
4	0.301		0.507		0.306	
5	0.427	0.363	0.522	0.487	0.235	0.318
6	0.359		0.507		0.318	
7	0.320		0.464		0.306	
8	0.349		0.493		0.259	
9	0.359		0.464		0.353	
10	0.379		0.449		0.376	

(j) 1FN

Sl. No.	Length of Secant					
	103 mm		69 mm		85 mm	
	$(N_L)_{\parallel}$	$(\bar{N}_L)_{\parallel}$	$(N_L)_{\perp}$	$(\bar{N}_L)_{\perp}$	$(N_L)_{I}$	$(\bar{N}_L)_{I}$
1	0.223		0.379		0.306	
2	0.243		0.430		0.294	
3	0.272		0.418		0.294	
4	0.243		0.456		0.365	
5	0.272	0.264	0.443	0.497	0.271	0.309
6	0.291		0.405		0.365	
7	0.291		0.468		0.306	
8	0.262		0.430		0.294	
9	0.252		0.456		0.318	
10	0.291		0.456		0.282	

Set 2 : (a) 3RC

Sl. No.	Length of Secant					
	104 mm		69 mm		104.5 mm	
	$(N_L)_{\parallel}$	$(\bar{N}_L)_{\parallel}$	$(N_L)_{\perp}$	$(\bar{N}_L)_{\perp}$	$(N_L)_{I}$	$(\bar{N}_L)_{I}$
1	0.240		0.159		0.191	
2	0.269		0.217		0.172	
3	0.231		0.217		0.143	
4	0.135		0.159		0.163	
5	0.135	0.188	0.188	0.198	0.172	0.166
6	0.154		0.217		0.153	
7	0.221		0.188		0.163	
8	0.173		0.202		0.191	
9	0.192		0.188		0.143	
10	0.135		0.231		0.172	

(b) 3C

Sl. No.	Length of Secant					
	104.5 mm		68.5 mm		103.0 mm	
	$(N_L)_{\parallel}$	$(\bar{N}_L)_{\parallel}$	$(N_L)_{\perp}$	$(\bar{N}_L)_{\perp}$	$(N_L)_{I}$	$(\bar{N}_L)_{I}$
1	0.239		0.321		0.204	
2	0.182		0.292		0.233	
3	0.191		0.263		0.233	
4	0.210		0.292		0.194	
5	0.172	0.204	0.277	0.293	0.223	0.209
6	0.201		0.321		0.213	
7	0.220		0.321		0.175	
8	0.220		0.277		0.194	
9	0.229		0.321		0.223	
10	0.172		0.248		0.194	

(c) 2TCA

Sl. No.	Length of Secant					
	104.5 mm		68.5 mm		103.0 mm	
	$(N_L)_{\parallel}$	$(\bar{N}_L)_{\parallel}$	$(N_L)_{\perp}$	$(\bar{N}_L)_{\perp}$	$(N_L)_{I}$	$(\bar{N}_L)_{I}$
1	0.268		0.350		0.291	
2	0.229		0.336		0.291	
3	0.268		0.350		0.262	
4	0.239		0.365		0.252	
5	0.287	0.243	0.263	0.325	0.281	0.268
6	0.229		0.292		0.252	
7	0.248		0.306		0.243	
8	0.182		0.306		0.281	
9	0.258		0.350		0.262	
10	0.220		0.336		0.252	

(d) 2TC

Sl. No.	Length of Secant					
	104.5 mm		69 mm		103.0 mm	
	$(N_L)_{\parallel}$	$(\bar{N}_L)_{\parallel}$	$(N_L)_{\perp}$	$(\bar{N}_L)_{\perp}$	$(N_L)_{I}$	$(\bar{N}_L)_{I}$
1	0.210		0.333		0.262	
2	0.258		0.362		0.252	
3	0.220		0.348		0.252	
4	0.268		0.333		0.281	
5	0.258	0.232	0.333	0.346	0.272	0.271
6	0.297		0.333		0.243	
7	0.163		0.377		0.262	
8	0.191		0.377		0.281	
9	0.249		0.348		0.311	
10	0.210		0.319		0.291	

(e) 2FC

Sl. No.	Length of Secant					
	105 mm		69 mm		103.0 mm	
	$(N_L)_{\parallel}$	$(\bar{N}_L)_{\parallel}$	$(N_L)_{\perp}$	$(\bar{N}_L)_{\perp}$	$(N_L)_{I}$	$(\bar{N}_L)_{I}$
1	0.276		0.391		0.272	
2	0.238		0.377		0.272	
3	0.228		0.420		0.281	
4	0.228		0.362		0.233	
5	0.228	0.238	0.391	0.397	0.272	0.272
6	0.238		0.406		0.262	
7	0.200		0.391		0.281	
8	0.219		0.377		0.272	
9	0.267		0.435		0.291	
10	0.257		0.420		0.281	

(f) 3RN

Sl. No.	Length of Secant					
	104.5 mm		69 mm		104.7 mm	
	$(N_L)_{\parallel}$	$(\bar{N}_L)_{\parallel}$	$(N_L)_{\perp}$	$(\bar{N}_L)_{\perp}$	$(N_L)_{I}$	$(\bar{N}_L)_{I}$
1	0.163		0.217		0.200	
2	0.153		0.203		0.191	
3	0.115		0.203		0.200	
4	0.191		0.232		0.181	
5	0.182	0.195	0.203	0.206	0.172	0.187
6	0.201		0.203		0.181	
7	0.239		0.188		0.191	
8	0.239		0.188		0.172	
9	0.229		0.217		0.162	
10	0.239		0.203		0.219	

(g) 3N

Sl. No.	Length of Secant					
	104.7 mm		69 mm		104.0 mm	
	$(N_L)_{\parallel}$	$(\bar{N}_L)_{\parallel}$	$(N_L)_{\perp}$	$(\bar{N}_L)_{\perp}$	$(N_L)_{I}$	$(\bar{N}_L)_{I}$
1	0.200		0.304		0.279	
2	0.219		0.289		0.269	
3	0.200		0.319		0.288	
4	0.248		0.261		0.259	
5	0.267	0.225	0.304	0.301	0.269	0.263
6	0.258		0.319		0.259	
7	0.162		0.348		0.298	
8	0.200		0.304		0.250	
9	0.219		0.289		0.192	
10	0.277		0.275		0.269	

(h) 2TNA

Sl. No.	Length of Secant					
	105.5 mm		68.5 mm		104.5 mm	
	$(N_L)_{\parallel}$	$(\bar{N}_L)_{\parallel}$	$(N_L)_{\perp}$	$(\bar{N}_L)_{\perp}$	$(N_L)_{I}$	$(\bar{N}_L)_{I}$
1	0.332		0.379		0.277	
2	0.284		0.350		0.258	
3	0.351		0.321		0.306	
4	0.322		0.350		0.306	
5	0.360	0.321	0.336	0.347	0.258	0.279
6	0.341		0.306		0.325	
7	0.351		0.336		0.239	
8	0.322		0.379		0.297	
9	0.303		0.350		0.258	
10	0.246		0.365		0.268	

(i) 2TN

Sl. No.	Length of Secant					
	105.5 mm		68.2 mm		103.0 mm	
	$(N_L)_{\parallel}$	$(\bar{N}_L)_{\parallel}$	$(N_L)_{\perp}$	$(\bar{N}_L)_{\perp}$	$(N_L)_{I}$	$(\bar{N}_L)_{I}$
1	0.341		0.410		0.281	
2	0.322		0.337		0.311	
3	0.284		0.439		0.272	
4	0.199		0.381		0.281	
5	0.275	0.297	0.469	0.394	0.272	0.282
6	0.303		0.439		0.272	
7	0.322		0.352		0.281	
8	0.341		0.396		0.272	
9	0.294		0.337		0.291	
10	0.294		0.381		0.291	

(j) 2FN

Sl. No.	Length of Secant					
	105.5 mm		68.5 mm		103.0 mm	
	$(N_L)_{\parallel}$	$(\bar{N}_L)_{\parallel}$	$(N_L)_{\perp}$	$(\bar{N}_L)_{\perp}$	$(N_L)_{I}$	$(\bar{N}_L)_{I}$
1	0.161		0.409		0.320	
2	0.133		0.482		0.272	
3	0.208		0.394		0.281	
4	0.180		0.423		0.281	
5	0.180	0.178	0.423	0.433	0.243	0.282
6	0.189		0.394		0.320	
7	0.208		0.467		0.291	
8	0.161		0.467		0.262	
9	0.189		0.409		0.262	
10	0.171		0.467		0.291	

Set 3 : (a) L1RC

Sl. No.	Length of Secant					
	104.5 mm		70 mm		102.5 mm	
	$(N_L)_{\parallel}$	$(\bar{N}_L)_{\parallel}$	$(N_L)_{\perp}$	$(\bar{N}_L)_{\perp}$	$(N_L)_{I}$	$(\bar{N}_L)_{I}$
1	0.277		0.340		0.312	
2	0.287		0.298		0.254	
3	0.277		0.355		0.293	
4	0.296		0.312		0.263	
5	0.287	0.280	0.326	0.332	0.234	0.269
6	0.287		0.355		0.263	
7	0.277		0.340		0.312	
8	0.258		0.326		0.254	
9	0.287		0.340		0.244	
10	0.268		0.326		0.263	

(b) L1C

Sl. No.	Length of Secant					
	102.5 mm		70.5 mm		104.2 mm	
	$(N_L)_{\parallel}$	$(\bar{N}_L)_{\parallel}$	$(N_L)_{\perp}$	$(\bar{N}_L)_{\perp}$	$(N_L)_{I}$	$(\bar{N}_L)_{I}$
1	0.293		0.411		0.297	
2	0.293		0.355		0.316	
3	0.302		0.350		0.316	
4	0.302		0.397		0.306	
5	0.312	0.2898	0.411	0.3895	0.287	0.2995
6	0.283		0.397		0.316	
7	0.273		0.397		0.316	
8	0.293		0.369		0.258	
9	0.293		0.411		0.287	
10	0.254		0.397		0.296	

(c) 1TCAL

Sl. No.	Length of Secant					
	104.5 mm		70.5 mm		103.0 mm	
	$(N_L)_{\parallel}$	$(\bar{N}_L)_{\parallel}$	$(N_L)_{\perp}$	$(\bar{N}_L)_{\perp}$	$(N_L)_{I}$	$(\bar{N}_L)_{I}$
1	0.335		0.440		0.359	
2	0.383		0.482		0.340	
3	0.364		0.454		0.388	
4	0.402		0.440		0.437	
5	0.383	0.3705	0.468	0.454	0.398	0.379
6	0.354		0.454		0.340	
7	0.421		0.454		0.320	
8	0.316		0.440		0.369	
9	0.383		0.440		0.437	
10	0.364		0.468		0.398	

(d) L1TC

Sl. No.	Length of Secant					
	104 mm		70.5 mm		104.5 mm	
	$(N_L)_{\parallel}$	$(\bar{N}_L)_{\parallel}$	$(N_L)_{\perp}$	$(\bar{N}_L)_{\perp}$	$(N_L)_{I}$	$(\bar{N}_L)_{I}$
1	0.269		0.468		0.287	
2	0.259		0.454		0.287	
3	0.288		0.553		0.287	
4	0.308		0.454		0.268	
5	0.336	0.281	0.440	0.472	0.306	0.283
6	0.259		0.468		0.277	
7	0.288		0.425		0.277	
8	0.279		0.482		0.287	
9	0.279		0.496		0.249	
10	0.250		0.482		0.306	

(e) L1FC

Sl. No.	Length of Secant					
	104.2 mm		71 mm		102.5 mm	
	$(N_L)_{\parallel}$	$(\bar{N}_L)_{\parallel}$	$(N_L)_{\perp}$	$(\bar{N}_L)_{\perp}$	$(N_L)_{I}$	$(\bar{N}_L)_{I}$
1	0.230		0.563		0.380	
2	0.201		0.577		0.429	
3	0.249		0.577		0.409	
4	0.278		0.591		0.341	
5	0.240	0.239	0.648	0.560	0.332	0.356
6	0.278		0.563		0.302	
7	0.221		0.535		0.332	
8	0.241		0.493		0.312	
9	0.211		0.521		0.351	
10	0.240		0.535		0.371	

(f) L1RN

Sl. No.	Length of Secant					
	105 mm		70.5 mm		102.5 mm	
	$(N_L)_{\parallel}$	$(\bar{N}_L)_{\parallel}$	$(N_L)_{\perp}$	$(\bar{N}_L)_{\perp}$	$(N_L)_{I}$	$(\bar{N}_L)_{I}$
1	0.371		0.355		0.410	
2	0.333		0.355		0.351	
3	0.343		0.326		0.341	
4	0.371		0.397		0.361	
5	0.362	0.337	0.397	0.372	0.322	0.347
6	0.324		0.383		0.341	
7	0.343		0.440		0.371	
8	0.286		0.425		0.351	
9	0.343		0.369		0.361	
10	0.295		0.369		0.263	

(g) L1N

Sl. No.	Length of Secant					
	105 mm		71 mm		102.0 mm	
	$(N_L)_{\parallel}$	$(\bar{N}_L)_{\parallel}$	$(N_L)_{\perp}$	$(\bar{N}_L)_{\perp}$	$(N_L)_{I}$	$(\bar{N}_L)_{I}$
1	0.381		0.507		0.323	
2	0.267		0.451		0.372	
3	0.305		0.465		0.363	
4	0.381		0.535		0.333	
5	0.343	0.346	0.493	0.484	0.294	0.344
6	0.381		0.451		0.392	
7	0.390		0.422		0.333	
8	0.333		0.465		0.343	
9	0.343		0.535		0.333	
10	0.333		0.521		0.353	

(h) 1TNAL

Sl. No.	Length of Secant					
	104 mm		70.5 mm		102.0 mm	
	$(N_L)_{\parallel}$	$(\bar{N}_L)_{\parallel}$	$(N_L)_{\perp}$	$(\bar{N}_L)_{\perp}$	$(N_L)_{I}$	$(\bar{N}_L)_{I}$
1	0.317		0.525		0.333	
2	0.423		0.610		0.372	
3	0.327		0.539		0.382	
4	0.394		0.511		0.411	
5	0.356	0.369	0.596	0.5603	0.372	0.382
6	0.385		0.567		0.451	
7	0.394		0.596		0.402	
8	0.298		0.553		0.392	
9	0.394		0.567		0.353	
10	0.404		0.539		0.353	

(i) L1TN

Sl. No.	Length of Secant					
	104.2 mm		70.5 mm		104.2 mm	
	$(N_L)_{\parallel}$	$(\bar{N}_L)_{\parallel}$	$(N_L)_{\perp}$	$(\bar{N}_L)_{\perp}$	$(N_L)_{I}$	$(\bar{N}_L)_{I}$
1	0.326		0.610		0.479	
2	0.307		0.596		0.441	
3	0.307		0.652		0.422	
4	0.345		0.638		0.422	
5	0.316	0.329	0.539	0.604	0.403	0.414
6	0.316		0.624		0.393	
7	0.364		0.596		0.364	
8	0.355		0.610		0.422	
9	0.316		0.581		0.412	
10	0.336		0.596		0.384	

(j) L1FN

Sl. No.	Length of Secant					
	104.2 mm		70.5 mm		104.5 mm	
	$(N_L)_{\parallel}$	$(\bar{N}_L)_{\parallel}$	$(N_L)_{\perp}$	$(\bar{N}_L)_{\perp}$	$(N_L)_{I}$	$(\bar{N}_L)_{I}$
1	0.388		0.612		0.431	
2	0.278		0.652		0.392	
3	0.388		0.681		0.383	
4	0.278		0.681		0.373	
5	0.316	0.303	0.667	0.657	0.344	0.388
6	0.259		0.652		0.402	
7	0.259		0.652		0.354	
8	0.307		0.610		0.392	
9	0.259		0.638		0.431	
10	0.297		0.681		0.383	

TABLE III : Grain Thickness along N.D. (at 500X)

Set 1 (a) 1RC

Sl. No.	Length of Secant (mm)	No. of grains	Grain thickness (mm)	Av. grain thickness (mm)
1	60.0	14	4.28	
2	63.5	17	3.73	
3	63.5	15	4.23	4.01
4	68.0	16	4.25	
5	60.5	17	3.56	

(b) 1C

Sl. No.	Length of Secant (mm)	No. of grains	Grain thickness (mm)	Av. grain thickness (mm)
1	64.5	26	2.48	
2	67.0	22	3.04	
3	61.5	20	3.07	2.86
4	59.5	22	2.70	
5	62.5	21	2.97	

(c) 1TCA

Sl. No.	Length of Secant (mm)	No. of grains	Grain thickness (mm)	Av. grain thickness (mm)
1	65.0	28	2.32	
2	67.0	25	2.68	
3	67.5	24	2.81	2.66
4	66.0	24	2.75	
5	66.5	24	2.77	

(d) 1TC

Sl. No.	Length of Secant (mm)	No. of grains	Grain thickness (mm)	Av. grain thickness (mm)
1	63.5	23	2.76	
2	67.5	23	2.93	
3	63.0	26	2.42	2.63
4	62.5	25	2.50	
5	66.0	26	2.54	

(e) 1FC

Sl. No.	Length of Secant (mm)	No. of grains	Grain thickness (mm)	Av. grain thickness (mm)
1	66.5	48	1.38	
2	65.5	42	1.56	
3	67.5	43	1.57	1.50
4	66.5	44	1.51	
5	64.0	43	1.48	

(f) 1RN

Sl. No.	Length of Secant (mm)	No. of grains	Grain thickness (mm)	Av. grain thickness (mm)
1	61.5	18	3.41	
2	65.0	20	3.25	
3	62.0	23	2.69	3.00
4	65.0	26	2.50	
5	63.0	20	3.15	

(g) 1N

Sl. No.	Length of Secant (mm)	No. of grains	Grain thickness (mm)	Av. grain thickness (mm)
1	63.5	29	2.18	
2	61.5	27	2.27	
3	60.5	26	2.32	2.32
4	63.0	25	2.52	
5	61.5	27	2.27	

(h) 1TNA

Sl. No.	Length of Secant (mm)	No. of grains	Grain thickness (mm)	Av. grain thickness (mm)
1	60.5	27	2.24	
2	63.5	27	2.35	
3	65.5	26	2.52	2.25
4	67.5	34	1.98	
5	65.5	30	2.18	

(i) 1TN

Sl. No.	Length of Secant (mm)	No. of grains	Grain thickness (mm)	Av. grain thickness (mm)
1	64.5	32	2.01	
2	60.5	30	2.01	
3	62.5	29	2.15	2.09
4	64.5	30	2.15	
5	65.0	31	2.09	

(j) 1FN

Sl. No.	Length of Secant (mm)	No. of grains	Grain thickness (mm)	Av. grain thickness (mm)
1	49.5	36	1.37	
2	56.5	38	1.49	
3	5.75	39	1.47	1.45
4	48.0	34	1.41	
5	56.5	37	1.52	

Set 2 (a) 3RC

Sl. No.	Length of Secant (mm)	No. of intersecting grains	Grain thickness (mm)	Av. grain thickness (mm)
1	53.0	04	13.25	
2	54.5	09	6.05	
3	60.0	07	8.57	
4	58.5	05	11.70	
5	62.0	07	8.86	9.30
6	55.0	05	11.00	
7	55.5	07	7.93	
8	54.5	06	9.08	
9	58.0	07	8.30	
10	59.5	07	8.40	

(b) 3C

Sl. No.	Length of Secant (mm)	No. of intersecting grains	Grain thickness (mm)	Av. grain thickness (mm)
1	52.0	08	6.50	
2	58.0	09	6.40	
3	55.0	08	6.90	
4	57.5	10	5.75	
5	50.0	07	7.10	6.30
6	50.0	10	5.00	
7	56.0	09	6.20	
8	48.0	09	5.30	
9	53.0	09	5.80	
10	49.0	06	8.20	

(c) 2TCA

Sl. No.	Length of Secant (mm)	No. of intersecting grains	Grain thickness (mm)	Av. grain thickness (mm)
1	57.0	15	3.80	
2	58.0	15	3.86	
3	57.5	14	4.10	
4	57.0	14	4.07	
5	50.5	13	3.88	4.20
6	54.0	11	4.90	
7	60.5	15	4.03	
8	53.0	10	5.30	
9	55.0	13	4.20	
10	59.0	15	3.90	

(d) 2TC

Sl. No.	Length of Secant (mm)	No. of intersecting grains	Grain thickness (mm)	Av. grain thickness (mm)
1	60.0	16	3.75	
2	59.0	17	3.47	
3	61.5	17	3.61	
4	61.0	17	3.58	
5	62.0	19	3.26	3.50
6	60.0	15	4.00	
7	58.5	17	3.44	
8	62.0	17	3.65	
9	62.0	19	3.26	
10	53.0	17	3.12	

(e) 2FC

Sl. No.	Length of Secant (mm)	No. of intersecting grains	Grain thickness (mm)	Av. grain thickness (mm)
1	61.0	22	2.77	
2	62.5	20	3.12	
3	65.5	23	2.85	
4	61.5	22	2.79	
5	61.5	22	2.79	2.99
6	61.0	19	3.21	
7	58.0	17	3.41	
8	60.0	22	2.73	
9	58.0	17	3.41	
10	59.5	21	2.89	

(f) 3RN

Sl. No.	Length of Secant (mm)	No. of intersecting grains	Grain thickness (mm)	Av. grain thickness (mm)
1	57.5	08	7.20	
2	59.5	09	6.60	
3	64.5	10	6.45	
4	51.5	09	5.70	
5	56.5	11	5.10	6.30
6	57.5	08	7.20	
7	66.5	10	6.65	
8	62.5	11	5.68	
9	62.5	12	5.20	
10	51.0	07	7.20	

(g) 3N

Sl. No.	Length of Secant (mm)	No. of intersecting grains	Grain thickness (mm)	Av. grain thickness (mm)
1	64.0	17	3.76	
2	63.0	20	3.15	
3	63.5	18	3.30	
4	62.5	19	3.53	
5	64.0	16	3.25	3.50
6	64.5	17	3.90	
7	63.5	19	3.71	
8	63.0	19	3.35	
9	64.5	18	3.35	
10	64.0	19	3.51	

(h) 2TNA

Sl. No.	Length of Secant (mm)	No. of intersecting grains	Grain thickness (mm)	Av. grain thickness (mm)
1	62.0	21	2.95	
2	64.5	26	2.48	
3	64.0	28	2.28	
4	64.0	26	2.46	
5	68.5	24	2.85	2.54
6	63.5	27	2.35	
7	60.5	22	2.75	
8	65.5	30	2.18	
9	58.5	23	2.54	
10	55.5	22	2.52	

(i) 2TN

Sl. No.	Length of Secant (mm)	No. of intersecting grains	Grain thickness (mm)	Av. grain thickness (mm)
1	58.0	24	2.41	
2	64.0	24	2.66	
3	62.0	25	2.48	
4	63.5	23	2.54	
5	64.0	27	2.37	2.44
6	66.0	29	2.27	
7	54.5	26	2.09	
8	61.5	22	2.79	
9	59.0	23	2.56	
10	54.5	24	2.27	

(j) 2FN

Sl. No.	Length of Secant (mm)	No. of intersecting grains	Grain thickness (mm)	Av. grain thickness (mm)
1	50.0	23	2.17	
2	59.0	26	2.26	
3	47.5	18	2.63	
4	53.5	31	1.72	
5	56.5	32	1.76	2.09
6	47.5	23	2.06	
7	57.5	29	1.98	
8	56.5	26	2.17	
9	56.0	29	1.93	
10	52.5	23	2.28	

Set 3 (a) L1RC

Sl. No.	Length of Secant (mm)	No. of intersecting grains	Grain thickness (mm)	Av. grain thickness (mm)
1	62.0	16	3.88	
2	63.0	14	4.50	
3	60.5	19	3.18	
4	61.5	20	3.07	
5	60.5	16	3.78	3.31
6	63.0	14	4.50	
7	64.0	17	3.73	
8	60.0	19	3.37	
9	62.0	16	3.75	
10	59.5	20	3.10	

(b) L1C

Sl. No.	Length of Secant (mm)	No. of intersecting grains	Grain thickness (mm)	Av. grain thickness (mm)
1	61.0	21	2.90	
2	57.5	18	3.20	
3	60.5	22	2.75	
4	61.0	18	3.39	
5	60.5	19	3.18	3.02
6	63.5	22	2.89	
7	65.5	20	3.27	
8	63.0	23	2.74	
9	62.0	20	3.10	
10	60.5	22	2.75	

(c) 1TCAL

Sl. No.	Length of Secant (mm)	No. of intersecting grains	Grain thickness (mm)	Av. grain thickness (mm)
1	62.5	32	1.95	
2	64.5	28	2.30	
3	67.0	30	2.23	
4	60.5	29	2.08	
5	62.5	31	2.02	2.12
6	59.0	27	2.20	
7	61.0	27	2.26	
8	61.0	28	2.20	
9	64.5	32	2.02	
10	60.5	31	1.95	

(d) L1TC

Sl. No.	Length of Secant (mm)	No. of intersecting grains	Grain thickness (mm)	Av. grain thickness (mm)
1	63.5	31	2.05	
2	61.5	35	1.76	
3	65.5	42	1.56	
4	65.0	38	1.71	
5	65.5	38	1.72	1.75
6	64.0	35	1.83	
7	64.0	38	1.68	
8	63.5	39	1.63	
9	65.0	38	1.71	
10	65.5	35	1.87	

(e) L1FC

Sl. No.	Length of Secant (mm)	No. of intersecting grains	Grain thickness (mm)	Av. grain thickness (mm)
1	64.0	49	1.31	
2	64.5	44	1.45	
3	62.0	46	1.35	
4	59.0	40	1.47	
5	65.0	43	1.51	1.48
6	63.5	42	1.51	
7	64.0	36	1.77	
8	63.5	45	1.41	
9	63.5	42	1.51	
10	65.0	43	1.51	

(f) L1RN

Sl. No.	Length of Secant (mm)	No. of intersecting grains	Grain thickness (mm)	Av. grain thickness (mm)
1	62.0	23	2.69	
2	65.5	24	2.73	
3	62.0	25	2.48	
4	57.5	17	3.38	
5	60.0	19	3.15	2.82
6	63.5	22	2.88	
7	62.0	22	2.82	
8	55.5	19	2.92	
9	61.5	25	2.46	
10	54.5	20	2.72	

(g) L1N

Sl. No.	Length of Secant (mm)	No. of intersecting grains	Grain thickness (mm)	Av. grain thickness (mm)
1	65.0	32	2.03	
2	64.0	32	2.00	
3	64.5	33	1.95	
4	63.0	32	1.97	
5	64.5	37	1.74	1.92
6	64.5	32	2.01	
7	65.5	37	1.77	
8	64.0	32	2.00	
9	66.5	33	2.01	
10	65.0	37	1.76	

(h) 1TNAL

Sl. No.	Length of Secant (mm)	No. of intersecting grains	Grain thickness (mm)	Av. grain thickness (mm)
1	62.5	38	1.64	
2	64.5	37	1.74	
3	63.0	38	1.65	
4	65.0	36	1.80	
5	65.5	41	1.62	1.62
6	66.5	41	1.62	
7	64.5	45	1.43	
8	61.5	39	1.58	
9	66.5	46	1.44	
10	65.5	38	1.72	

(i) L1TN

Sl. No.	Length of Secant (mm)	No. of intersecting grains	Grain thickness (mm)	Av. grain thickness (mm)
1	63.0	46	1.37	
2	65.0	47	1.38	
3	62.0	45	1.37	
4	65.5	46	1.42	
5	63.0	39	1.61	1.43
6	65.5	45	1.45	
7	61.0	44	1.38	
8	60.5	40	1.51	
9	64.0	45	1.42	
10	63.0	46	1.37	

(j) L1FN

Sl. No.	Length of Secant (mm)	No. of intersecting grains	Grain thickness (mm)	Av. grain thickness (mm)
1	60.0	48	1.25	
2	62.5	48	1.30	
3	63.0	53	1.20	
4	62.0	46	1.35	
5	64.5	49	1.32	1.27
6	62.5	50	1.25	
7	64.0	53	1.21	
8	63.5	54	1.17	
9	64.0	51	1.25	
10	64.5	47	1.37	

TABLE IV : Data for Polar Graphs

Sample	Angle θ°	N_L	L cm
1RC	0	2.71	5.15
	30	2.33	5.95
	60	2.99	7.35
	90	2.99	6.40
	120	2.86	7.35
	150	2.44	6.15
	180	2.28	5.30

Sample	Angle θ°	N_L	L cm
1C	0	4.86	5.35
	30	4.03	6.20
	60	3.56	7.30
	90	4.34	6.45
	120	4.02	7.45
	150	3.47	6.05
	180	3.65	6.20

Sample	Angle θ°	N_L	L cm
1TCA	0	4.42	5.20
	30	4.64	6.05
	60	4.29	7.45
	90	4.50	6.45
	120	4.21	7.35
	150	4.38	5.85
	180	4.00	5.00

Sample	Angle θ°	N_L	L cm
1TC	0	4.50	5.20
	30	4.00	6.00
	60	4.07	7.60
	90	4.98	6.10
	120	4.21	7.60
	150	3.93	6.10
	180	4.20	5.25

Sample	Angle θ°	N_L	L cm
1FC	0	3.65	5.20
	30	4.63	6.05
	60	5.09	7.40
	90	5.38	6.50
	120	5.06	7.50
	150	4.59	6.10
	180	3.85	5.20

Sample	Angle θ°	N_L	L cm
1RN	0	3.20	5.65
	30	2.90	6.50
	60	4.03	7.40
	90	4.03	6.45
	120	4.02	7.40
	150	3.20	5.60
	180	3.40	4.75

Sample	Angle θ°	N_L	L cm
1N	0	3.02	5.30
	30	4.10	6.10
	60	4.20	7.40
	90	4.25	6.35
	120	4.50	7.30
	150	3.80	6.05
	180	3.07	5.20

Sample	Angle θ°	N_L	L cm
1TNA	0	4.20	5.40
	30	6.30	6.20
	60	6.30	7.60
	90	6.40	6.60
	120	6.00	7.55
	150	5.90	5.95
	180	4.20	5.20

Sample	Angle θ°	N_L	L cm
1TN	0	3.20	5.05
	30	4.20	5.90
	60	5.10	7.40
	90	6.80	6.45
	120	4.80	7.35
	150	4.30	6.00
	180	3.20	5.20

Sample	Angle θ°	N_L	L cm
1FN	0	1.80	5.40
	30	5.50	6.20
	60	7.10	7.50
	90	6.82	6.45
	120	6.70	7.45
	150	4.50	5.75
	180	2.20	4.90

Sample	Angle θ°	N_L	L cm
3RC	0	2.07	5.30
	30	1.80	6.20
	60	1.40	7.65
	90	1.49	6.70
	120	1.30	7.70
	150	1.70	5.90
	180	1.98	5.05

Sample	Angle θ°	N_L	L cm
3C	0	2.45	5.30
	30	1.50	6.15
	60	1.90	7.15
	90	1.77	6.20
	120	2.10	7.10
	150	1.17	5.90
	180	2.35	5.10

Sample	Angle θ°	N_L	L cm
2TCA	0	2.31	5.20
	30	2.78	6.10
	60	2.91	6.85
	90	3.02	5.95
	120	2.87	6.95
	150	2.80	6.05
	180	2.31	5.20

Sample	Angle θ°	N_L	L cm
2TC	0	2.88	5.20
	30	2.30	6.05
	60	2.72	7.35
	90	3.50	6.40
	120	2.70	7.45
	150	2.15	6.05
	180	3.07	5.20

Sample	Angle θ°	N_L	L cm
2FC	0	2.80	5.00
	30	2.40	5.80
	60	3.10	7.40
	90	3.54	6.40
	120	3.10	7.40
	150	2.83	6.35
	180	2.70	5.50

Sample	Angle θ°	N_L	L cm
3RN	0	1.58	5.10
	30	1.70	5.95
	60	2.90	7.55
	90	2.60	6.55
	120	2.80	7.60
	150	1.78	6.15
	180	1.68	5.30

Sample	Angle θ°	N_L	L cm
3N	0	2.55	5.10
	30	2.60	5.85
	60	2.60	7.40
	90	2.80	6.35
	120	2.85	7.35
	150	2.90	6.25
	180	2.50	5.40

Sample	Angle θ°	N_L	L cm
2TNA	0	3.90	5.30
	30	4.50	6.15
	60	4.10	7.70
	90	3.60	6.65
	120	3.90	7.70
	150	3.60	6.15
	180	3.80	5.25

Sample	Angle θ°	N_L	L cm
2TN	0	3.36	5.35
	30	2.60	6.20
	60	3.50	7.75
	90	3.65	6.75
	120	3.60	7.80
	150	2.50	6.05
	180	3.46	5.20

Sample	Angle θ°	N_L	L cm
2FN	0	1.33	5.25
	30	2.11	6.15
	60	2.50	7.10
	90	3.90	6.20
	120	2.90	7.20
	150	1.95	6.15
	180	1.50	5.30

Sample	Angle θ°	N_L	L cm
L1RC	0	2.42	4.95
	30	2.96	5.75
	60	3.20	7.50
	90	3.54	6.50
	120	3.12	7.05
	150	2.52	6.35
	180	2.55	5.50

Sample	Angle θ°	N_L	L cm
	0	3.11	4.50
	30	3.40	5.30
	60	3.70	7.45
L1C	90	3.85	6.50
	120	3.33	7.50
	150	3.21	6.55
	180	2.81	5.70

Sample	Angle θ°	N_L	L cm
	0	3.11	5.15
	30	3.31	6.05
	60	4.29	7.45
1TCAL	90	4.65	6.45
	120	4.56	7.45
	150	3.64	6.05
	180	3.24	5.25

Sample	Angle θ°	N_L	L cm
	0	4.47	5.15
	30	4.00	6.00
	60	4.67	7.50
L1TC	90	5.20	6.55
	120	4.40	7.50
	150	3.63	6.05
	180	4.34	5.30

Sample	Angle θ°	N_L	L cm
L1FC	0	2.77	5.05
	30	4.27	5.85
	60	5.75	7.30
	90	5.85	6.50
	120	5.69	7.55
	150	3.71	6.20
	180	2.96	5.40

Sample	Angle θ°	N_L	L cm
L1RN	0	3.30	5.15
	30	3.50	6.00
	60	3.83	7.05
	90	4.43	6.10
	120	3.97	7.05
	150	3.90	6.10
	180	3.58	5.30

Sample	Angle θ°	N_L	L cm
L1N	0	4.08	5.15
	30	4.60	6.10
	60	5.20	7.55
	90	5.56	6.65
	120	5.10	7.65
	150	4.30	6.05
	180	3.81	5.25

Sample	Angle θ°	N_L	L cm
1TNAL	0	4.27	5.15
	30	4.37	5.95
	60	5.37	7.45
	90	5.89	6.45
	120	5.27	7.40
	150	4.26	6.10
	180	4.70	5.30

Sample	Angle θ°	N_L	L cm
L1TN	0	3.56	5.05
	30	3.90	5.90
	60	4.90	7.50
	90	5.90	6.50
	120	5.20	7.50
	150	4.20	6.15
	180	3.55	5.35

Sample	Angle θ°	N_L	L cm
L1FN	0	3.50	5.15
	30	4.20	5.95
	60	6.00	7.50
	90	6.61	6.50
	120	5.87	7.50
	150	4.30	6.05
	180	3.62	5.25

MME-1994-M-PRA (OR